SYNTHESIS AND CHARACTERIZATION OF HIGH AND LOW VALENT URANIUM NITROGEN COMPLEXES AND COPPER CATALYZED CROSS- COUPLING REACTIONS OF BROMINATED COMPOUNDS

by

**Kristen Gettys**

A Dissertation

Submitted to the Faculty of Purdue University

In Partial Fulfillment of the Requirements for the degree of

Doctor of Philosophy
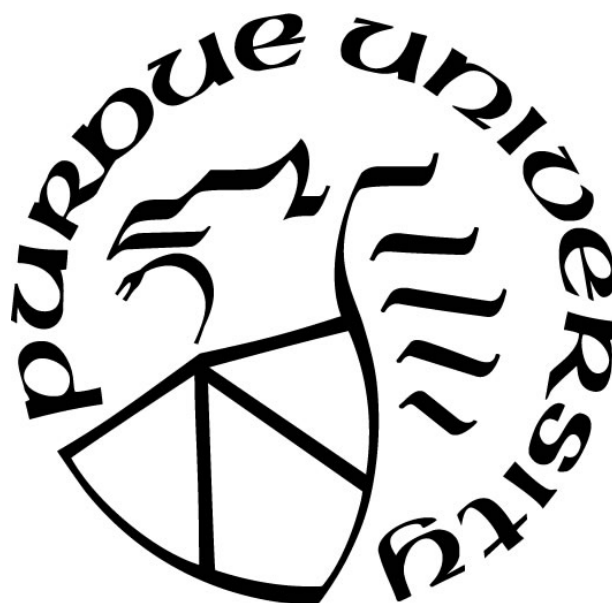
Department of Chemistry

West Lafayette, Indiana

December 2018

THE PURDUE UNIVERSITY GRADUATE SCHOOL
STATEMENT OF COMMITTEE APPROVAL

Dr. Suzanne Bart, Chair

    Department of Chemistry

Dr. Mark Lipton

    Department of Chemistry

Dr. Christopher Uyeda

    Department of Chemistry

Dr. Paul Wenthold

    Department of Chemistry

Approved by:

    Dr. Christine Hrycyna

        Head of the Graduate Program

To Mom, for your unending support and love.

ACKNOWLEDGMENTS

First and foremost, to Suzanne: I will never be able to thank you enough for giving me the ultimate second chance and being an incredible advisor, mentor, and resource. I have learned so much from you over the past year and a half and I only regret that I didn't make the flying leap to your group sooner.

To my group: Caleb, Ezra, Scott, Tyler, and Shane, you guys always kept me on my toes and made sure that work was never boring. May you always remember the proper way to quench KH, take joy in acid washing all the hard water stains off the condensers, and don't forget to play the Shaman every now and then in my absence!

To the other three of our core-four: Allison, break open another bottle of peach André; we have some celebrating to do! Thank you for hours spent discussing departmental gossip, tears shared because people are stupid, unending laughter, and all of your support. Anna, you have become such an incredible friend over the past couple of years and I have loved every crazy adventure we've had (but particularly the one involving the chocolate cake shake)! Carly, you listened to more "I can't believe we actually have to deal with this" rants than anyone and I will forever be grateful for the encouragement you gave me after I decided to make my mental health my first priority. Thank you all for your incredible support!

To my forever bestie: Emma, we started this wild (stupid?) ride together and I would have been completely lost without you. I love you like you are my sister and I miss

our seemingly endless talks on the phone. Here's to life after grad school and rekindling a friendship that is far too precious to let go.

To my Studio b family (also known as fierce woman tribe): You beautiful people are the best gift I could have asked for and these last two years would have been so much less fulfilling without you. The love that flows through you all is strong enough to pull people back from the "pit of despair" and you will never know how deeply you've touched countless lives. Thank you for reminding me that I do actually love to dance, that I am stronger than I think, and that, collectively, we can change the world. May the Pound music always be louder than loud, the toning weights always get CRUSHED, and never forget that we all love Salsa!

To my favorite rebels: Michelle, you never cease to amaze me with your strength and perseverance despite everything that gets thrown on your plate. I will never undermine the power of simply 'saying hello' because it led me to one of the best friends I've ever had. Amanda, you're the big sister I never had and the soul sister I always wanted. You push me past the limits I set for myself in every possible way (I mean just look at my lunges now!) and you inspire me to be a better person every single day. Thank you for countless late-night chats, drinks on the porch, priceless words of wisdom, never EVER losing faith in me or my ideas, and always having a phenomenal playlist to go with it all. And to Dan, Wes, Will, Lucy, and Tess: thank you all for accepting me into your home on so many occasions. Even if you never understand the joy you brought to my life just by having dinner or sharing Halloween candy or sitting on the couch watching tv, I will never forget it.

To Susan: You're the best aunt/second mom I could ever ask for. You have been there for me throughout this entire process and, at times, you were the only one who really understood how I felt. I will never be able to repay you for how much you have given me; I can only hope to be the same source of love and stability to someone else in the future that you have been to me.

Finally, to my parents: You always told me I could do anything I set my mind to and I finally proved it to myself. This was an incredibly rocky road, but you never once stopped supporting me and I will always remember that. I could not have gotten where I am today without your love.

TABLE OF CONTENTS

LIST OF TABLES

LIST OF FIGURES

LIST OF SCHEMES

LIST OF ABBREVIATIONS

AD	adamantyl
BN	benzyl
Detp	2,6-diethylphenyl
DIPA	di-isopropyl amine
DIPEA	di-isopropyl ethylamine
DIPP	2,6-diisoproylphenyl
DippCDI	*N,N*-2,6-diisopropylphenylcarbodiimide
DMAP	4-dimethylaminopyridine
DMF	dimethyl formamide
EtOAc	ethyl acetate
*i*PrCDI	*N,N*-isopropylcarbodiimide
ITI	inverse trans influence
MeCN	acetonitrile
MeOH	methanol
Mes	2,4,6-trimethylphenyl
$^{Mes}PDI^{Me}$	2,6-(2,4,6-Me$_3$-C$_6$H$_2$-N=CMe)$_2$C$_5$H$_3$N
*p*Tol	4-methylphenyl
*t*BuBpy	4,4'-tert butyl bipyridine
thf	tetrahydrofuran
tppo	triphenylphosphine oxide
Tpy	terpyridine
VT	variable temperature

ABSTRACT

Author: Gettys, Kristen, E. PhD
Institution: Purdue University
Degree Received: December 2018
Title: Organometallic Explorations in Catalysis and Synthesis
Committee Chair: Suzanne Bart

It is well-known that f-block elements can exhibit coordination modes which surpass those of the transition metals. With uranyl and uranium bis(imido) complexes a strong preference is shown for the oxo or imido ligands in the *trans-* position; a phenomenon which is known as the inverse trans- influence which is unique to high valent actinides. However, when a third imido is added to the complex, a decrease in bond order occurs and this preference is diminished. Through the synthesis of several novel coordination complexes of tris(2,6-diisopropylphenyl)imido uranium [U(NDipp)$_3$] with a variety of ligands, we were able to analyze the energy differentials between bonding modes in both the solution and solid state. Furthermore, density functional theory calculations were employed to model the energetic preferences between these geometries. The combination of analyses gives rise to the observation that the orientation of the imido substituents is fluxional depending on the rigidity of the supporting ligands, and oftentimes exhibits low energetic barriers for the formation of different conformers.

Uranium tris(imido) species bearing *trans*-imidos are desirable synthons as they can be used to mimic reactivity of more complicated uranium oxide polymeric systems. Such systems are advantageous as they are easily soluble in organic solvents, making them amenable to standard characterization methods and ligand substitution strategies. Our group has previously shown that uranium tris(imidos), easily synthesized from [(^{Mes}PDI^{Me})U(THF)]$_2$ and various azides, feature axial imido substituents exhibiting differing bond characteristics than the adjacent equatorial imido substituent. The aim of this work is to show that multiple analogues of mixed imido products can be formed from either the aforementioned dimer or stable tris(imido) synthons by exploiting reactivity differences between the axial and equatorial positions.

Presented herein are novel copper-catalyzed ring opening reactions of cyclopropanols and various electrophiles to synthesize a variety of beta-functionalized ketones. The reactions feature mild conditions and tolerates a wide selection of functional groups leading to complex products which can be used in the synthesis of bioactive molecules.

CHAPTER 1.   LEWIS BASE ADDUCTS OF URANIUM TRIS(IMIDO) COMPLEXES

1.1   Introduction

Our group has recently reported the synthesis of multiple uranium tris(imido) complexes; one supported by solvent ligands ((thf)$_3$U(NDipp)$_3$ (**1-thf$_3$**) (Dipp = 2,6-diisoproylphenyl)) and the other two supported by a redox-active ligand ((^{Mes}PDI^{Me})U(NMes)$_3$ (**1-PDI-Mes**) (^{Mes}PDI^{Me} = 2,6-(2,4,6-Me$_3$-C$_6$H$_2$-N=CMe)$_2$C$_5$H$_3$N) (Mes = 2,4,6-trimethylphenyl), (^{Mes}PDI^{Me})U(NDipp)$_3$ (**1-PDI-Dipp**)) (Figure 1.1).[1,2] These complexes were the first of their kind and showed for the first time that uranium was capable of supporting three confirmed multiple bonds at a single center. The synthesis and characterization of these complexes was well overdue, as many of their transition metal analogs M(UNR)$_3$(L)$_x$ have been known for nearly 30 years.[3–7]
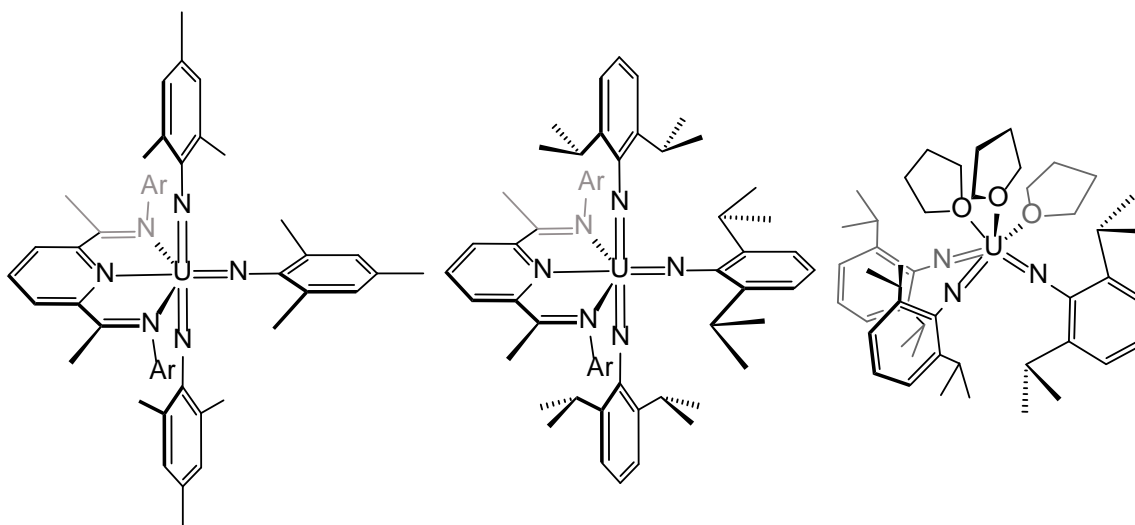
Figure 1.1 Structural representations of **1-PDI-Mes**, **1-PDI-Dipp**, and **1-thf$_3$** respectively.

Structural data of uranium (VI) complexes bearing multiply-bonded ligands is comprised predominantly of molecules displaying the UO$_2^{2+}$ or UNR$_2$L$_2$ formalism with

the ligands existing in the *trans-* position.[8] Contrary to the transition metals, high valent actinides exhibit stabilization through strongly donating *trans*-ligands as is evidenced by shortened and bond distances. The stability and driving force towards the formation of this framework arises from the inverse *trans*-influence (ITI), which involves the mixing of core 6p orbital density with that of the 5f.[9] For the bis(imido) complexes, only complexes bearing the highly bulky and electron donating Cp^* ligands, $Cp^R_2U(NR)_2$,[10,11] deviate from the *trans-* orientation of the imido substituents.

Synthesis of linear uranium bis imidos began in 2005 by James Boncella and co-workers with the synthesis of $U(NPh)_2L_2$ (L = thf, I).[12] From that seminal publication, a vast library of syntheses emerged along with examples of reactivity. In 2006 they discovered that, not only could the equatorial ligands be substituted, but one of the imidos could be replaced with an oxo ligand through the addition of a single equivalent of water.[13,14] Further studies by Boncella and colleagues provided great insight to the reactivity of uranium bis(imidos) but never culminated in the synthesis of a uranium tris(imido).

The synthetic routes towards **1-PDI-Dipp** and **1-thf₃** are similar in that uranium tris(iodide) is mixed with a reducing reagent, then oxidized to uranium (VI) upon addition of azide. Although these complexes have parallel syntheses and bear identical imido-based substituents, they are structurally unrelated with **1-PDI-Dipp** being pseudo *mer*-octahedral and **1-thf₃** being pseudo *fac*-octahedral. Whereas bis(imidos) display a strong preference for *trans-* multiply-bonded substituents, the addition of a third imido appears to diminish this preference. In previous work we have shown that the increased π-donation from the third imido substituent has been shown to weaken the *trans-* bonding manifold such that preference for the *trans-* orientation is overcome.[2,15]

In contrast to this observed phenomenon, fluxional geometries are not known for the transition metal tris(imido) analogs $[M(NR)_3]$ which most commonly display a bent pyramidal imido orientation. (Figure 1.2a) Throughout the early to mid-1990's an entire library of tris(imidos) were synthesized including group V (Nb, Ta),[3] group VI (Mo, W),[4,16] group VII (Re, Tc),[5,6] and group VIII metals (Os).[7] The prevalent bent pyramidal geometry observed for all molecules, excluding the Re and Os examples, arises from increased bonding with multiple *d* orbitals, as well as minimized *trans*-influence repulsions. The only

variation from this pyramidal geometry is noted in the d^2 Os(NDipp)$_3$ and [Re(NDipp)$_3$]$^-$ complexes, as occupation of the dz^2 orbital forces adaptation of a trigonal planar geometry (Figure 1.2b).[7] While the T-shaped orientation of the imido substituents (Figure 1.2c) in **1-PDI-Dipp** and **1-PDI-Mes** seems unique in comparison to transition metal analogs, this coordination geometry is logical when the steric nature of the PDI ligand is considered. Likewise, the coordination geometry of **1-thf$_3$** is also predictable, as it bears a bonding formulism similar to its transition metal analogs.

a.   b.   c.

Pyramidal   Trigonal   T-shaped
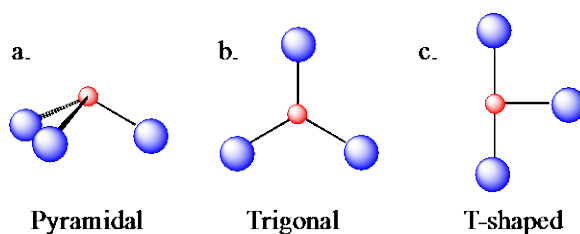
Figure 1.2 Geometries for tris(imido) complexes.

Due to the interesting structural differences between these two complexes, new coordination complexes of **1-thf$_3$** were sought out to further investigate the types of coordination complexes available for the uranium tris(imido). Interestingly, upon addition of a single equivalent of ^{Mes}PDI^{Me} to **1-thf$_3$**, the quantitative conversion to **1-PDI-Dipp** occurred with the loss of all thf ligands. This led to the hypothesis that other Lewis base adducts of the [U(NR)$_3$] framework could be constructed taking advantage of the rapid THF dissociation.

In our previous report,[17] we stated that the coordinated thf ligands of **1-thf$_3$** are highly labile, with rapid dissociation/association occurring in solution, as was noted by highly broadened thf resonances in the ^{1}H NMR spectrum (Scheme 1.1). In the presence of non-coordinating solvents (toluene/pentane), crystals of (thf)$_2$U(NDipp)$_3$ (**1-thf$_2$**) could be isolated at -35 °C and analyzed by X-ray diffraction. Refinement of the data revealed a penta-coordinate uranium center with two bound THF ligands and three imido substituents (Figure 1.3). The symmetry/coordination geometry of this complex lies in between a C$_{3v}$

(trigonal bipyramidal) and C_{2v} (square pyramidal) symmetric complex. The U=N bonds in **1-thf$_2$** are slightly shorter with respect to **1-thf$_3$**, with U-N bond distances ranging from 1.966(2) to 1.995(2) Å. The N1-U1-N3 bond angle of 149.48° is slightly more obtuse than the other two, N1-U1-N2 = 101.46° and N2-U1-N3 = 108.98°, and, using geometric calculations developed by Muetterties and Guggenberger,[18] the molecular structure is calculated to be closer to the C_{2v} symmetric structure than the D_{3h} symmetric structure. Despite the pseudo *trans-* orientation of the imido substituents, no axial contraction is noted. The U-O bond distances for the two thf ligands of 2.411(2) and 2.456(2) Å, are significantly truncated from the U-O distances seen in **1-thf$_3$** (2.595 – 2.618 Å). The orientation of the imido substituents in **1-thf$_2$** is very similar to the predicted gas phase structure of UO$_3$, whose trans-oxo substituents deviate from the idealized T-shaped orientation (165 – 158°).
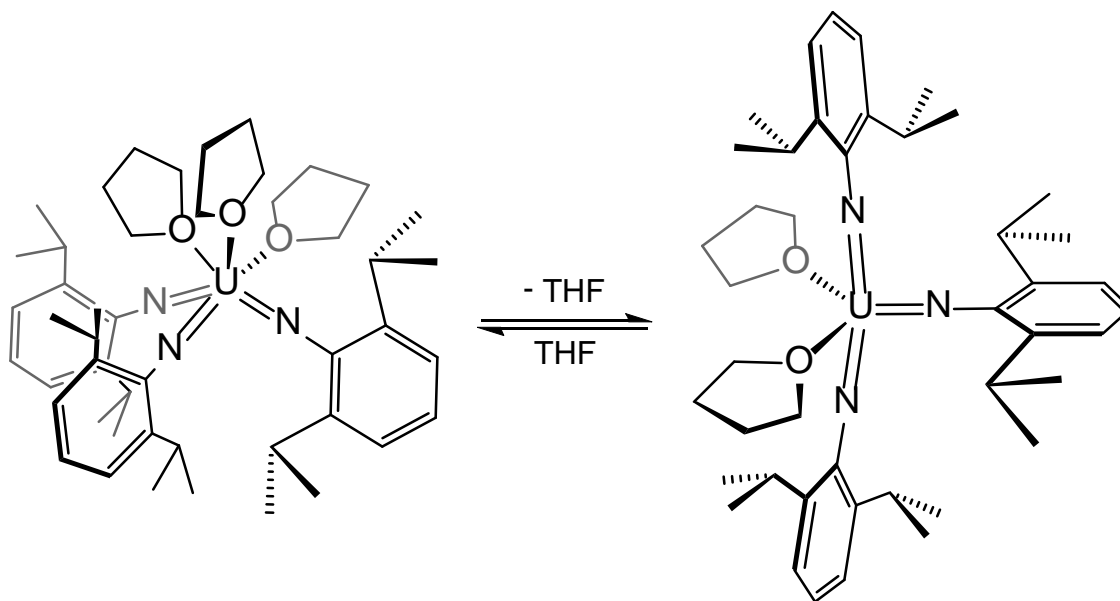
Scheme 1.1 Equilibrium between **1-thf$_3$** and **1-thf$_2$** in solution
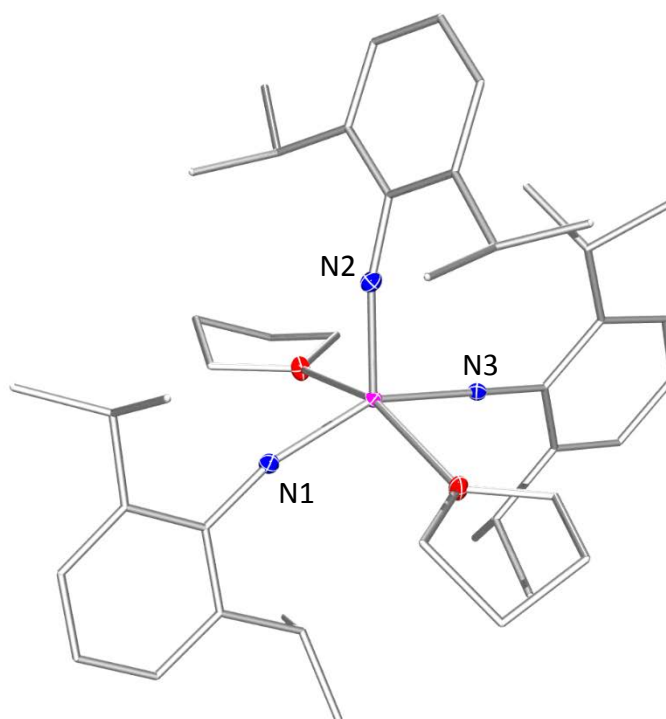
Figure 1.3 Molecular structure of **1-thf₂** with non-carbon atoms displayed at 30% probability ellipsoids. Hydrogen atoms and outer sphere solvent molecules have been omitted for clarity.

Despite this difference in coordination geometry from **1-thf₃**, attempts at analysis of these crystals by ^{1}H NMR spectroscopy revealed no difference from parent complex, with only signals from the imido substituents being visible. This suggests that **1-thf₃** and **1-thf₂** are in a rapid equilibrium with one another in solution, and that the solution phase structure depicted by ^{1}H NMR spectroscopy is likely a superposition of **1-thf₃** and **1-thf₂**, with the two being very similar in symmetry (Scheme 1.1).

Since it was known that complete substitution of the THF ligands with another supporting ligand (^Mes^PDI^Me^) forced a complete geometry change in the imido substituents, calculations at the PBE/ZORA/TZ2P level of theory were sought for the energy differences in these two conformations. By comparing the calculated bond distances of **1-thf₃** in both

the *fac* and *mer* conformations with the experimentally gathered data (Table 1.1), an energy diagram of the different conformations could be constructed (Figure 1.4).

Table 1.1 Selected bond distances for **1-thf₃** and calculated bond metrics for both *fac-* and *mer-* isomers of **1–thf₃**.

(thf)₃U(NDipp)₃			
	Expt.	**Calculated** *fac*	**Calculated** *mer*
Bond	Distance (Å)		
U1-N1	1.986(14)	2.006	1.955
U1-N2	2.000(16)	2.008	2.010
U1-N3	2.010(15)	2.009	1.995
U1-O1	2.595(13)	2.699	2.534
U1-O2	2.616(13)	2.698	2.831
U1-O3	2.618(12)	2.696	2.532
Bond	Degree (°)		
N1-UI-N2	99.7(5)	104.5	96.76
N1-UI-N3	99.8(5)	103.0	166.59
N2-UI-N3	101.6(5)	102.4	96.65
N1-UI-O1	165.9(2)	159.4	87.61
N2-UI-O2	162.2(5)	162.4	179.39
N3-UI-O3	162.2(4)	161.3	87.56

The change in energy of the bond can be calculated by subtracting the interaction energy (ΔE_{int}) from the total deformation energy (ΔE_{def}). The interaction energy takes into account steric interactions, including Pauli repulsion and electrostatic interaction, as well as orbital interactions while the total deformation energy is a summation of the fragmented energies of the two fragments formed. When these calculations are applied to the calculated bond distances in Table 1.1, an interesting observation is made. The **1-PDI-Dipp** similar, but heretofore unobserved, *mer* conformer of **1-thf₃** is significantly higher in energy than either **1-thf₂** or *fac* **1-thf₃** thus yielding explanation as to why it has yet to be detected.
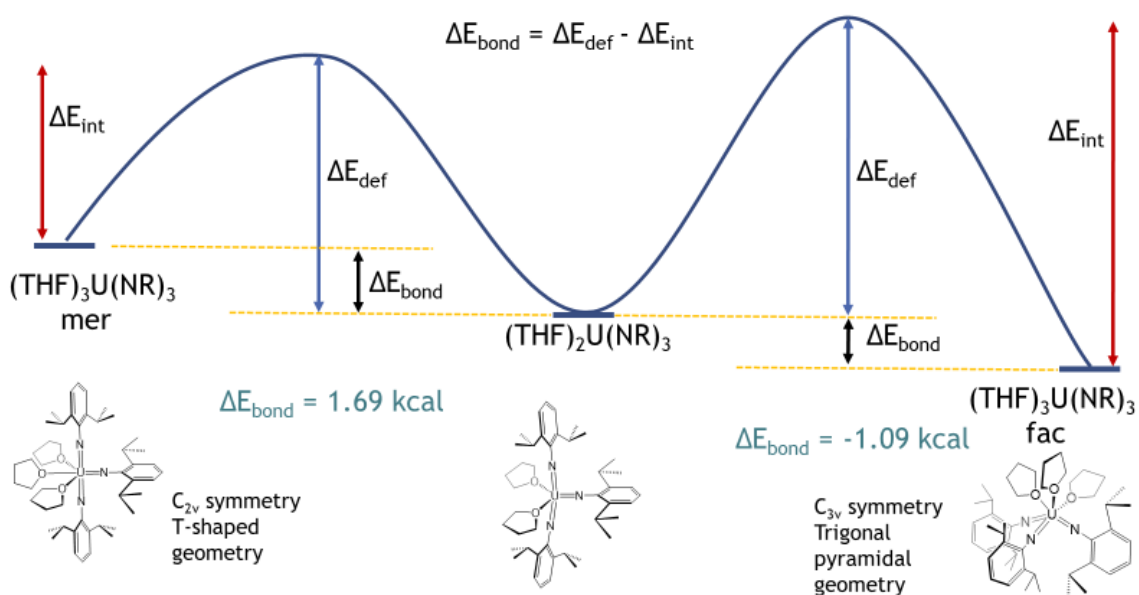
Figure 1.4 Energy diagram between possible conformers of thf supported U(NDipp)₃.

While ligand dissociation from tris(imido) complexes is not unprecedented, the drastic structural changes we have observed resulting from ligand dissociation are unusual. Since orbital overlap typically dictates the orientation of these highly donating substituents, investigating the changes of conformation with *f*-block atoms gives more possibility of fluctuation than *d*-block metals. To investigate this phenomenon further we sought to investigate the incorporation of more highly donating ligands.

1.2   Results and Discussion

Since the structures of **1-PDI-Dipp** and **1-thf₃** had such drastically different geometries, a handful of ligands were selected to probe the ligand effect. A selection of mono-, bi- and tridentate ligands were used, as well as the oxygen containing triphenylphosphine oxide (Scheme 1.2).
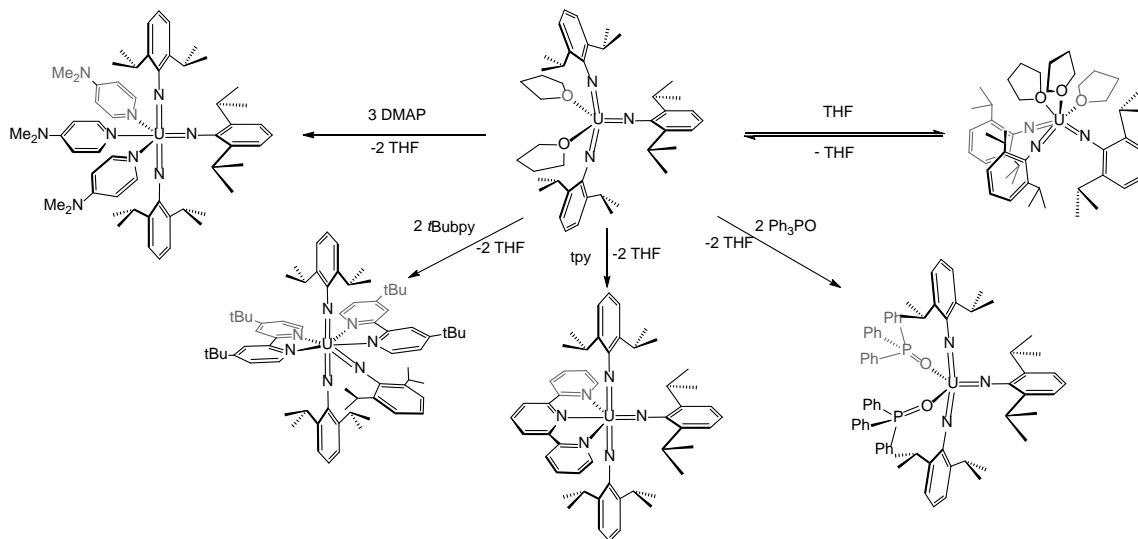
Scheme 1.2 Synthesis of Lewis base derivatives of U(NDipp)₃(L)ₙ.

We began with the addition of three equivalents of 4-dimethylaminopyridine (DMAP) to a toluene solution of **1-thf₃**. Removal of the solvent *in vacuo* resulted in isolation of (dmap)₃U(NDipp)₃ (**1-dmap₃**) in good yield (91%). Despite being synthesized from **1-thf₃**, analysis of crystals of **1-dmap₃** by X-ray diffraction reveals a T-shaped orientation of the imido substituents with an overall *mer*-octahedral conformation much like **1-PDI-Dipp** (Figure 1.5). The two axial U=N bonds, related by a N-U-N binding angle of 168.33°, display bond distances of 2.005(5) and 1.974(4) Å, which are slightly truncated with respect to the equatorial U=N bond of 2.028(4) Å. The two *trans* U-N$_{dmap}$ interactions show typical U-N dative distances, with bond distances of 2.555(6) and 2.573(4) Å. (ref) The U-N$_{dmap}$ bond *trans* to the equatorial imido, however, is elongated by over 0.1 Å, with a bond distance of 2.698(5) Å. This can be attributed to a *trans*-influence but is in contrast to what is commonly observed in high valent uranium.
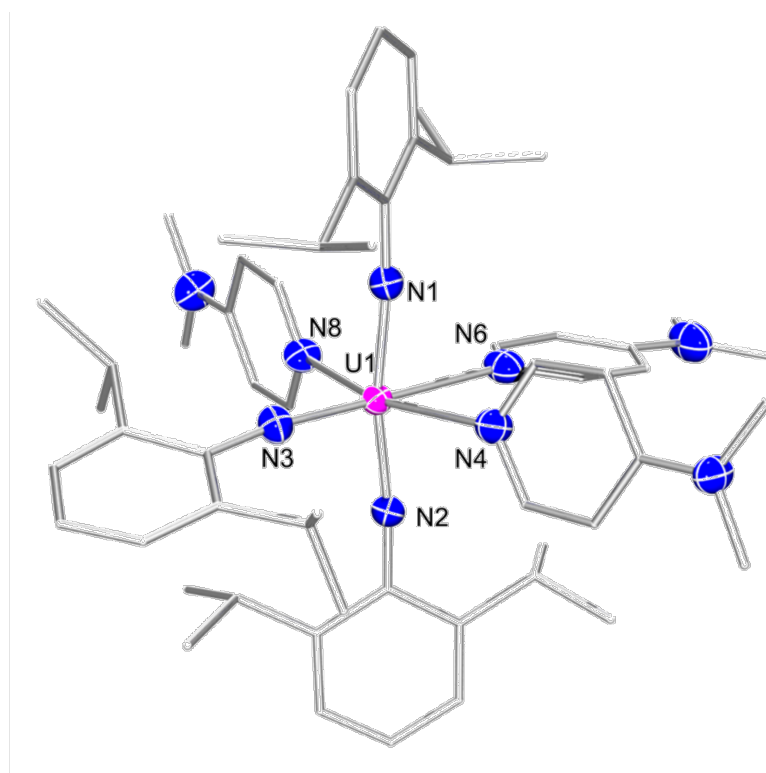
Figure 1.5 Molecular structure of **1-dmap$_3$** with non-carbon atoms displayed as 30% probability ellipsoids. Hydrogen atoms and outer sphere solvent molecules have been omitted for clarity.

The T-shaped orientation of imido substituents in the solid-state structure of **1-dmap$_3$** is nearly identical to that of **1-PDI-Dipp**, despite the coordinative freedom of the DMAP ligands. However, analysis of **1-dmap$_3$** by ^{1}H NMR spectroscopy does not agree with the solid-state structure (Figure 1.6). While the ^{1}H NMR spectrum of **1-PDI-Dipp** agrees with the solid-state structure with two sets of imido based resonances in a 2:1 ratio concurrent with a C$_{2v}$ symmetric molecule, the ^{1}H NMR spectrum of **1-dmap$_3$** looks nearly identical to **1-thf$_3$**, with only a single set of resonances for all three imido substituents. A large broad doublet at 1.44 ppm is assigned as the *i*Pr-CH$_3$, with its corresponding *i*PrCH resonating at 5.41 ppm. The *p*-ArH resonance has shifted to 5.19 ppm and the *m*-ArH resonance is found at 7.99 ppm. At first, the signals for the dmap ligands seem completely

absent. However, upon closer investigation, spectra taken over the course of 24 hours show the disappearance of free dmap and a growth of free thf (Figure 1.7). Using this information we observe the signals for the coordinated dmap ligands being significantly broadened, but visible at 1.95, 5.79, and 9.20 ppm. In agreement with the solution behaviour seen for **1-thf₃**, the breadth and distribution of ligand resonances would suggest rapid association and dissociation, leading to a solution state structure more similar to a theoretical (dmap)₂U(NDipp)₃ (**1-dmap₂**) (Scheme 1.3) Unfortunately, attempts at isolation of crystals of **1-dmap₂** by similar methods as was done for **1-thf₂**, only afforded crystals of **1-dmap₃** despite the use of only two equivalents of ligand.
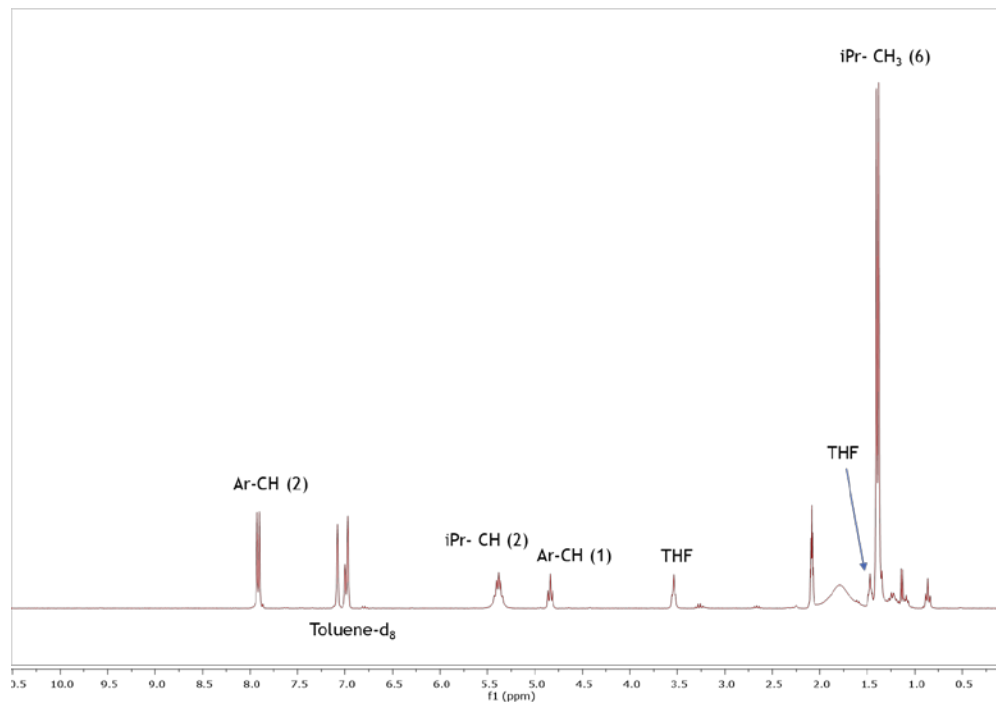
Figure 1.6 ^{1}H NMR spectrum of **1-dmap₃** at room temperature in toluene-d_8.
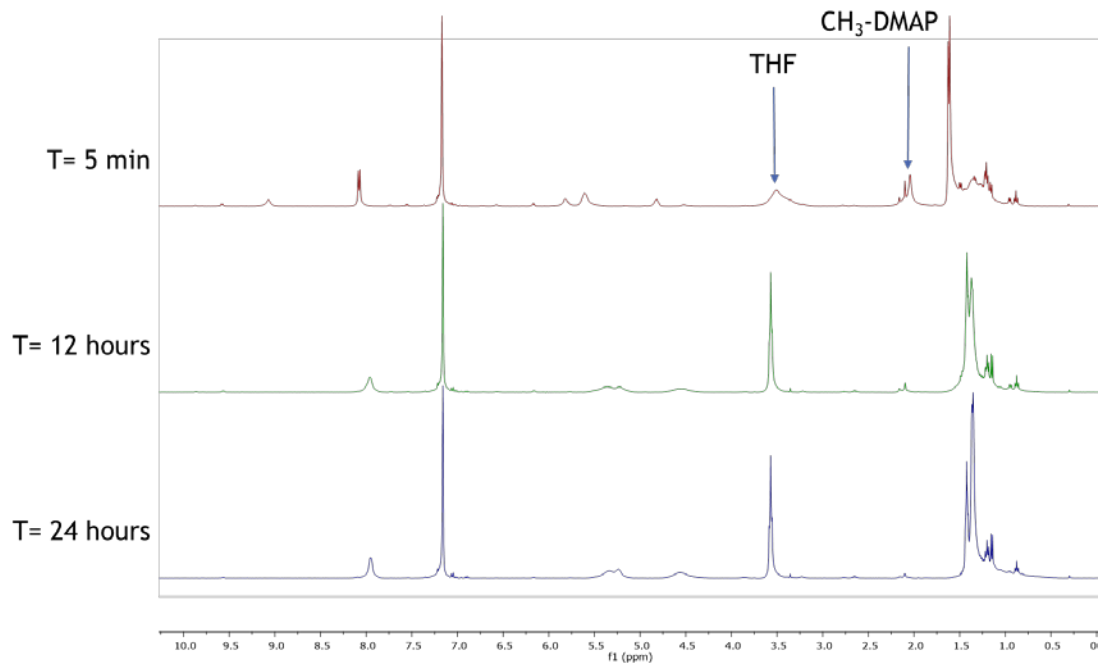
Figure 1.7 ^{1}H NMR spectrum in benzene-d_6 at room temperature of DMAP ligands displacing thf ligands on uranium tris(imido).
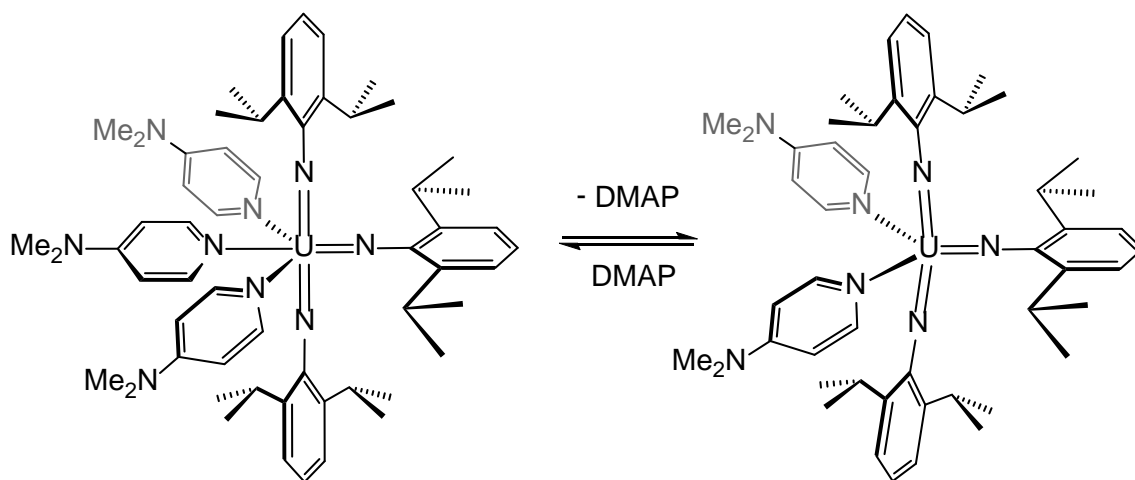
Scheme 1.3 Equilibrium between **1-dmap₃** and **1-dmap₂** in solution.

Since the molecular structure of **1-dmap₃** was in stark contrast to what had previously been observed and calculated for **1-thf₃,** the question arose whether the

formation of meridional **1-dmap₃** was a structural anomaly. To address this, variable temperature ^{1}H NMR spectroscopy was employed (Figure 1.8). Starting at 50 ˚C, the spectrum of **1-dmap₃** displays sharp resonances for the imido substituents, however upon cooling these resonances begin to broaden and shift drastically which broaden into the baseline at -20 ˚C. Continued cooling reveals a new set of resonances, which sharpen to clarity at -40 ˚C. This new conformer displays 12 resonances, indicative of a change in symmetry to C₂v, similar to the solution structure of **1-PDI-Dipp**.
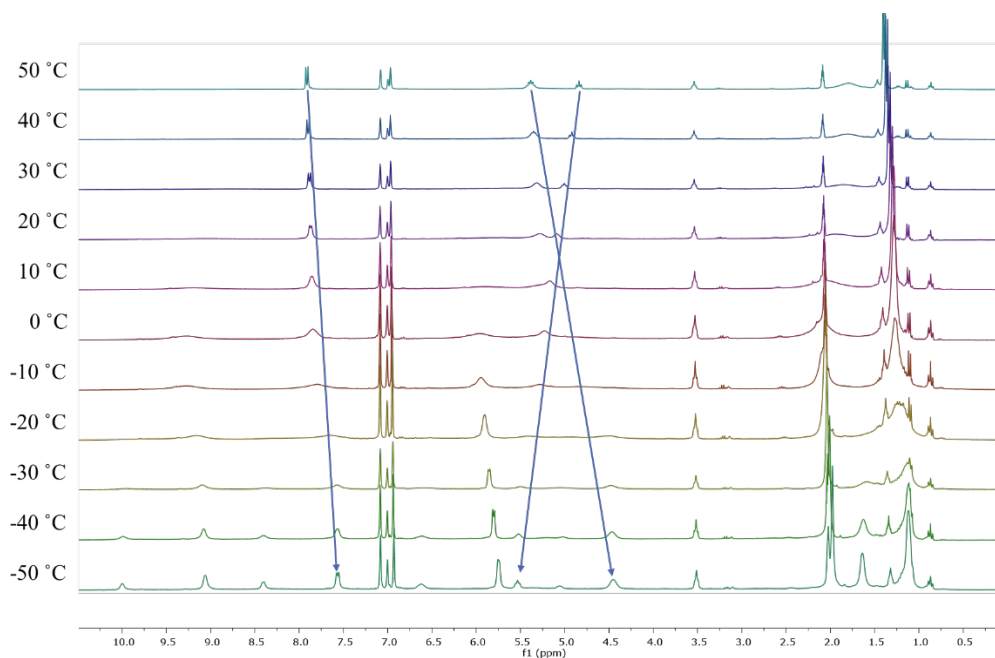
Figure 1.8 Variable temperature ^{1}H NMR spectra of **1-dmap₃** from 50 ˚C to -50 ˚C in toluene-d_8.

Initial assignment of the ^{1}H NMR spectrum at -40 ˚C was complicated by the lack of signal splitting and the temperature independent paramagnetism. However, application of 2D correlation spectroscopy (COSY) allowed for complete assignment to be made. A large resonance found at 1.11 ppm, integrating to 24H, is assigned to the axial-iPrCH₃ substituents, with the corresponding axial-iPrCH resonance at 4.47 ppm. The p-ArH and m-ArH resonances for the axial imido complex are found at 5.53 and 7.57 ppm,

respectively. A smaller signal at 1.64 ppm is assigned to the equatorial-iPrCH$_3$, integrating to 12H, which correlates to a 2H iPrCH resonance at 6.61 ppm. The resonances at 5.06 and 8.40 ppm integrating to 1H and 2H respectively are assigned to the p-ArH and m-ArH of the equatorial imido substituent. A large resonance at 2.02 ppm is assigned to the NMe$_2$ substituents of the dmap ligands. Two sets of resonances are also found further downfield, corresponding to inequivalent ArH$_{dmap}$ substituents. A large 6H resonance at 5.75 ppm is responsible for all three of the dmap-m-ArH resonances as determined by correlation spectroscopy. This resonance has two cross peaks in the spectrum; a 4H resonance at 9.06 ppm, and a 2H signal at 10.00 ppm, corresponding to the *trans*-dmap and the *cis*-dmap-*o*-ArH protons. It is reasonable to expect that the dmap ligand residing in the *trans*-position from the equatorial imido would give slightly differing shifts from those in the *cis*-position. This C$_{2v}$ symmetric conformer matches exactly the symmetry seen in the solid state, suggesting that the meridional tris(imido) complex is indeed the lower energy conformer and is not the result of some crystal packing effect.

Similar computational calculations were done for the possible complexes involving dmap as were done for **1-thf$_3$** (Figure 1.9). However, when dmap is employed as the ligand in this system, we see the bis-ligand complex being higher in energy than either of the tris-ligand conformers. Since the *mer* orientation of the imidos is significantly lower in energy than either the bis-ligand or *fac* orientation, it is reasonable that this was the observed geometry in the crystallized complex.
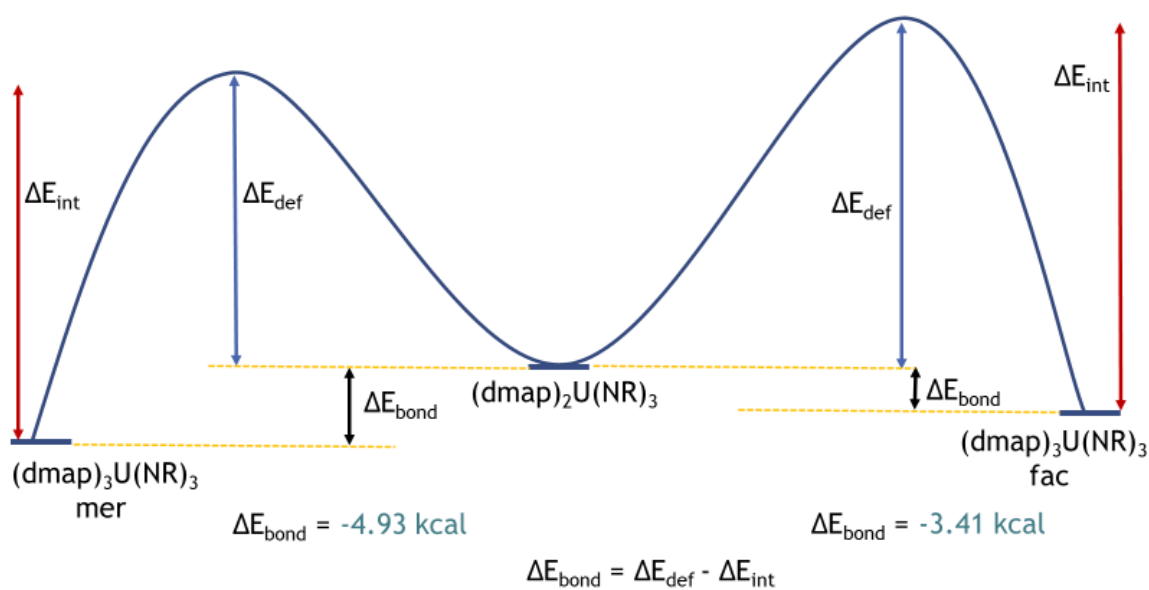
Figure 1.9 Energy diagram of three possible conformers of dmap supported U(NDipp)$_3$.

These solution- and solid-state behaviors are identical when employing bi- and tri-dentate ligands. Coordination complexes of U(NDipp)$_3$ bearing 4,4'-di-tert-butyl-2,2'-bipyridine (tBubpy) ligands and 2,2';6',2''-terpyridine (tpy), (tBubpy)$_2$U(NDipp)$_3$ (**1-tBubpy$_2$**) and (tpy)U(NDipp)$_3$ (**1-tpy**) respectively, are easily synthesized in a manner analogous to **1-dmap$_3$**. Crystallographic analysis of both **1-tBubpy$_2$** and **1-tpy** reveal the three imido substituents in a T-shaped orientation, identical to **1-dmap$_3$**. (Figure 1.10 and 1.11 respectively). For **1-tBubpy$_2$**, the two trans imido substituents, related by a bonding angle of 167.1(4)°, again show truncated U-N bond distances of 1.999(11) and 2.000(13) Å, for U1-N1 and U1-N2 respectively. The equatorial imido bond is slightly elongated, displaying a U-N bond distance of 2.090(9) Å. The orientation of the tBubpy ligands in **1-tBubpy$_2$** is very similar to what is seen for the bis-ligand U(V) bis(imido) halide complexes, (tBubpy)$_2$UX$_2$(NDipp)$_2$ (X = Cl, Br, I) synthesized by Boncella and coworkers.[13] For **1-tpy**, the trans U=N bonds (1.94(2) and 1.97(13) Å) (169(2)°) are slightly contracted with respect to the *cis*-U=N bond (2.11(4) Å). The U-N distances for the tpy ligand are on par with that of the neutral U-N bonds in **1-PDI-Dipp** and other U(VI)-N dative interactions.
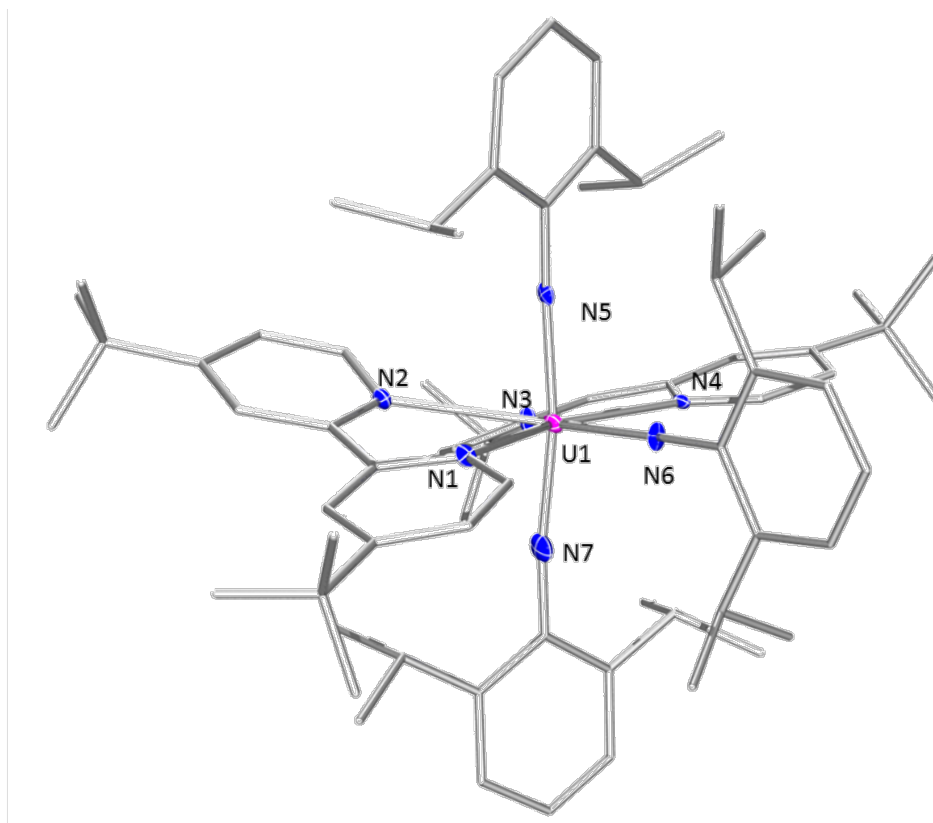
Figure 1.10 Molecular structure of **1-*t*Bubpy$_2$** with non-carbon atoms displayed as 30% probability ellipsoids. Hydrogen atoms and outer sphere solvent molecules have been omitted for clarity.

Despite bearing chelating ligands, the solution state structures of **1-*t*Bubpy$_2$** and **1-tpy** analyzed by ^{1}H NMR spectroscopy show similar (although less drastic) ligand dissociation behaviours as both **1-thf$_3$** and **1-dmap$_3$**. Even **1-tpy,** bearing the planar tridentate tpy ligand, displays only a single set of resonances corresponding to the diisopropylphenyl imido substituents at room temperature. For **1-*t*Bubpy$_2$** the ^{1}H NMR spectrum displays highly broadened resonances, with four signals corresponding to the three Dipp imido substituents. However, analogous to **1-dmap$_3$**, ^{1}H NMR spectroscopic analysis of both **1-tpy** and **1-*t*Bubpy$_2$** at low temperatures reveal C$_{2v}$ symmetric structures, in accordance with their solid-state structures.
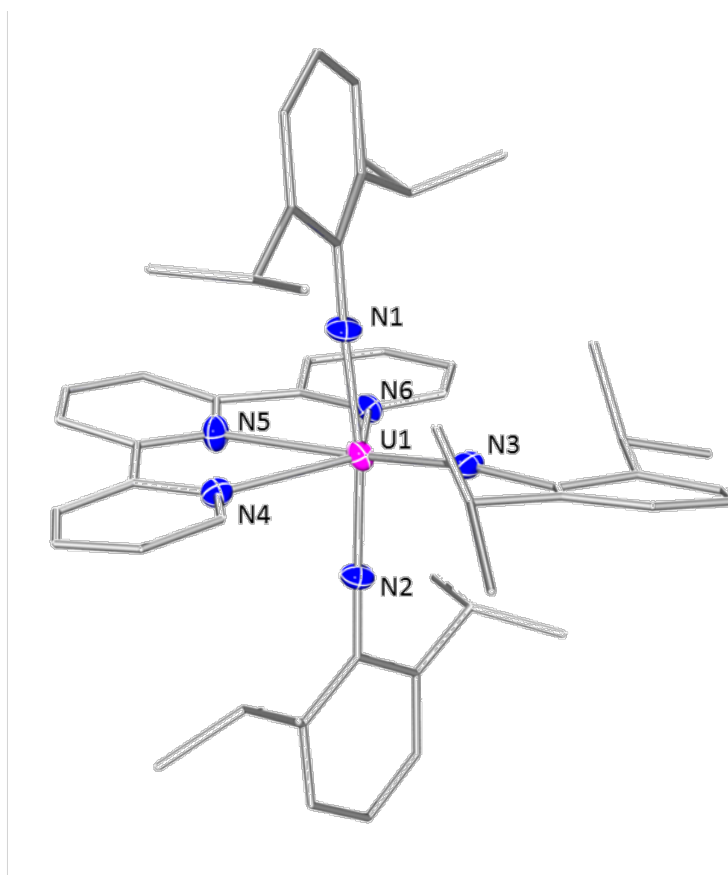
Figure 1.11 Molecular structure of **1-tpy** with non-carbon atoms displayed as 30% probability ellipsoids. Hydrogen atoms and outer sphere solvent molecules have been omitted for clarity.

In an attempt to obtain a purely (L)$_2$U(NDipp)$_3$ complex, the bulky triphenylphosphine oxide (tppo) ligand was employed, as incorporation of three tppo ligands seemed unlikely. Addition of two equivalents of triphenylphosphine oxide to a stirring solution of **1-thf$_3$**, followed by the removal of volatiles in *vacuo*, results in the isolation of (tppo)$_2$U(NDipp)$_3$ (**1-tppo$_2$**) in good yields (89%). Analysis of this complex by ^{1}H NMR spectroscopy depicts a highly symmetric product, with four signals corresponding to the Dipp moiety, and integration confirms the coordination of only two tppo ligands. Also, unlike **1-thf$_3$** and **1-dmap$_3$**, the room temperature signals observed through ^{1}H NMR spectroscopy corresponding to both the ligand and the imido substituents are quite sharp and clearly defined, indicating little fluctuation in the solution state structure. Unfortunately, structural characterization of **1-tppo$_2$** by X-ray diffraction could not be

accomplished due to the poor crystallinity of the product. However, analysis by VT ^{1}H NMR spectroscopy, reveals that **1-tppo$_2$** retains its solution state symmetry even at low temperatures, and resonances corresponding to the either the ligand or the imido substituents showing no temperature dependence, with only slight broadening of signals at low temperatures. This would indicate a solution state structure of **1-tppo$_2$** similar to that of **1-thf$_2$**, which, due to its solid-state structure, would likely display a D$_{3h}$ symmetric ^{1}H NMR spectrum. The solution and solid-state symmetry of these five coordinate complexes however provides substantial evidence for the observed symmetry of the coordinatively saturated complexes at ambient temperatures.

The ground state structures can also be noted by vibrational spectroscopy when looking at the U=N-C stretching vibrations. For complexes **1-tpy**, **1-tBubpy$_2$**, and **1-dmap$_3$** we see a single vibration that that correspond to the axial imido, 1235, 1230 and 1240 cm^{-1} respectively, and equatorial imido substituents at 1206, 1205, and 1208 cm^{-1} respectively. However, analysis of **1-tppo$_2$** by IR spectroscopy reveals only one broad U=N-C vibration at 1244 cm^{-1}.

In order to derive the nature of the bonding in these complexes for comparison, a deeper analysis of the computational calculations of these species was undertaken. To accomplish this, comparisons between **1-thf$_2$**, **1-thf$_3$**, and **1-dmap$_3$**, as well as the theoretical facial conformation of (dmap)$_3$U(NDipp)$_3$ (*fac*-**1-dmap$_3$**) and meridional conformation of **1-thf$_3$** (*mer*-**1-thf$_3$**) were analyzed.

When considering the two meridional complexes, similarities can be drawn between the calculated structures and **1-PDI-Dipp** in that molecular orbital depictions of these complexes show a high degree of competition between the three U=N bonds for uranium based orbital density. This results in many of the U=N bonding orbitals displaying contributions from all three imido nitrogens. Both *mer*-**1-thf$_3$** and **1-dmap$_3$** show a similar set of U-N bonding orbitals as were seen for **1-PDI-Dipp** with a maximum U5f orbital contributions of 19 and 20% for **mer-1-thf$_3$** (Figure 1.12) and **1-dmap$_3$** (Figure 1.13) respectively.
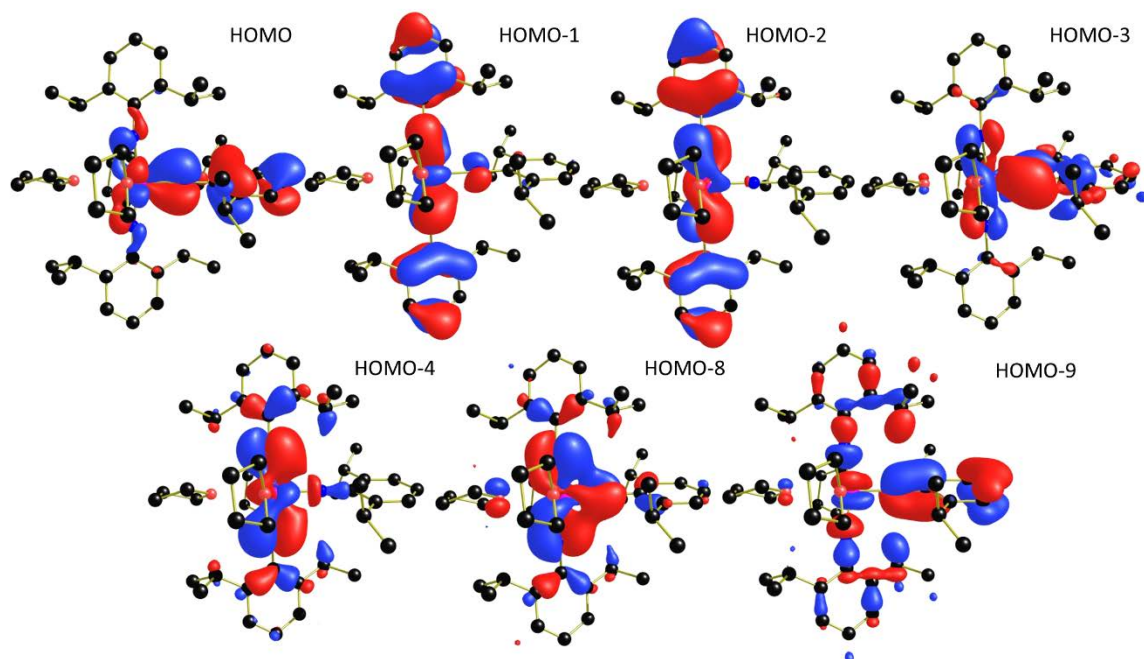
Figure 1.12 Highest occupied molecular orbitals of *mer*-**1-thf₃**.
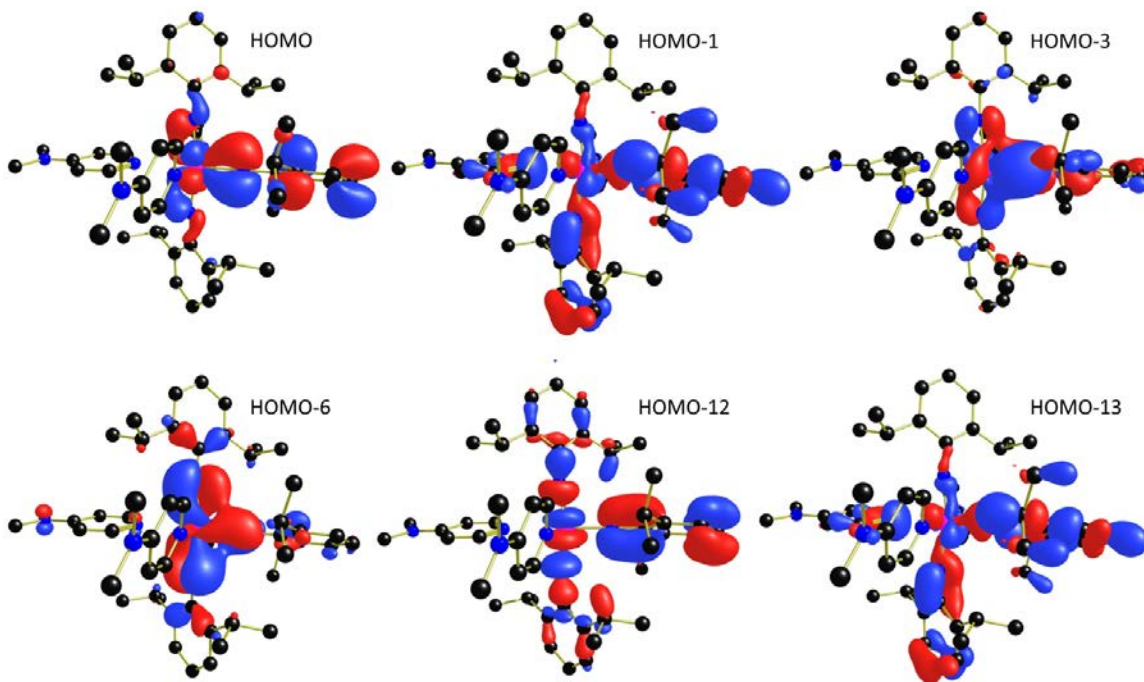
Figure 1.13 Highest occupied molecular orbitals of **1-dmap₃**.

Interestingly, **1-thf₃** (Figure 1.14) displays no purely σ-bonding orbitals, with π-bonding being the primary contributor to the U-N bond system. Also of interest, the U-N orbital contributions are slightly lower than what is noted in the meridional complexes, with the highest orbital contribution of 16%. Much like **1-PDI-Dipp**, all of the tris(imido) complexes show decreased bond orders; a feature highlighted with Nalewaski-Mrozek[19] bond orders ranging from 2.17 – 2.27, which are consistent with U-N double bonds with slight triple-bonding character.
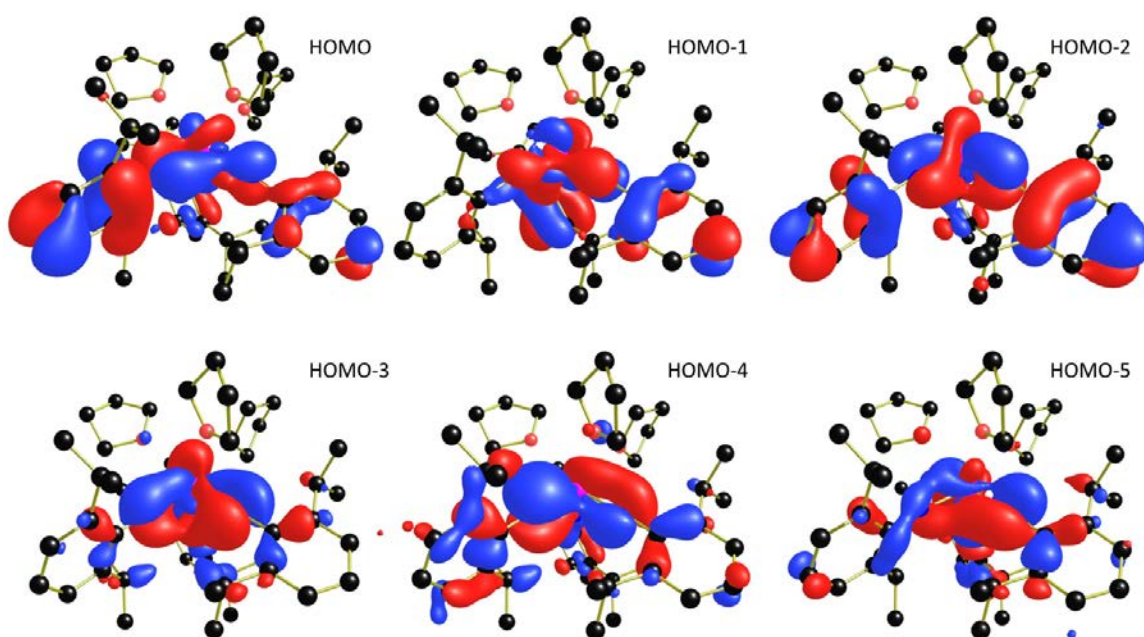
Figure 1.14 Highest occupied molecular orbitals of **1-thf₃**.

In conclusion, the coordination chemistry of the investigated molecules is based primarily on the bonding dispersion of the imido substituents and ligands. While **1-thf₃** most closely resembles transition metal analogs exhibiting a bent trigonal pyramidal structure, we have shown that substitution with any other Lewis basic ligand yields a unique t-shaped geometry. Further studies are required to investigate whether an associatie mechanism is at play in contrast to the dissociative mechanism explored through calculations.

1.3   Experimental

General Considerations: All air- and moisture-sensitive manipulations were performed by using standard Schlenk techniques or in an MBraun inert atmosphere drybox with an atmosphere of purified nitrogen. The MBraun drybox is equipped with a coldwell designed for freezing samples in liquid nitrogen as well as two -35 °C freezers for cooling samples and crystallizations. Solvents for sensitive manipulations were dried and deoxygenated by using literature procedures.[20] Benzene-d_6, toluene-d_8, and tetrahydrofuran-d_8 were purchased from Cambridge Isotope Laboratories, dried with molecular sieves and sodium, and degassed by 3 freeze–pump–thaw cycles. (THF)$_3$U(NDipp)$_3$ (**1-thf$_3$**) was prepared according to literature procedures. DMAP, *t*BuBpy, Tpy, and tppo ligands were purchased in solid form, degassed overnight on a Schlenk line, and used without further purification.

^{1}H and ^{13}C NMR spectra were recorded on a Varian Inova 300 spectrometer operating at 299.992 MHz. All chemical shifts are reported relative to the peak for SiMe$_4$, using ^{1}H and ^{13}C (residual) chemical shifts of the solvent as a secondary standard. Infrared spectra were recorded on a Thermo Nicolet 6700 FTIR spectrophotometer with a DTGS TEC detector as a solution deposition on a KBr window. Samples were stored under an inert atmosphere until transferred to the spectrometer. Electronic absorption measurements were recorded at 294 K in THF in sealed 1 cm quartz cuvettes with data collection performed on a Jasco V-6700 spectrophotometer under inert conditions.

Data for **1-dmap$_3$** were collected on a Bruker AXS APEXII CCD diffractometer featuring a fine focus sealed tube X-ray source with a plane graphite incident beam monochromator operating with Mo Kα radiation ($\lambda = 0.71073$ Å). Data for **1-thf$_2$** and **1-tpy** were collected on Bruker AXS D8 Quest diffractometer equipped with a solid state 100 cm2 Photon 100 CMOS area detector and an I-μ-S microsource X-ray tube, laterally graded multilayer (Goebel) mirror for monochromatization and also operating with Mo Kα radiation ($\lambda = 0.71073$ Å). Data for **1-tBubpy$_2$** were collected on a Bruker AXS X8 Prospector CCD diffractometer featuring an I-μ-S microsource X-ray tube with a laterally graded multilayer (Goebel) mirror for monochromatization and operating with Cu Kα radiation ($\lambda = 1.54184$ Å). All instruments were equipped with Oxford Cryostream low temperature devices. Single crystals for X-ray diffraction were coated with

poly(isobutylene) oil in a glovebox and mounted on a Mitegen micromesh mount and quickly transferred to the goniometer head into the 100 K coldstream of the diffractometer. Initial unit cells were determined, data collection strategies set up and frames collected using APEX2,[21] processed using SAINT,[22] and the files scaled and corrected for absorption using SADABS[23] or TWINABS.[24] The space groups were assigned and the structures were solved by direct methods using XPREP within the SHELXTL suite of programs[25,26] and refined by full matrix least squares against F^2 with all reflections using Shelxl2014[23] and the graphical interface Shelxle.[27] If not specified otherwise H atoms attached to carbon atoms were positioned geometrically and constrained to ride on their parent atoms, with carbon hydrogen bond distances of 0.95 Å for alkene and aromatic C-H, 1.00, 0.99 and 0.98 Å for aliphatic C-H, CH_2 and CH_3 moieties, respectively. Methyl H atoms were allowed to rotate but not to tip to best fit the experimental electron density. $U_{iso}(H)$ values were set to a multiple of $U_{eq}(O/C/N)$ with 1.5 for CH_3 and OH, and 1.2 for C-H, CH_2 and N-H units, respectively. Additional details relating to disorder and twinning are given for each structure in their crystallographic experimental details sections, below.

Synthesis of (dmap)₃U(NDipp)₃ (1-dmap₃). A 20 mL scintillation vial was charged with a single equivalent of **1-thf₃** (0.100 g, 0.102 mmol), three equivalents of N,N-dimethylaminopyridine (0.037 g, 0.306 mmol), and 5 mL toluene. The reaction was stirred for 20 minutes, after which time the volatiles were removed *in vacuo.* The leftover brown material was washed with pentane and the resulting solid (yield: 0.105 g, 0.092 mmol, 91%) was identified as (dmap)₃U(NDipp)₃ (**1-dmap₃**). ^{1}H NMR (300 MHz, 20 °C, C_6D_6): δ = 1.40 (d, ^3J(H,H) = 6 Hz, 36H, *i*Pr-C*H₃*), 1.95 (vbs, 18H, dmap-C*H₃*), 5.19 (bs, 3H, *p*-Ar-

H), 5.41 (bs, 6H, m-Ar-*H*), 5.79 (vbs, 6H, dmap-Ar-*H*), 7.99 (d, ^3J(H,H) = 6 Hz, 6H, *m*-Ar-*H*), 9.20 (vbs, 6H, dmap-Ar-*H*); ^{1}H NMR (300 MHz, 50 ºC toluene-*d*$_8$): δ = 1.44 (d, ^3J(H,H) = 6 Hz, 36H, *i*Pr-C*H*$_3$), 1.81 (vbs, 18H, dmap-C*H*$_3$), 4.84 (bs, 3H, *p*-Ar-*H*), 5.39 (bs, 6H, *i*PrC*H*), 7.92 (d, ^3J(H,H) = 6 Hz, 6H, *m*-Ar-*H*); ^{1}H NMR (300 MHz, -50 ºC toluene-*d*$_8$): δ = 1.23 (s, 24H, *trans-i*Pr-C*H*$_3$), 1.75 (s, 12H, *cis-i*Pr-C*H*$_3$), 2.14 (s, 18H, dmap-C*H*$_3$), 4.57 (s, 4H, *trans-i*PrC*H*), 5.17 (s, 1H, *cis-p*-Ar-*H*), 5.64 (s, 2H, *trans-p*-Ar-*H*), 5.87 (s, 6H, dmap-Ar-*H* x 2), 6.73 (s, 2H, *cis-i*PrC*H*), 7.68 (s, 4H, *trans-m*-Ar-*H*), 8.51 (s, 2H, *cis-m*-Ar-*H*), 9.17 (s, 4H, *trans*-dmap-Ar-*H*), 10.11 (s, 4H, *cis*-dmap-Ar-*H*); analysis (calcd., found for C$_{57}$H$_{81}$N$_9$U): C (60.57, 60.34), H (7.22, 7.55), N (11.15, 10.89).

Figure 1.15 2D COSY spectrum of **1-dmap$_3$** in toluene-*d*$_8$ at -40 ˚C.

Table 1.2. Selected experimental bond metrics for **1–dmap₃** and calculated bond metrics for both *fac-* and *mer-* isomers of **1–dmap₃**.

(dmap)₃U(NDIPP)₃			
	Expt.	Calculated *fac*	Calculated *mer*
Bond	Distance (Å)		
U1-N1	2.005(5)	1.988	2.012
U1-N2	1.974(4)	2.002	2.013
U1-N3	2.028(4)	2.013	2.015
U1-N4	2.573(4)	2.607	2.720
U1-N6	2.698(5)	2.746	2.713
U1-N8	2.555(6)	2.593	2.716
Bond	Degree (°)		
N1-UI-N2	168.33(18)	167.10	104.14
N1-UI-N3	95.81(18)	96.60	103.90
N2-UI-N3	95.84(17)	96.28	103.65
N4-UI-N6	83.66(18)	83.66	82.74
N4-UI-N8	166.22(17)	162.22	83.11
N6-UI-N8	82.79(18)	82.79	83.09
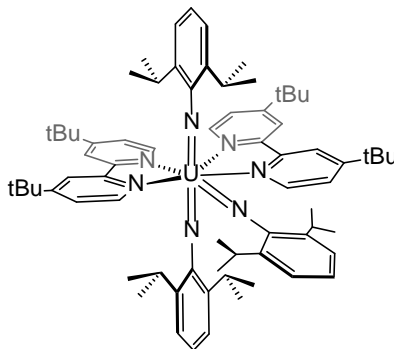
Synthesis of (*t*Bubpy)₂U(NDIPP)₃ (1-*t*Bubpy₂). A 20-mL scintillation vial was charged with one equivalent of **1-thf₃** (0.100 g, 0.102 mmol), two equivalents of 4,4'-di-*tert*-butyl-2,2'-bipyridine (0.054 g, 0.204 mmol), and 5 mL diethyl ether. The reaction was stirred for 20 minutes, after which time the volatiles were removed *in vacuo.* The leftover dark brown material was washed with pentane and the remaining solid (yield: 0.117 g, 0.090 mmol, 88%) was identified as (*t*Bubpy)₂U(NDIPP)₃ (**1-*t*Bubpy₂**). In ^{1}H NMR analysis rings pointing towards the equatorial imido are classified as bpyA and rings pointing towards each other are bpyB. ^{1}H NMR (300 MHz, 20 ℃ toluene-d_8): δ = 0.67 (bs, 36H, *i*Pr-C*H₃*), 1.16 (s, 36H, bpy-*t*Bu), 3.71 (bs, 6H, *i*PrC*H*), 5.03 (bs, 3H, *p*-Ar-*H*), 6.89 (s, 6H, *m*-Ar-*H*), 7.33 (bs, 2H, bpy-Ar*H*), 8.53 (s, 4H, bpy-Ar*H*), 10.29 (s, 2H, bpy-Ar*H*), 10.43 (s, 4H, bpy-Ar*H*); ^{1}H NMR (300 MHz, 50 ℃ toluene-d_8): δ = 0.89 (bs, 36H, *i*Pr-C*H₃*), 1.19 (s, 36H, bpy-*t*Bu), 4.81 (bs, 6H, *i*PrC*H*), 5.01 (bs, 3H, *p*-Ar-*H*), 7.68 (s, 6H, *m*-Ar-*H*), 8.52 (s, 4H, bpy-Ar*H*), 10.13 (s, 4H, bpy-Ar*H*), 10.75 (s, 4H, bpy-Ar*H*); ^{1}H NMR (300 MHz, -50 ℃ toluene-d_8): δ = 0.60 (d, ^3J(H,H) = 6 Hz, 12H, *trans-i*Pr-C*H₃*), 0.91 (d, 12H, ^3J(H,H) = 6 Hz, *trans-i*Pr-C*H₃*), 1.09 (s, 18H, bpyB-tBu), 1.15 (s, 18H, bpyA-tBu), 1.58 (d, ^3J(H,H) = 6 Hz, 12H, *cis-i*Pr-C*H₃*), 3.67 (sept, ^3J(H,H) = 6 Hz, 4H, *trans-i*PrC*H*), 4.81 (t, ^3J(H,H) = 9 Hz, 1H, *cis-p*-Ar-*H*), 5.28 (t, ^3J(H,H) = 9 Hz, 2H, *trans-p*-Ar-*H*), 6.56 (d, 2H, bpyB-Ar*H*), 6.77 (d, 2H, bpyA-Ar*H*), 7.14 (s, 2H, *cis-i*PrC*H*), 7.41 (d, 4H, *trans-m*-Ar-*H*), 8.52 (s, 2H, bpyB-Ar*H*), 8.59 (s, 2H, bpyA-Ar*H*), 8.74 (d, 2H, *cis-m*-Ar-*H*), 9.47 (d, 2H, bpyB-Ar*H*), 10.84 (d, 2H, bpyA-Ar*H*).
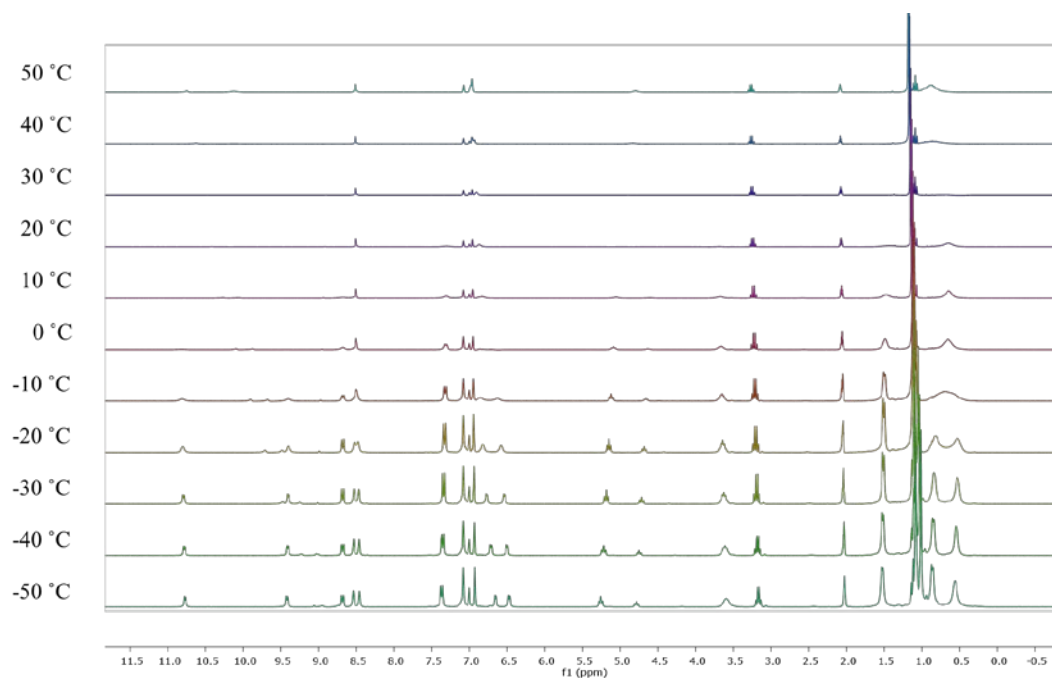
Figure 1.16 Variable temperature ^{1}H NMR spectra of **1-tBuBpy$_2$** from 50 ˚C to -50 ˚C in toluene-d_8.
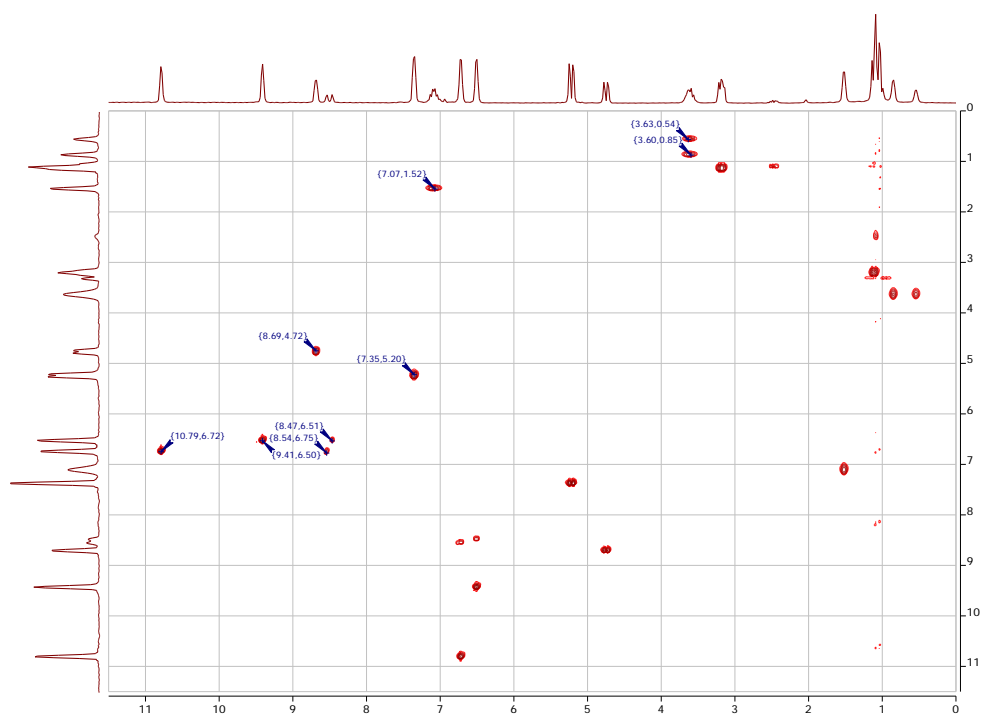
Figure 1.17 2D COSY spectrum of **1-tBuBpy$_2$** in toluene-d_8 at -50 ˚C.
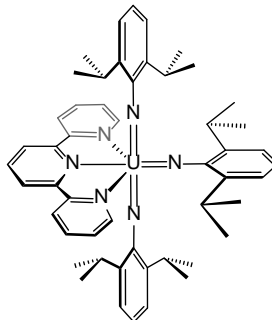
Synthesis of (tpy)U(NDipp)$_3$ (1-tpy). A 20-mL scintillation vial was charged with a single equivalent of **1-thf$_3$** (0.100 g, 0.102 mmol) and dissolved in diethylether. To this was added a single equivalent of 2,2';6'2"-terpyridine (0.024 g, 0.102 mmol) and this solution was stirred for 1 hour. After this time, the volatiles were removed *in vacuo* and the remaining dark black solid (yield: 0.097 g, 0.097 mmol, 96 %) was collected. ^{1}H NMR (300 MHz, CD$_2$Cl$_2$, 25 ºC, TMS): δ = 0.94 (d, [3]*J*(H,H) = 9Hz, 36H), 4.49 (bs, 6H), 4.76 (bs, 3H), 7.30 (d, [3]*J*(H,H) = 6 Hz, 4H), 7.82 (t, [3]*J*(H,H) = 6 Hz, 2H), 8.22 (t, [3]*J*(H,H) = 6 Hz, 2H), 8.40 (t, [3]*J*(H,H) = 6 Hz, 1H) 8.45 (d, [3]*J*(H,H) = 6 Hz, 2H), 8.53 (d, [3]*J*(H,H) = 6 Hz, 2H), 9.51 (d, [3]*J*(H,H) = 6 Hz, 2H); ^{1}H NMR (300 MHz, thf-*d$_8$*, 30 ºC, TMS) δ = 0.88 (d, [3]*J*(H,H) = 6Hz, 36H), 4.61 (bs, 9H), 7.23 (d, [3]*J*(H,H) = 6 Hz, 4H), 7.95 (m, 2H), 8.36 (m, 2H), 8.51 (t, 1H), 8.73 (m, 2H), 8.80 (m, 2H), 9.66 (d, 2H); ^{1}H NMR (300 MHz, thf-*d$_8$*, -50 ºC, TMS): δ = 0.48 (d, [3]*J*(H,H) = 6Hz, 24H, *trans-i*PrCH$_3$), 1.10 (d, [3]*J*(H,H) = 6Hz, 12H *cis-i*PrCH$_3$), 3.91 (bs, 5H, both *trans-i*PrCH and *cis-p*-ArH), 4.77 (t, [3]*J*(H,H) = 9Hz, 2H, *trans-p*-ArH), 6.76 (bs, 2H, *cis-i*PrCH), 6.96 (d, [3]*J*(H,H) = 6Hz, 4H, *trans-m*-ArH), 7.99 (d, [3]*J*(H,H) = 9Hz, 2H, *cis-m*-ArH), 8.01 (m, 2H), 8.43 (bs, 2H), 8.58 (bs, 1H), 8.89 (bs, 4H), 10.22 (bs, 2H).
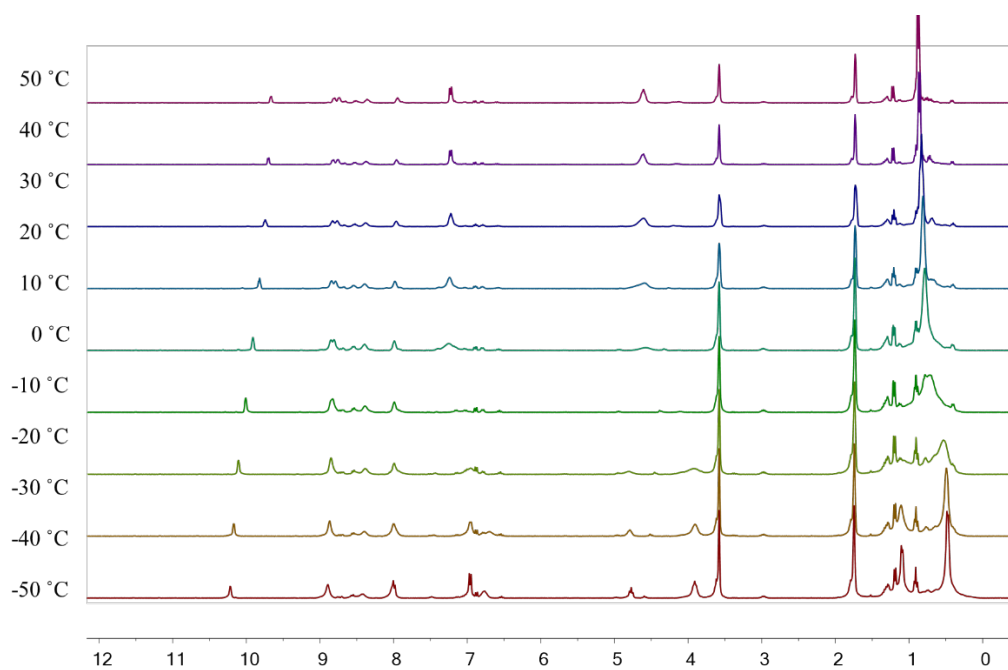
Figure 1.18 Variable temperature ^{1}H NMR spectra of **1-tpy** from 50 ˚C to -50 ˚C in toluene-d_8.
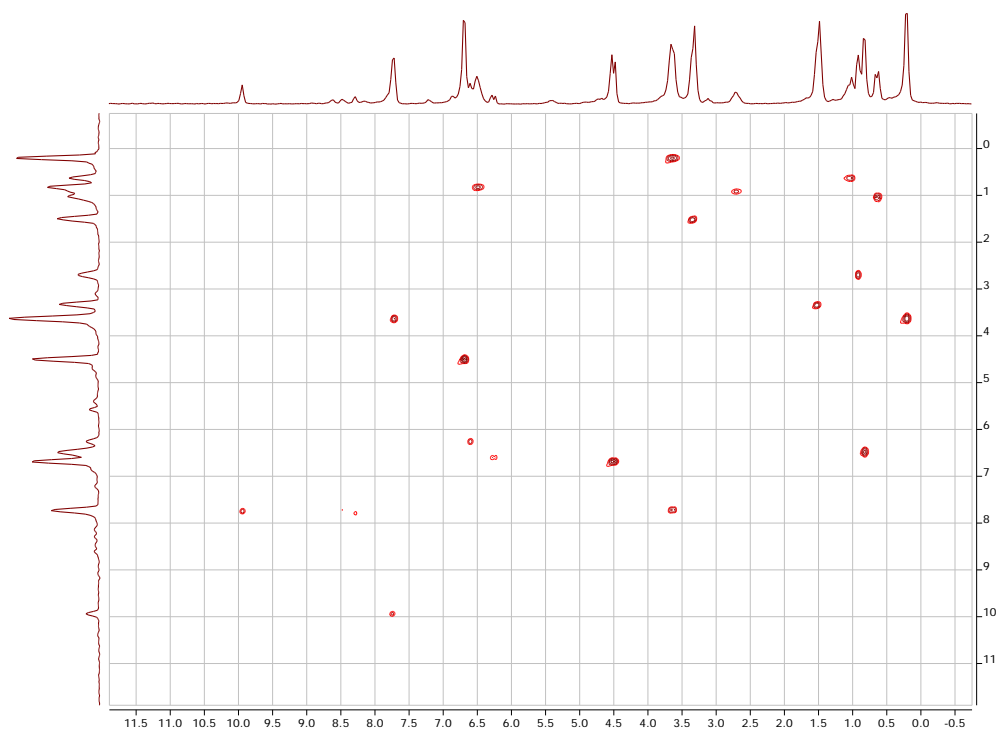
Figure 1.19 2D COSY spectrum of **1-tpy** in toluene-d_8 at -50 ˚C.

Crystallization of (thf)₂U(NDIPP)₃ (1-thf₂). Crystals suitable for analysis by X-Ray diffraction analysis were grown from a concentrated solution of **1-** in toluene/pentane. Crystallization was aided by complexation with PMe₃.

Table 1.3 Selected experimental bond metrics and calculated bond metrics for **1-thf₂**

(thf)₂U(NDIPP)₃		
	Expt.	*Calc.*
Bond	**Distance (Å)**	
U1-N1	1.998(5)	1.995
U1-N2	1.974(4)	1.966
U1-N3	2.028(4)	1.977
U1-O1	2.573(4)	2.411
U1-O2	2.698(5)	2.457
Bond	**Degree (°)**	
N1-UI-N2	149.48(10)	149.5
N1-UI-N3	108.98(10)	109.0
N2-UI-N3	101.46(10)	101.5
O1-UI-O2	156.99(8)	157.0
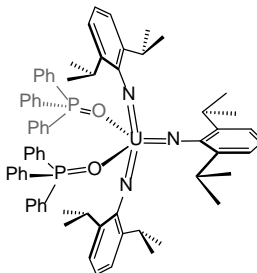
Synthesis of (Ph$_3$PO)$_2$U(NDipp)$_3$ (1-tppo$_2$). A 20-mL scintillation vial was charged with one equivalent of **1-thf$_3$** (0.100 g, 0.102 mmol), two equivalents of triphenlyphosphine oxide (0.035 g, 0.204 mmol), and 5 mL toluene. The reaction was stirred for 20 minutes, after which time the volatiles were removed *in vacuo* and the leftover powdery brown material was analyzed by ^{1}H NMR spectroscopy showing pure (Ph$_3$PO)$_2$U(NDipp)$_3$ (**1-tppo$_2$**) (yield: 0.120 g, 0.09 mmol, 89%). ^{1}H NMR (300 MHz, 25 ℃, C$_6$D$_6$): δ = 1.35 (d, ^3J(H,H) = 6 Hz, 36H, *i*Pr-C*H*$_3$), 4.02 (t, ^3J(H,H) = 6 Hz, 3H, *p*-Ar-*H*), 5.73 (sept., ^3J(H,H) = 6 Hz, 6H, *i*PrC*H*), 6.92 (m, 9H, Ph$_3$PO), 8.35 (m, 6H, Ph$_3$PO), 8.37 (d, ^3J(H,H) = 6 Hz, 6H, *m*-Ar-*H*), ^{1}H NMR (300 MHz, 25 ℃, toluene-*d$_8$*): δ = 1.29 (d, ^3J(H,H) = 6 Hz, 36H, *i*Pr-C*H*$_3$), 3.94 (t, ^3J(H,H) = 6 Hz, 3H, *p*-Ar-*H*), 5.66 (sept., ^3J(H,H) = 6 Hz, 6H, *i*PrC*H*), 6.98 (m, 9H, Ph$_3$PO), 7.99 (m, 6H, Ph$_3$PO), 8.29 (d, ^3J(H,H) = 6 Hz, 6H, *m*-Ar-*H*), ^{1}H NMR (300 MHz, 50 ℃, toluene-*d$_8$*): δ = 1.26 (d, ^3J(H,H) = 6 Hz, 36H, *i*Pr-C*H*$_3$), 3.88 (t, ^3J(H,H) = 6 Hz, 3H, *p*-Ar-*H*), 5.64 (sept., ^3J(H,H) = 6 Hz, 6H, *i*PrC*H*), 6.98 (m, 9H, Ph$_3$PO), 7.98 (m, 6H, Ph$_3$PO), 8.27 (d, ^3J(H,H) = 6 Hz, 6H, *m*-Ar-*H*), ^{1}H NMR (300 MHz, -40 ℃, toluene-*d$_8$*): δ = 1.34 (s, 36H, *i*Pr-C*H*$_3$), 4.00 (bs, 3H, *p*-Ar-*H*), 5.62 (bs., 6H, *i*PrC*H*), 6.85 (s, 9H, Ph$_3$PO), 7.96 (s, 6H, Ph$_3$PO), 8.35 (s, 6H, *m*-Ar-*H*), (analysis (calcd., found for C$_{72}$H$_{81}$N$_3$P$_2$UO$_2$): C (65.49, 64.96), H (6.18, 5.84), N (3.18, 2.98).

CHAPTER 2.   SYNTHESIS OF MIXED TRIS(IMIDO) URANIUM COMPLEXES

2.1   Introduction

Uranium tris(imido) species bearing *trans*-imidos are desirable synthons as they can be used to mimic reactivity of more complicated uranium oxide polymeric systems. Such systems are advantageous as they are easily soluble in organic solvents, making them amenable to standard characterization methods and ligand substitution strategies. Our group has previously shown that uranium tris(imidos), easily synthesized from [(^Mes^PDI^Me^)U(THF)]$_2$ and various azides, feature axial imido substituents exhibiting differing bond characteristics than the adjacent equatorial imido substituent.[1] The aim of this work is to show that multiple analogues of mixed imido products can be formed from either the aforementioned dimer or stable tris(imido) synthons by exploiting reactivity differences between the axial and equatorial positions.

It is well known that the stabilization of UO_2^{2+} comes from the inverse trans influene (ITI) and features strong uranium-oxygen bonds which are notoriously difficult to functionalize.[9] Because of this influence, any ligands which reside in the equatorial plane are labile and exchangeable. However, studying this molecule in organic solvents is complicated by its insolubility. Since imido ligands are isoelectronic with oxo ligands yet exhibit significantly better solubility, crystallinity, and are less prone to polymerization, they are ideal for studying the reactivity of these types of molecules.

The previous chapter discusses the differences between the energy levels of *mer-* and *fac-* tris(imido) uranium complexes. A noticeable difference is seen when the imidos are in the mer- coordination form between the bond distances of the equatorial and axial imidos. When considering the ITI, it is reasonable to attribute the shortening of the axial imido bonds to uranium stabilization, thus suggesting that the equatorial bond is weaker and, therefore, more labile. Previous studies in our group, as well as others, have shown that mono- and bis-imidos can undergo multiple bond metathesis[23–37] as well as protonolysis[14,33,43–46] reactions whereby the imido substituent is exchanged with another moiety. The intended purpose of this project was to show that similar methods could be

employed to exchange the equatorial imido of uranium tris(imido) complexes with other imidos. The following chapter details the progressions towards proving this concept.

2.2   Results and Discussion

There are three proposed ways in which uranium mixed tris(imido) complexes could be synthesized: 1) direct synthesis from the reduced PDI-U dimer, 2) multiple-bond metathesis with carbodiimides, and 3) protonolysis with anilines (Scheme 2.1).
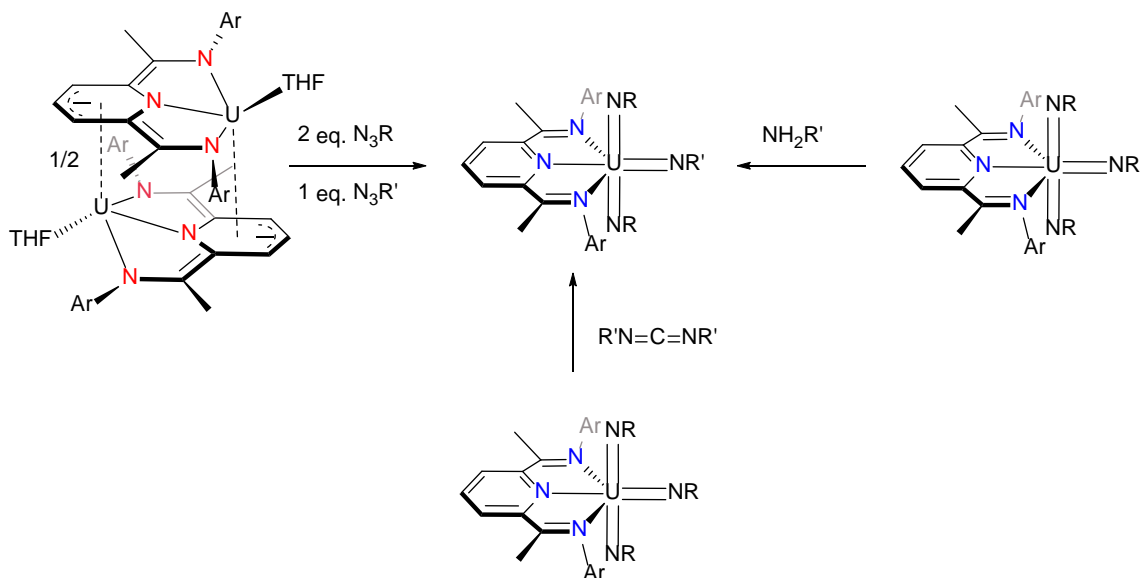
Scheme 2.1 Possible synthetic pathways towards mixed uranium tris(imidos).

The first pathway towards a mixed uranium tris(imido) begins with the aforementioned uranium PDI dimer. Through mixing a solution of the dimer with a solution of Dipp and Mes azides in a 2:1 ratio, an immediate effervescence is observed, and the resulting product is the desired mixed imido (Scheme 2.2). It should be noted that despite the possibility of six different products, only one product is formed and in excellent yield. These six separate products could represent both formations of homo tris(imidos), homo axial imidos with a differing equatorial imido, and mixed axial imidos with either substituent in the equatorial position (Figure 2.1). Regardless of whether this reaction was carried out such that the azides were first mixed together then added to the dimer, or

whether one azide was added before the other, the major product of the reaction remained the same. It was noted, however, that pre-mixing the azides before addition resulted in a slightly higher yield and purification by recrystallization was simplified.
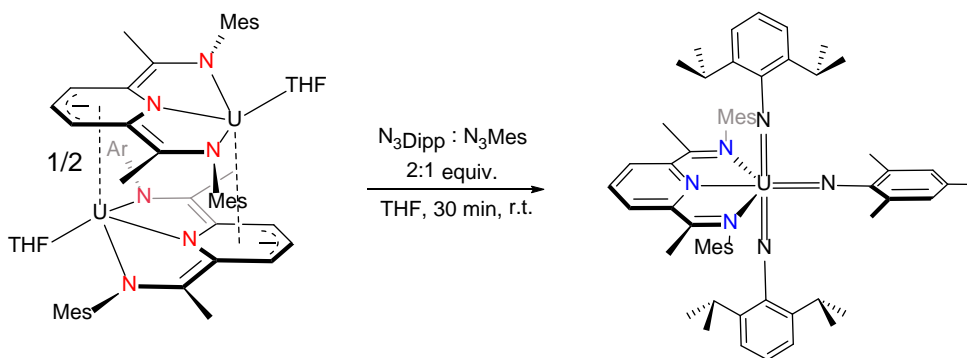
Scheme 2.2 First synthetic route towards mixed tris(imidos).
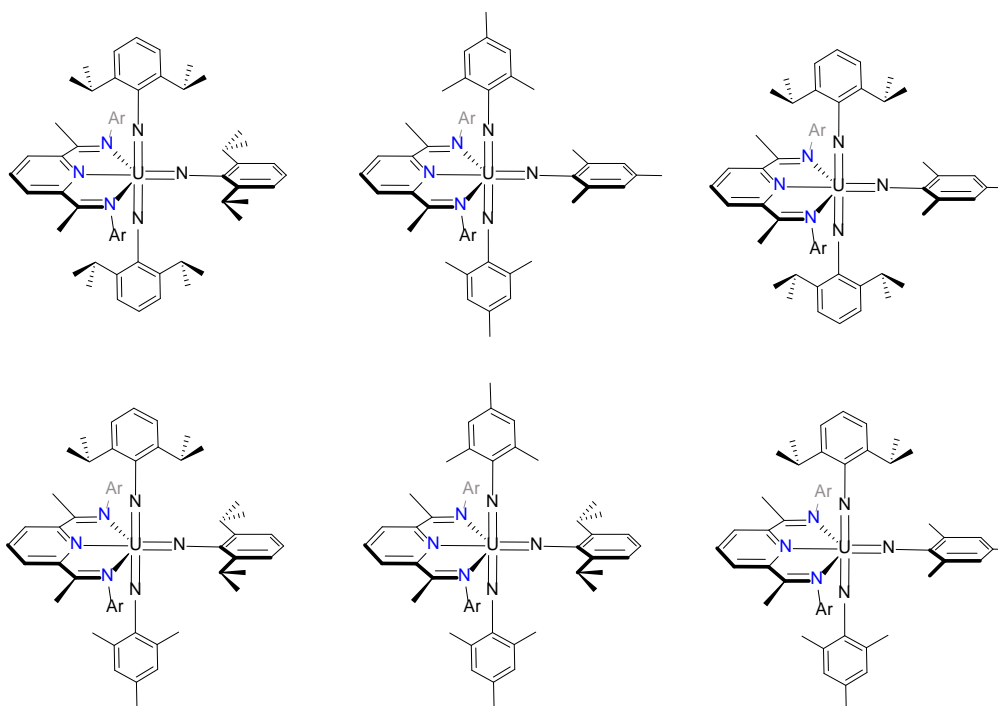
Figure 2.1 All possible products from Scheme 2.2.

NMR spectroscopy of the final product reveals resonances which initially suggest three unique imidos. There are two septets in drastically different chemical environments, therefore it is reasonable to presume that there are two DIPP imidos, one in the equatorial position, and the other in the axial position. There are also signature resonances of the MES imido which are shifted from the previously published homo-MES tris(imido). However, when single crystals of this product are grown and analyzed from a concentrated solution of THF and pentane, it is apparent that the, originally desired, mixed complex (**PDI-U-(NDipp)₂(NMes)**) has been formed (Figure 2.2)
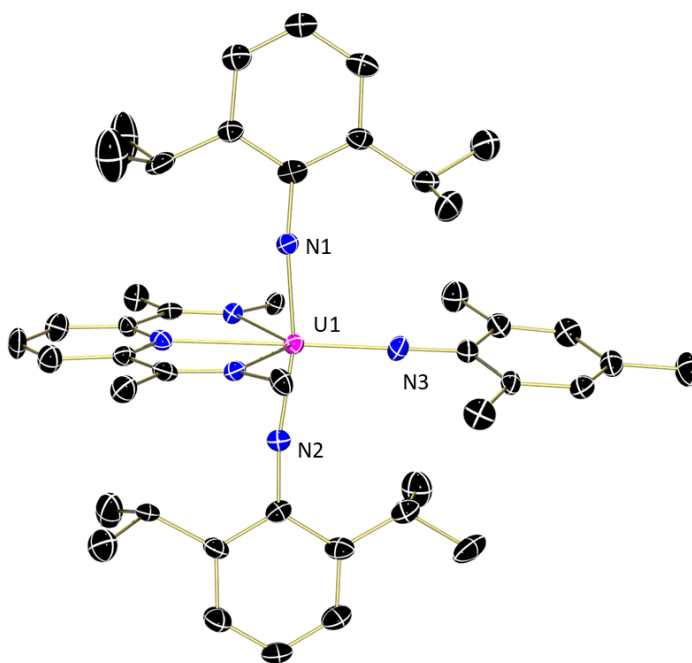
Figure 2.2 Molecular structure of **PDI-U-(NDipp)₂(NMes)** shown at 30% probability ellipsoids. Hydrogen atoms, PDI mesityl groups, and co-crystallized solvent atoms have been omitted for clarity.

Further analysis of the crystal structure reveals why the initial ^{1}H NMR spectroscopic study was misleading. Due to the steric bulk of the PDI mesityl groups coupled with the di-isopropyl phenyl imido groups, rotation of the imido substituents is

limited leading to different chemical environments of the isopropyl groups on either side of the diisopropyl phenyl rings. Analysis of the bond lengths between the tris(Dipp), tris(MES), and mixed product show little differences (Table 2.1). All three of the structures show significant bond elongation along the equatorial imido bond, although the mixed species does also exhibit elongation of one of the axial imidos.

Table 2.1 Comparison of imido bond distances between homo tris(imidos) and the synthesized mixed tris(imido).

	U-N1	U-N2	U-N3
PDI-U(NDipp)$_3$	1.967(7) □	1.965(7) □	2.022(8) □
PDI-U(NMes)$_3$	1.992(5) □	1.992(5) □	2.024(5) □
PDI-U(NDipp)$_2$(NMes)	1.997(7) □	1.967(7) □	2.027(8) □

After discovering the peculiarity of the single product formation, investigations began on the reduction potential of the azides. Electrochemical studies done by Adharsh Raghavan show that azides bearing more aliphatic/donating substituents are poorer oxidants than those bearing more electron withdrawing substituents (Table 2.2). Based on the observations from the aforementioned experiment and the observed reduction potentials, it was hypothesized that mixed imidos could be constructed when two equivalents of a more oxidizing azide were combined with one equivalent of poorer oxidizing azide. In order to test this hypothesis, an experiment was devised whereby two equivalents of Dipp azide would be combined with one equivalent of DETP (diethylphenyl) azide as the difference in reduction potential between the two azides was 0.196 V (Scheme 2.3).

Table 2.2 Table showing the reduction potentials of multiple available azides from poorest oxidant (most electron donating group) to best oxidant (most electron withdrawing group).

$$R-N=\overset{+}{N}=\overset{-}{N} + 2e^- \longrightarrow R-N^{2-} + N_2$$

Azide	Reduction potential (V)
Adamantyl (Ad)	-3.195
Benzyl (Bn)	-3.015
2,6-diisopropyl (Dipp)	-2.942
2,4,6-trimethyl (Mes)	-2.816
2,6-diethyl (Detp)	-2.746
4-methyl (pTol)	-2.671

Poorer oxidant

Better oxidant
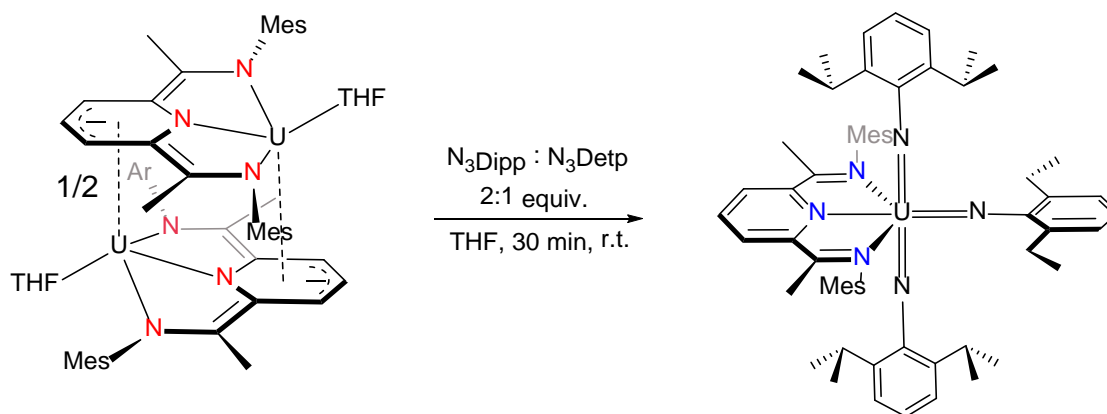
Scheme 2.3 Synthetic scheme for **PDI-U-(NDipp)₂(NDetp)**.

In keeping with the previous and hypothesized results, a single product was formed through the reaction of Dipp and Detp azides in THF at room temperature over the course of 30 minutes and was assigned as **PDI-U-(NDipp)₂(NDetp)** (Figure 2.4). Analysis with ^{1}H NMR spectroscopy shows similar signals as those seen in **PDI-U-(NDipp)₂(NMes)**. Unlike **PDI-U-(NDipp)₂(NMes)**, **PDI-U-(NDipp)₂(NDetp)** shows no significant axial bond lengthening along either of the imido bonds, although the bond lengths are elongated from either of the homo tris(imido) complexes (Table 2.3).
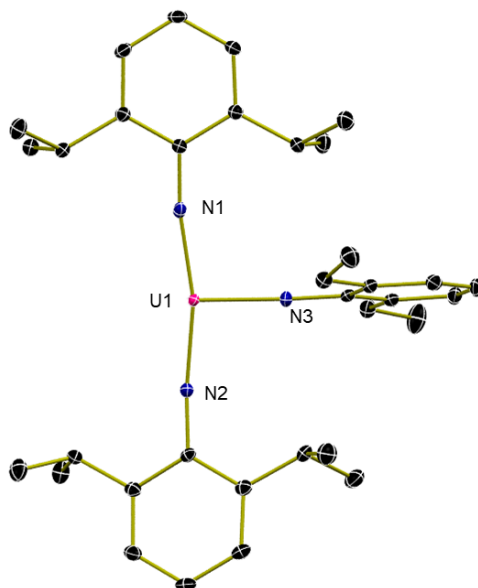
Figure 2.3 Crystal structure of **PDI-U-(NDipp)₂(NDetp)** shown at 30% probability ellipsoids. Hydrogen atoms, PDI ligand, and co-crystallized solvent atoms have been omitted for clarity.

Table 2.3 Comparison of imido bond distances between homo tris(imidos) and the synthesized mixed tris(imido).

	U-N1	U-N2	U-N3
PDI-U(NDipp)$_3$	1.967(7) Å	1.965(7) Å	2.022(8) Å
PDI-U(NDetp)$_3$	1.970(7) Å	1.900(7) Å	2.030(7) Å
PDI-U(NDipp)$_2$(NDetp)	1.987(3) Å	1.988(3) Å	2.033(3) Å

With two mixed tris(imido) compounds fully characterized, efforts began on the synthesis of all varieties of homo tris(imidos). With these compounds in hand, full analysis via NMR spectroscopy would provide all of the necessary information to do preliminary solution state characterization. Unfortunately, synthesis of PDI-U(N*p*Tol)$_3$ from the PDI dimer resulted in an NMR spectrum which only showed free PDI ligand. Likewise, all attempts to characterize this molecule via crystallization resulted in crystals of free PDI. It has been reasoned that the PDI ligand is lost from the compound due to the highly oxidizing nature of the *p*Tol imido. Without the ligand to stabilize the geometry of the complex, a lack of structural stability causes loss of NMR signal similar to what is observed in Chapter 1.

Although the synthesis of **PDI-U-(N*p*Tol)$_3$** did not work as planned, synthesis of a mixed species containing the *p*Tol imido were still attempted from the reduced PDI-uranium dimer. With a difference of reduction potential of 0.271 V between the Dipp and *p*Tol azides, synthesis of **PDI-U-(NDipp)$_2$(N*p*Tol)** was most likely to yield an appreciable result (Scheme 2.4). When four equivalents of Dipp azide were combined with two equivalents of pTol azide then added to the PDI-uranium dimer an immediate effervescence was observed. Although single crystals of the product were not isolated, a clean ^{1}H NMR spectrum was produced which clearly shows resonances attributable to two Dipp imido substituents as well as a single *p*Tol imido. The NMR spectrum also shows a significant quantity of the free PDI ligand. This is unsurprising as this ligand resides in the equatorial plane *trans* to the more oxidizing *p*Tol imido.
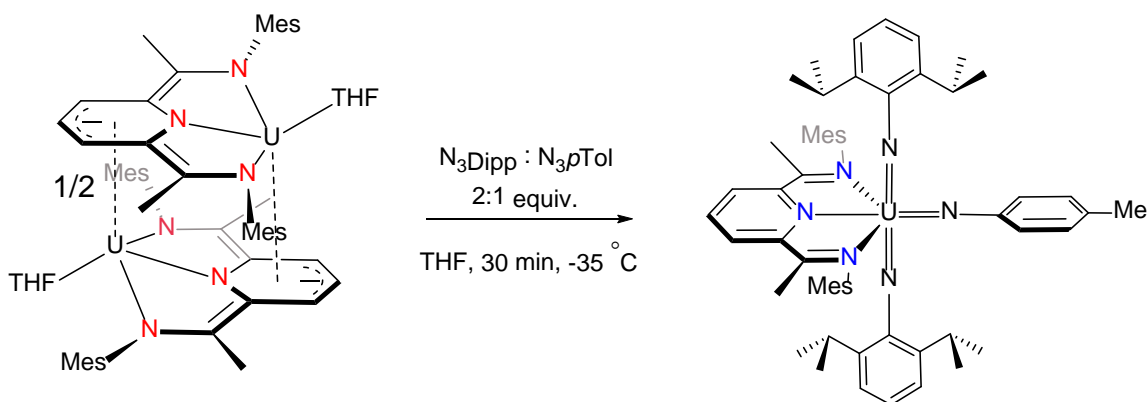
Scheme 2.4 Synthetic scheme for **PDI-U-(NDipp)₂(N*p*Tol)**.

Since the synthesis of **PDI-U-(NDipp)₂(N*p*Tol)** was successful, synthesis of other mixed imidos with the equatorial *p*Tol imido were attempted. The synthesis of these molecules was desired because the products could later be matched to those made through protonolysis as the *p*Tol-aniline would be the most reactive of the available anilines. However, synthesis of **PDI-U-(NMes)₂(N*p*Tol)** via the route shown in Scheme 2.5 resulted only in a small quantity of PDI-U(NMes)₃ and a large quantity of free PDI detectable by ^{1}H NMR spectroscopy. In contrast to this result, when the synthesis of **PDI-U-(NDetp)₂(N*p*Tol)** was attempted via a similar route, a large quantity of unreacted diethylphenyl azide was observed along with free PDI. It is believed that both routes resulted in the primary formation of *p*Tol tris(imido) with multiple other side products made as well.
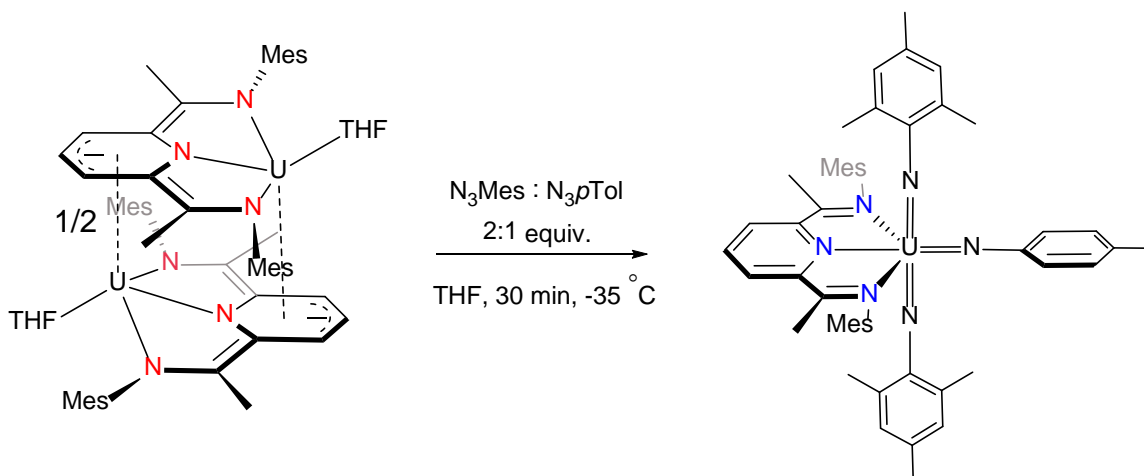
Scheme 2.5 Synthetic scheme for **PDI-U-(NMes)₂(N*p*Tol)**.

With a handful of uranium mixed (tris)imidos synthesized and characterized, efforts began towards studying the reactivity of homo (tris)imidos. The first route studied was multiple-bond metathesis with carbodiimides. Since azides containing fewer than four carbon atoms exhibit extreme instability, it was idealized that using diisopropyl carbodiimide (*i*PrCDI) would not only provide high reactivity due to its small steric nature, but also result in an imido that would otherwise be difficult or dangerous to produce.

Initial experiments involving the tris(imido) and *i*PrCDI in a one to one ratio yielded extraordinarily complicated reaction mixtures (Scheme 2.6). It was presumed that this occurred because of the ability of the carbodiimide to react twice, thus leading to a proposed mixture of mixed tris(imido), *N,N*-2,6-diisopropylphenylcarbodiimide (DippCDI), and *N*-(2,6-diisopropylphenyl)-*N*-isopropylcarbodiimide. In an effort to simplify the system, the equivalents of *i*PrCDI were reduced by half with the hopes that only the DippCDI would remain which could be easily separated from the uranium product(s) by differences in solubility. Unfortunately, the reaction provided a similar mix of products as was previously seen and most of the products were soluble in non-polar and polar solvents alike.
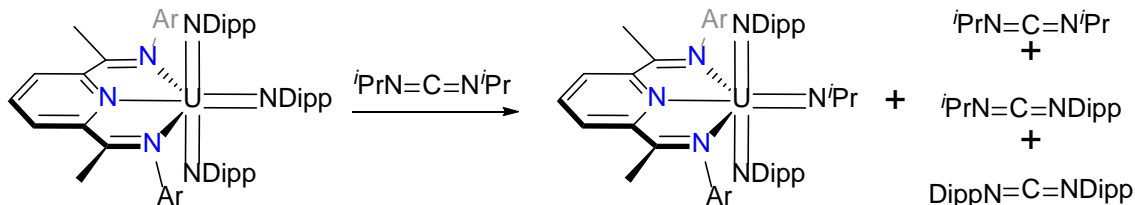
Scheme 2.6 Synthetic design of multiple bond metathesis with PDI supported tris(Dipp)imido and possible byproducts.

With few results coming from the multiple bond metathesis route, efforts were shifted towards investigating protonolysis. The addition of one equivalent of para-tolyl aniline again produced an NMR spectrum that was void of clear signals indicative of a uranium product, but the production of signals which could be attributed to Dipp aniline showed that a reaction was, in fact, occurring (Figure 2.4). Unfortunately, as free PDI, Dipp aniline, and para-tolyl aniline were the only signals visible from NMR and crystallization attempts were unsuccessful, verification of the final product could not be made.

Future progress with this project should be focused on protonolysis reactions with varying anilines. Removal of the aniline via pentane washes is complicated by the solubility of the uranium product(s) in pentane, even when chilled by the freezer. However, alkyl amines bearing electron withdrawing groups were not probed and could lead to products with less organic solubility. Although the reactivity of anilines and amines is assumed to be based on the pK_a of the nitrogen bound protons and trends similarly to the electrochemical results seen for the azides, much could be gained from testing the reactivity of simple primary amines since the steric factor may override the electronic factor.
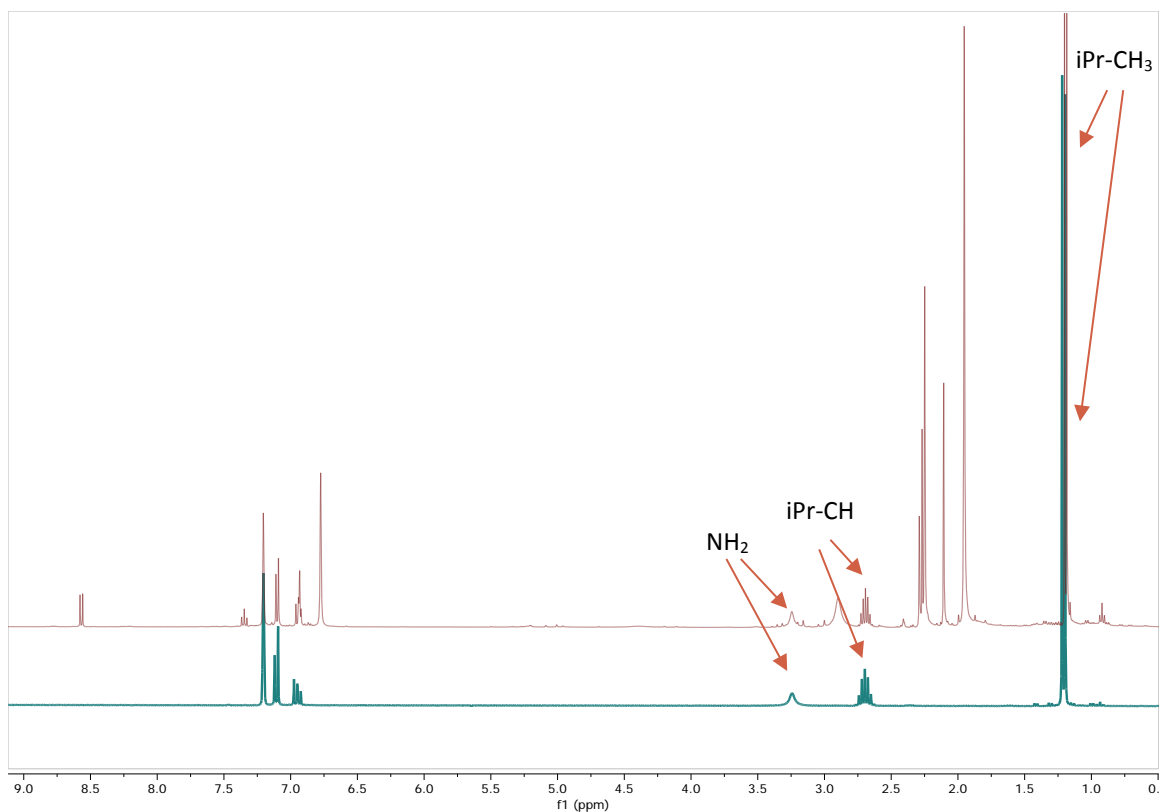
Figure 2.4 Superimposed NMR spectra in benzene-d_6 at room temperature of Dipp
aniline (blue) with reaction progression (maroon) with para-tolyl aniline.

In conclusion, uranium mixed tris(imidos) can be synthesized in a facile manner from
[PDI-U-thf]$_2$ via reaction with azides provided that the poorer oxidizing azide has a twofold
excess over the other. When azides were used which had less electron donating character
a common observation was that the supporting ^{Mes}PDI^{Me} ligand dissociated from the
complex. If this ligand were modified to have more electron donating character it might be
possible to prevent the dissociation from occurring which would allow for the synthesis of
homo and mixed tris(imidos) with stronger electron withdrawing groups attached. None of
the tris(imidos) showed any significant reactivity with carbodiimides despite the literature
precedent of uranium imidos undergoing multiple-bond metathesis with moieties such as
these. It is possible that the steric and electronic environment of these molecules is not
conducive to such reactivity. Finally, reactivity was observed when anilines were

introduced to uranium tris(imidos) but nothing beyond initial characterization of byproducts resulted from these studies.

2.3 Experimental

General Considerations: All air- and moisture-sensitive manipulations were performed by using standard Schlenk techniques or in an MBraun inert atmosphere drybox with an atmosphere of purified nitrogen. The MBraun drybox is equipped with a coldwell designed for freezing samples in liquid nitrogen as well as two -35 °C freezers for cooling samples and crystallizations. Solvents for sensitive manipulations were dried and deoxygenated by using literature procedures.[20] Benzene-d_6, toluene-d_8, and tetrahydrofuran-d_8 were purchased from Cambridge Isotope Laboratories, dried with molecular sieves and sodium, and degassed by 3 freeze–pump–thaw cycles. $^{Mes}PDI^{Me}$,[47] [PDI-U-thf]$_2$,[1] aryl azides,[48] and potassium graphite[49] were prepared according to literature procedures. *i*PrCDI was purchased in 99% purity from Sigma-Aldrich, degassed overnight on a Schlenk line, and used without further purification.

^1H and ^{13}C NMR spectra were recorded on a Varian Inova 300 spectrometer operating at 299.992 MHz. All chemical shifts are reported relative to the peak for SiMe$_4$, using ^1H and ^{13}C (residual) chemical shifts of the solvent as a secondary standard. Infrared spectra were recorded on a Thermo Nicolet 6700 FTIR spectrophotometer with a DTGS TEC detector as a solution deposition on a KBr window. Samples were stored under an inert atmosphere until transferred to the spectrometer. Electronic absorption measurements were recorded at 294 K in THF in sealed 1 cm quartz cuvettes with data collection performed on a Jasco V-6700 spectrophotometer under inert conditions.

Single crystals for X-ray diffraction were coated with poly(isobutylene) oil in a glovebox and mounted on a Mitegen micromesh mount and quickly transferred to the goniometer head into the 100 K coldstream of the diffractometer. Initial unit cells were determined, data collection strategies set up and frames collected using APEX2,[21] processed using SAINT,[22] and the files scaled and corrected for absorption using SADABS[23] or TWINABS.[24] The space groups were assigned and the structures were solved by direct methods using XPREP within the SHELXTL suite of programs[25,26] and refined by full matrix least squares against F^2 with all reflections using Shelxl2014[23] and

the graphical interface Shelxle.[27] If not specified otherwise H atoms attached to carbon atoms were positioned geometrically and constrained to ride on their parent atoms, with carbon hydrogen bond distances of 0.95 Å for alkene and aromatic C-H, 1.00, 0.99 and 0.98 Å for aliphatic C-H, CH_2 and CH_3 moieties, respectively. Methyl H atoms were allowed to rotate but not to tip to best fit the experimental electron density. $U_{iso}(H)$ values were set to a multiple of $U_{eq}(O/C/N)$ with 1.5 for CH_3 and OH, and 1.2 for C-H, CH_2 and N-H units, respectively. Additional details relating to disorder and twinning are given for each structure in their crystallographic experimental details sections, below.

Synthesis of PDI-U-(NDipp)$_2$(NMes). A 20 mL scintillation vial was loaded with 100 mg (0.071 mmol, 1 eq.) of [PDI-U-thf]$_2$ dissolved in 10 mL of toluene. In a separate vial, 58 mg of DippN$_3$ (0.284 mmol, 4 eq.) were mixed with 23 mg of MesN$_3$ (0.142 mmol, 2 eq.) in 1 mL of toluene. The mixture of azides was transferred to the vial containing the dimer and an additional 1 mL of toluene was used to rinse the vial. Upon addition of the azides, an immediate effervescence was observed and identified as loss of nitrogen. After stirring for 30 minutes at room temperature, volatile components were removed *in vacuo* leaving a black powdery product. After multiple washes with pentane, the product was identified as **PDI-U-(NDipp)$_2$(NMes)**. ^{1}H NMR (300 MHz, 20 ˚C, C$_6$D$_6$): δ = 0.71 (d, 12H, *i*Pr-C*H*$_3$), 1.53 (d, 12H, *i*Pr-C*H*$_3$), 1.71 (s, 6H, PDI-imide-C*H*$_3$), 2.02 (s, 6H, PDI-Mes-*o*-C*H*$_3$), 2.12 (s, 6H, Mes-*o*-C*H*$_3$), 3.68 (sept, 2H, *i*PrC*H*), 4.41 (s, 6H, imido-Mes-*o*-C*H*$_3$), 5.86 (s, 3H, imido-Mes-*p*-C*H*$_3$), 6.72 (s, 6H), 7.31 (s, 6H,), 7.78 (d, Dipp-*m*-Ar*H*), 8.18 (s, 2H, imido-Mes-*m*-Ar*H*), 8.44 (sept, 2H, *i*PrC*H*).
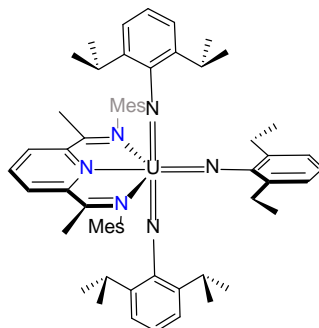
Synthesis of PDI-U-(NDipp)₂(NDetp). A 20 mL scintillation vial was loaded with 100 mg (0.071 mmol, 1 eq.) of [PDI-U-thf]₂ dissolved in 10 mL of toluene. In a separate vial, 58 mg of Dipp azide (0.284 mmol, 4 eq.) were mixed with 25 mg of Detp azide (0.142 mmol, 2 eq.) in 1 mL of toluene. The mixture of azides was transferred to the vial containing the dimer and an additional 1 mL of toluene was used to rinse the vial. Upon addition of the azides, an immediate effervescence was observed and identified as loss of nitrogen. After stirring for 30 minutes at room temperature, volatile components were removed *in vacuo* leaving a black powdery product. After multiple washes with pentane, the product was identified as **PDI-U-(NDipp)₂(NDetp)**. ^{1}H NMR (300 MHz, 20 °C, C₆D₆): δ = 0.71 (d, 12H, *i*Pr-C*H₃*), 1.53 (d, 12H, *i*Pr-C*H₃*), 1.71 (s, 6H, PDI-imide-C*H₃*), 2.02 (s, 6H, PDI-Mes-*o*-C*H₃*), 2.12 (s, 6H, Mes-*o*-C*H₃*), 3.68 (sept, 2H, *i*PrC*H*), 4.41 (s, 6H, imido-Mes-*o*-C*H₃*), 5.86 (s, 3H, imido-Mes-*p*-C*H₃*), 6.72 (s, 6H), 7.31 (s, 6H,), 7.78 (d, Dipp-*m*-Ar*H*), 8.18 (s, 2H, imido-Mes-*m*-Ar*H*), 8.44 (sept, 2H, *i*PrC*H*).
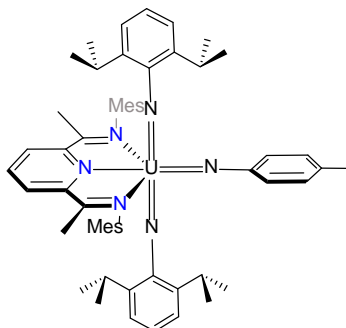
Synthesis of PDI-U-(NDipp)₂(N*p*Tol). A 20 mL scintillation vial was loaded with 100 mg (0.071 mmol, 1 eq.) of [PDI-U-thf]₂ dissolved in 10 mL of toluene. In a separate vial, 58 mg of DippN₃ (0.284 mmol, 4 eq.) were mixed with 18 mg of *p*TolN₃ (0.142 mmol, 2 eq.) in 1 mL of toluene. The mixture of azides was transferred to the vial containing the dimer and an additional 1 mL of toluene was used to rinse the vial. Upon addition of the azides, an immediate effervescence was observed and identified as loss of nitrogen. After stirring for 30 minutes at room temperature, volatile components were removed *in vacuo* leaving a black powdery product. After multiple washes with pentane, the product was identified as **PDI-U-(NDipp)₂(N*p*Tol)**. ^{1}H NMR (300 MHz, 20 ˚C, C₆D₆): δ = 0.69 (d, 12H, *i*Pr-C*H*₃), 1.46 (d, 12H, *i*Pr-C*H*₃), 1.71 (s, 6H, PDI-imide-C*H*₃), 2.06 (s, 12H, PDI-Mes-*o*-C*H*₃), 2.14 (s, 3H, *p*Tol-*p*-C*H*₃), 3.33 (sept, 4H, *i*PrC*H*), 4.19 (d, 2H, *p*Tol-*o*-C*H*₃), 5.74 (t, 2H, *i*Pr-*p*-C*H*), 6.76 (s, 6H, PDI-Mes-*p*-C*H*₃), 7.04 (d, 4H, *i*Pr-*m*-C*H*), 7.31 (t, 1H, PDI-pyr-*p*-C*H*), 8.49 (d, PDI-pyr-*m*-C*H*), 9.28 (2H, *p*Tol-*m*-C*H*).

CHAPTER 3.   REACTIVITY OF DIAZOALKANES WITH LOW VALENT URANIUM MOLECULES

3.1   Introduction

Attempts to create uranium Schrock-type alkylidenes have been largely unsuccessful due to an inability to synthesize a true uranium-carbon multiple bond. Initial attempts to create this type of molecule through reduction of a substituted diazomethane began by the group of Carol Burns in 2002.[50] In their system, $Cp^*_2U(Me)(OTf)$, which coordinates as a dimer, was introduced to diphenyldiazomethane. Instead of the desired loss of nitrogen, crystallographic evidence showed that rearrangement took place after insertion resulting in the first actinide hydrazonato complex to be formed. In 2007 Meyer published two structures showing differing coordination of diazomethane.[51] Initially, using (tBuArO)$_3$tacn   (trianion   of   1,4,7-tris(3,5-di-tert-butyl-2-   hydroxybenzyl)-1,4,7-triazacyclononane) they observed diazomethane coordinated to the uranium with a delocalized single electron throughout the diazomethane fragment. By adapting the tacn ligand with bulky adamantyl functionality, they were able to get coordination through the terminal nitrogen of the diazomethane. Exposing this molecule to heat did not result in the extrusion of nitrogen but, instead, resulted in C-H activation of one of the phenyl rings providing an indazole ligand. Most recently, John Arnold published a tris guanidate supported uranium III molecule which coordinated with diphenyldiazomethane in an end-on nearly linear fashion similar to what Meyer observed with the bulkier adamantyl functionalized tacn ligand.[52]

The objective of this project was to use diazomethane derivatives to test their varying reactivity with uranium species bearing a tris-pyrazole borate ligand as shown in Scheme 3.1. Diazomethanes are known to act as "masked" carbenes as the carbenes are typically formed through the extrusion of dinitrogen via either heat, light, or reduction. Since uranium is known to be a strongly reducing metal, it was proposed that the metal alone or, with the aid of potassium graphite, would be sufficient in reducing the diazomethane to the carbene. Likewise, if the nitrogen remained with the molecule, it could be used to study bonding motifs which may be less visible if more reactive molecules such as azides were used.
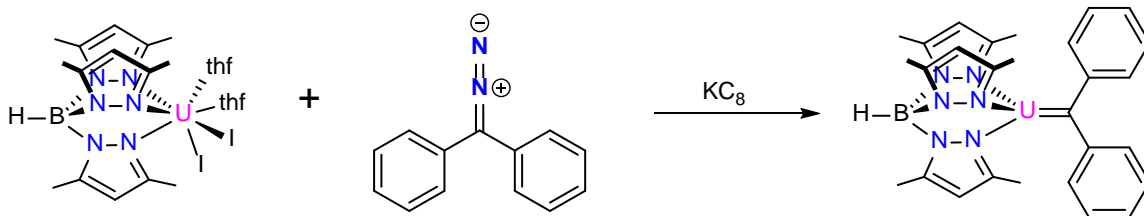
Scheme 3.1 Proposed synthesis of Tp* supported uranium alkylidene

3.2　　Results and Discussion

Primary reactions between Tp*UI$_2$ and diphenyldiazomethane were unsurprising in that no reduction was seen of the diazomethane fragment. However, an effect which had previously not been observed came to light; instead of the diazomethane coordinating to a single uranium, it was bridging between two ligand supported uranium atoms despite being combined in a one to one ratio. Thus, efforts towards investigating this type of molecule began with synthesizing an unreduced bridging coordinated species. These molecules could then undergo progressive reductions and oxidations thereby giving some insight on the reactivity of bridging diazomethane fragments. Scheme 3.2 shows the map of these reactions as well as the structures of all of the compounds formed.
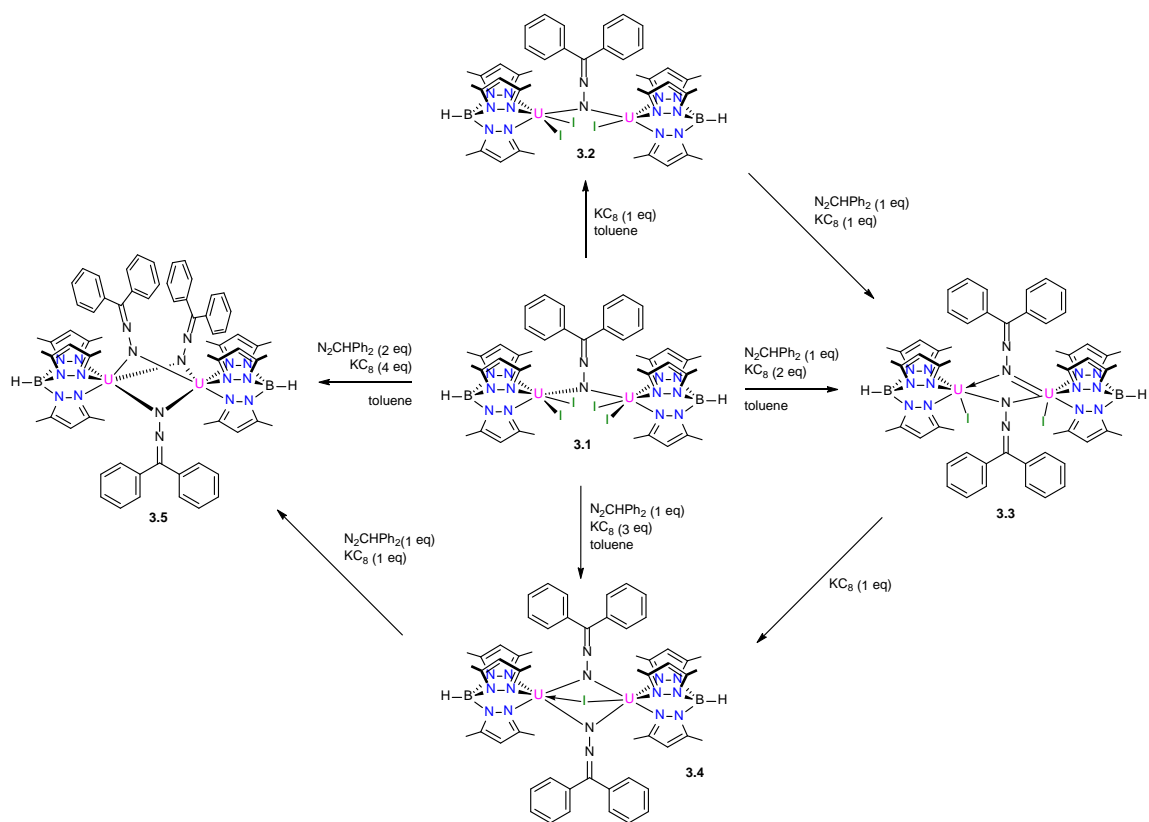
Scheme 3.2 Reaction map showing reduction series with diphenyldiazomethane.

The parent unreduced compound (**3.1**) is a tetra-iodo species with the diazomethane bridging the two uranium centers (Figure 3.1). Analysis of small red block crystals grown from benzene indicate that the bonding of the diazomethane fragment is nearing multiple bond character with the U1-N13 bond length being 2.182(2) Å. The U2-N13 and U2-N14 bond lengths are significantly longer at 2.396(2) and 2.361(2) Å respectively. Analysis of the C31-N14 bond length shows retention of the double bond character through a relatively short bond length of 1.309(3) Å. Analysis through electronic absorption spectroscopy for

this compound shows a characteristic resonance at 650 nm indicating that the overall oxidation state of the dimer is uranium (IV).[50]
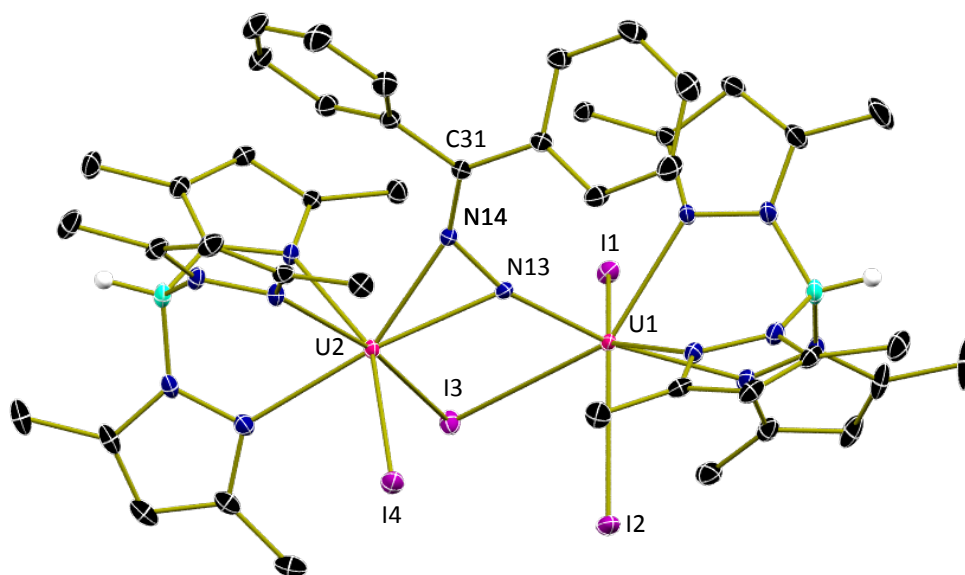
Figure 3.1 Molecular structure of **3.1** with atoms displayed as 30% probability ellipsoids and selected hydrogen atoms omitted for clarity.

Reduction of **3.1** with two equivalents of KC_8 in the presence of one equivalent of diazomethane yields a reddish-brown solution which can be crystallized from benzene to give needle-like red crystals. X-ray diffraction analysis of this compound yields a structure like that seen in Figure 3.2. It was of interest to note that, instead of both diazomethane fragments being shared equally between the two uranium atoms, they are both oriented the same direction towards one center.
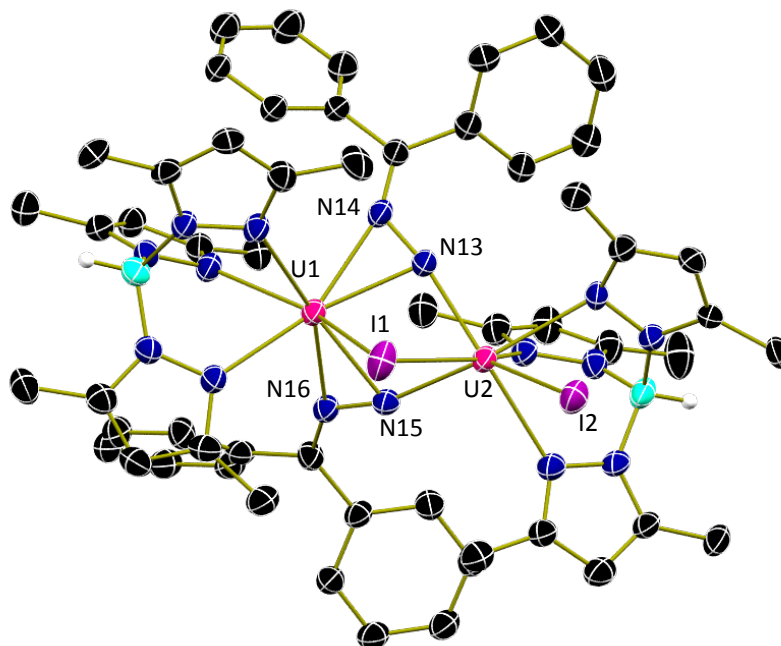
Figure 3.2 Molecular structure of **3.3** with atoms displayed as 30% probability ellipsoids and selected hydrogen atoms omitted for clarity.

When a closer look is taken at the bond lengths (Figure 3.3), it can be seen that the U2-N13 (2.200(8) Å) and U2-N15 (2.211(8) Å) bonds are significantly shorter than any of the U1-N bonds (2.344(8)-2.406(9) Å).This indicates a bonding motif similar to what was seen in **3.1** but, as fluxional coordination with diazomethanes has been previously observed[30], it could be a structural anomaly where the coordination between the two diazomethanes is in flux between the two uranium atoms.
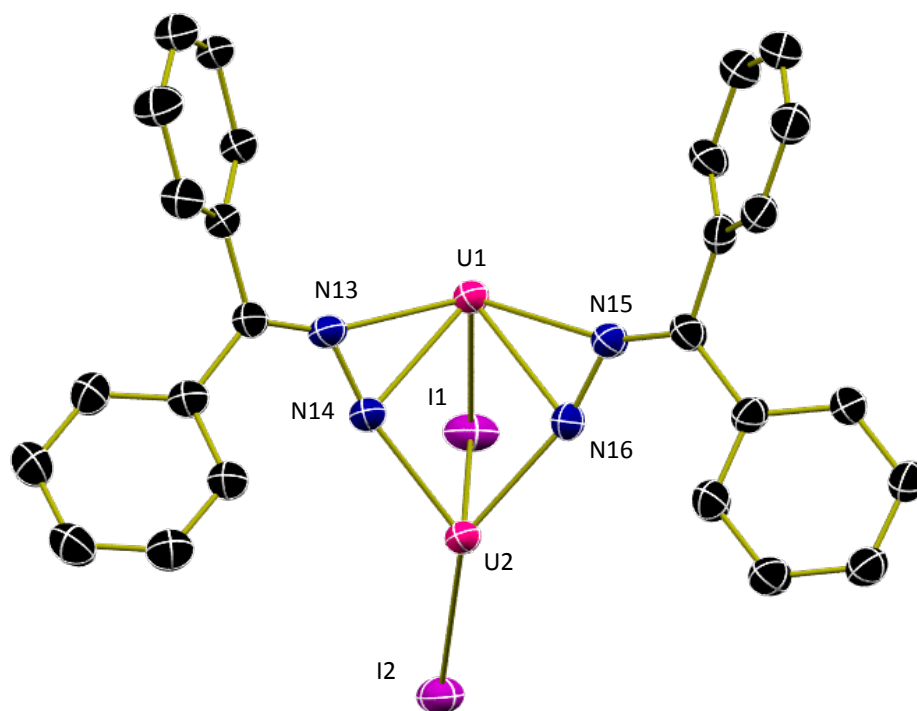
Figure 3.3 Molecular structure of **3.3** with atoms displayed as 30% probability ellipsoids with hydrogen atoms and Tp* ligands omitted for clarity.

The final iodinated structure in the series is synthesized through reduction of **3.1** with three equivalents of KC_8 in the presence of one equivalent of diazomethane or, alternatively, through the reduction of **3.3** with one equivalent of KC_8. This molecule, unlike **3.1** or **3.3**, does not exhibit as much symmetry with only one iodine atom being shared between the two uranium atoms. However, the same bonding preference is seen with the two diazomethane fragments oriented in the same direction and having significantly shorter bond lengths with U2 than U1. Unsurprisingly, the U2-N13 and U2-N15 bond lengths are shorter than those observed with **3.3** at 2.165(6) and 2.158(7) Å respectively. This is explained by the increased bonding with the two diazomethane fragments in lieu of the iodine and lends further proof that, throughout the entire reduction series, an overall oxidation state of +4 is maintained.
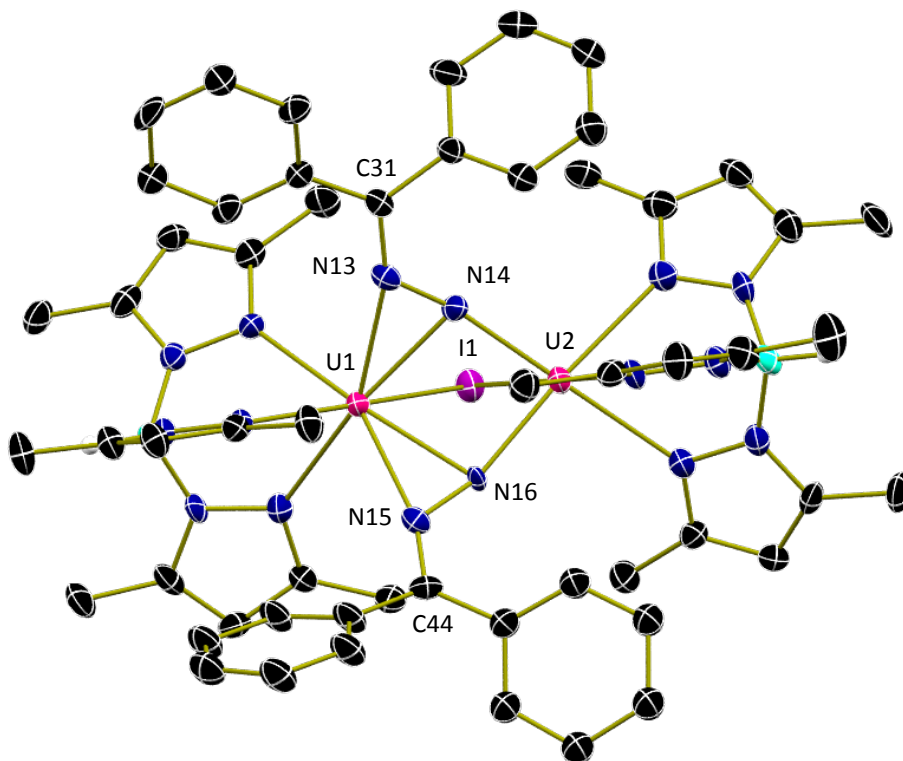
Figure 3.4 Crystal structure of **3.4** with atoms displayed as 30% probability ellipsoids and selected hydrogen atoms omitted for clarity.

Reduction with four equivalents of potassium graphite and two additional equivalents of diazomethane resulted in compound **3.5** (Figure 3.5). Compound **3.5** shows remarkable symmetry with the Tp* ligands eclipsed, and the diazomethane molecules evenly spaced between each pyrazole ring. This molecule shows the greatest bond lengths between uranium atoms and diazomethane nitrogens as is expected due to the steric demands of the three bridging diazomethane fragments. ^{1}H NMR of this molecule shows a complicated spectrum with no elements of symmetry. The alternation of one of the diazomethane fragments accounts for this observation even though the molecule, when viewed from the boron of one of the Tp* ligands, shows eclipsed Tp* ligands with perfectly interspaced diazomethane bridges.
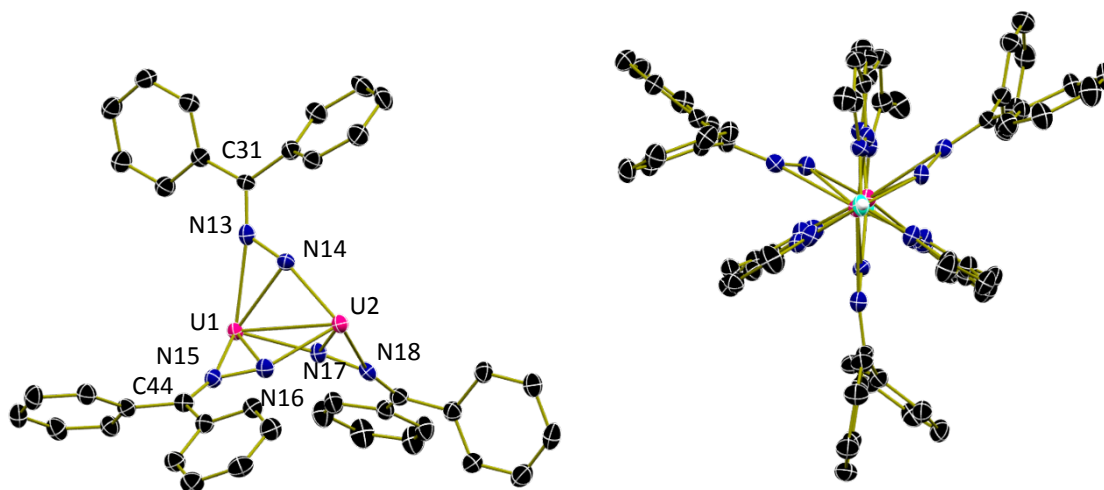
Figure 3.5 (Left) Molecular structure of compound **3.5** with atoms displayed as 30% probability ellipsoids and hydrogen atoms and Tp* ligands omitted for clarity. (Right) End-on view of entire molecule with Tp* ligands showing symmetry. Atoms displayed as 30% probability ellipsoids with selected hydrogen atoms omitted for clarity.

The synthesis of this series of molecules exemplifies further unique bonding modes of uranium. Initial synthesis of tetra-iodo **3.1** shows an initial oxidation of uranium from +3 to +4 however, further reduction and oxidation events through addition of potassium graphite and diazomethane do not appear to have effect on the overall +4 oxidation state. Since it is well known that uranium V molecules exhibit inherent instability, it is reasonable that the energy required to oxidize to that state is not possible with current reaction conditions. Additionally, reduction back to the +3 state, which would be required in order to form the desired alkylidene, appears to require a significantly stronger reduction agent than potassium graphite. Reduction with rubidium or cesium graphite might provide a different result.

Table 3.1 Table showing selected bond distances for compounds **3.1**, **3.3**, **3.4**, and **3.5**.

Bond	3.1	3.3	3.4	3.5
U-N(Tp*)	2.448(2)- 2.557(2) Å	2.478(8)- 2.545(8) Å	2.451(7)- 2.492(8) Å	2.499(6)- 2.563(5) Å
U1-N13	2.396(2) Å	2.344(8) Å	2.373(6) Å	2.408(5) Å
U1-N14	2.361(2) Å	2.406(9) Å	2.417(7) Å	2.443(5) Å
U2-N13	2.182(2) Å	2.200(8) Å	2.165(6) Å	2.208(5) Å
N13-N14	1.377(3) Å	1.352(11) Å	1.359(9) Å	1.323(8) Å
N14-C31	1.309(3) Å	1.316(13) Å	1.318(10) Å	1.322(8) Å
U1-N15	N/A	2.349(7) Å	2.332(7) Å	2.373(5) Å
U1-N16	N/A	2.368(8) Å	2.421(7) Å	2.470(6) Å
U2-N15	N/A	2.211(8) Å	2.158(7) Å	2.182(5) Å
N15-N16	N/A	1.338(11) Å	1.349(9) Å	1.333(7) Å
N16-C44	N/A	1.304(12) Å	1.335(11) Å	1.312(8) Å
U1-N17	N/A	N/A	N/A	2.203(5) Å
U2-N17	N/A	N/A	N/A	2.401(5) Å
U2-N18	N/A	N/A	N/A	2.446(5) Å
N17-N18	N/A	N/A	N/A	1.331(8) Å
N18-C57	N/A	N/A	N/A	1.319(8) Å

Although the products depicted above do not exhibit the desired bonding character which was originally sought, they do provide unique insight into the bonding nature of Tp* uranium species. For all of the molecules, the carbon nitrogen bond of any of the diazomethane fragments does not vary significantly from the accepted double bond length of 1.32 Å.[53,54] Additionally, all of the diazomethane fragments display a shortened bond

indicative of multiple bonding character[52] with one of the uranium atoms while the other uranium interacts with both nitrogens in a dative manner.

   Additional explorations of reactivity with these types of molecules gave disappointing results. When both compounds **3.1** and **3.5** were exposed to excess KC_8, both molecules showed a large degree of decomposition. Also, when reduction with Tp^*_2UI was attempted with the intent of the second bulky Tp^* ligand preventing the bridging effect seen previously, reduction attempts with KC_8 resulted in loss of one Tp^* ligand and formation of the same products as before.

   Since our group has seen a significant amount of success synthesizing molecules from the reduced $^{Mes}PDI^{Me}$ uranium dimer, reactions were designed using this material. It was envisioned that the electrons held in the PDI ligand would act as a more "direct" reducing agent and provide the desired uranium alkylidene. Although the desired product was not observed, a byproduct was crystallized from a reaction mixture which indicates that a uranium alkylidene had been transiently made. Attempts to trap this transient species are ongoing.

   In conclusion, while multiple studies have shown that multiple diazomethane derivatives coordinate with uranium moieties, this is the first example of diazomethane bridging between two supporting uranium atoms. As there are few examples of bridging uranium molecules in literature, this series provides great insight as to the possibility of uranium bonding modes.

3.3   Experimental

General Considerations: All air- and moisture-sensitive manipulations were performed by using standard Schlenk techniques or in an MBraun inert atmosphere drybox with an atmosphere of purified nitrogen. The MBraun drybox is equipped with a coldwell designed for freezing samples in liquid nitrogen as well as two -35 °C freezers for cooling samples and crystallizations. Solvents for sensitive manipulations were dried and deoxygenated by using literature procedures.[20] Benzene-d_6, toluene-d_8, and tetrahydrofuran-d_8 were purchased from Cambridge Isotope Laboratories, dried with molecular sieves and sodium, and degassed by 3 freeze–pump–thaw cycles. Tp^*UI_2,[55]

diphenyldiazomethane,[56] and potassium graphite[49] were prepared according to literature procedures.

^{1}H and ^{13}C NMR spectra were recorded on a Varian Inova 300 spectrometer operating at 299.992 MHz. All chemical shifts are reported relative to the peak for SiMe$_4$, using ^{1}H and ^{13}C (residual) chemical shifts of the solvent as a secondary standard. Infrared spectra were recorded on a Thermo Nicolet 6700 FTIR spectrophotometer with a DTGS TEC detector as a solution deposition on a KBr window. Samples were stored under an inert atmosphere until transferred to the spectrometer. Electronic absorption measurements were recorded at 294 K in THF in sealed 1 cm quartz cuvettes with data collection performed on a Jasco V-6700 spectrophotometer under inert conditions.

Data for all crystals were collected on a Bruker AXS X8 Prospector CCD diffractometer featuring an I-μ-S microsource X-ray tube with a laterally graded multilayer (Goebel) mirror for monochromatization and operating with Cu Kα radiation (λ = 1.54184 Å). All instruments were equipped with Oxford Cryostream low temperature devices. Single crystals for X-ray diffraction were coated with poly(isobutylene) oil in a glovebox and mounted on a Mitegen micromesh mount and quickly transferred to the goniometer head into the 100 K coldstream of the diffractometer. Initial unit cells were determined, data collection strategies set up and frames collected using APEX2,[21] processed using SAINT,[22] and the files scaled and corrected for absorption using SADABS[23] or TWINABS.[24] The space groups were assigned and the structures were solved by direct methods using XPREP within the SHELXTL suite of programs[25,26] and refined by full matrix least squares against F^2 with all reflections using Shelxl2014[23] and the graphical interface Shelxle.[27] If not specified otherwise H atoms attached to carbon atoms were positioned geometrically and constrained to ride on their parent atoms, with carbon hydrogen bond distances of 0.95 Å for alkene and aromatic C-H, 1.00, 0.99 and 0.98 Å for aliphatic C-H, CH$_2$ and CH$_3$ moieties, respectively. Methyl H atoms were allowed to rotate but not to tip to best fit the experimental electron density. U$_{iso}$(H) values were set to a multiple of U$_{eq}$(O/C/N) with 1.5 for CH$_3$ and OH, and 1.2 for C-H, CH$_2$ and N-H units, respectively. Additional details relating to disorder and twinning are given for each structure in their crystallographic experimental details sections, below.

Synthesis of Tp*₂U₂I₄N₂CPh₂: A 20-mL scintillation vial was charged with two equivalents (500 mg, 0.5 mmol) of Tp*UI₂ and 10 mL of toluene. The solution was stirred at room temperature for 5 minutes before one equivalent a 0.5 M solution of diphenyldiazomethane in toluene was added dropwise over 5 minutes. An immediate color change was observed as the deep blue/purple uranium solution turned brick red upon addition of the magenta diazomethane. The reaction was stirred at room temperature for 2 hours before volatile compounds were removed *in vacuo* leaving a dark brown residue. Repeated washings with toluene afforded a fine golden powder which was identified as **Tp*₂U₂I₄N₂CPh₂** in 60% yield. ^{1}H NMR (300 MHz, 25 ˚C, C₆D₆): δ = -13.80 (s, 2H, Tp*B-H), -7.91 (s,18H, Tp*Me), 2.11 (s, 6H, Tp*C-H), 4.61 (s, 18H, Tp*Me), 15.26 (s, 2H), 16.87 (s, 1H, Ph-*p*-H), 17.09 (s, 2H), 20.54 (s, 1H, Ph-*p*-H), 30.61 (s, 2H), 32.45 (s, 2H).

Synthesis of Tp*₂U₂I₂(N₂CPh₂)₂: A 20-mL scintillation vial was charged with Tp*₂U₂I₄N₂CPh₂ in 5 mL of toluene. Two equivalents of KC₈ and one equivalent of diazomethane were then added and the slurry was left to stir at room temperature for 30 minutes. The slurry was filtered over celite to remove graphite and KI and the resulting reddish-brown solution was concentrated to afford a dark reddish-brown residue. Recrystallization from toluene afforded **Tp*₂U₂I₂(N₂CPh₂)₂** in an 85% yield. ^{1}H NMR (300 MHz, 25 ˚C, C₆D₆): δ = -25.34 (s, 4H), -12.04 (s, 1H, Tp*B-H), -7.90 (s, 9H, Tp*Me), -4.77 (s, 2H), 0.27 (s, 1H, Tp*B-H), 1.85 (s, 2H), 2.11 (s, 9H, Tp*Me), 4.36 (s, 9H, Tp*Me), 6.77 (s, 9H, Tp*Me), 17.23 (s, 4H), 22.63 (s, 4H), 25.72 (s, 4H).

Synthesis of Tp*₂U₂I(N₂CPh₂)₂: A 20-mL scintillation vial was charged with Tp*₂U₂I₄N₂CPh₂ in 5 mL of toluene. Three equivalents of KC₈ and one equivalent of diazomethane were then added and the slurry was left to stir at room temperature for 30 minutes. The slurry was filtered over celite to remove graphite and KI and the resulting reddish-brown solution was concentrated to afford a dark reddish-brown residue. Recrystallization from toluene afforded **Tp*₂U₂I(N₂CPh₂)₂** ^{1}H NMR (300 MHz, 25 ˚C, C₆D₆): δ = -28.36 (s, 4H), -13.94 (s, 1H, Tp*B-H), -8.32 (s, 9H, Tp*Me), -4.57 (s, 2H), 0.12 (s, 1H, Tp*B-H), 1.56 (s, 2H), 1.91 (s, 9H, Tp*Me), 3.76 (s, 9H, Tp*Me), 7.12 (s, 9H, Tp*Me), 15.43 (s, 4H), 23.67 (s, 4H), 26.21 (s, 4H).

Synthesis of Tp*$_2$U$_2$(N$_2$CPh$_2$)$_3$: A 20-mL scintillation vial was charged with Tp*$_2$U$_2$I$_4$N$_2$CPh$_2$ in 5 mL of toluene. Four equivalents of KC$_8$ and two equivalents of diazomethane were then added and the slurry was left to stir at room temperature for 30 minutes. The slurry was filtered over celite to remove graphite and KI and the resulting reddish-brown solution was concentrated to afford a dark reddish-brown residue. Recrystallization from toluene yielded **Tp*$_2$U$_2$(N$_2$CPh$_2$)$_3$** in a 79% yield. ^{1}H NMR (300 MHz, 25 ˚C, C$_6$D$_6$): δ = -18.95, -16.99, -13.71, -12.65, -8.60, -3.85, -3.52, -2.90, -2.38, -0.15, 0.28, 1.33, 1.66, 1.87, 2.11, 2.25, 2.40, 3.15, 3.81, 4.20, 3.15, 3.81, 4.20, 4.97, 5.65, 7.03, 7.74, 9.01, 9.62, 9.80, 10.97, 11.53, 12.16, 12.18, 13.11, 14.12, 14.67, 15.64, 16.87, 17.57, 20.53.

CHAPTER 4.   COPPER CATALYZED SYNTHESIS OF FLUORO- AND ALKYL- SUBSTITUTED DICARBONYLS

4.1   Introduction

Synthesis of carbon-carbon alkyl bonds, particularly via transition-metal catalyzed reactions, remains a topic of constant discussion due to its importance in natural product synthesis, medicinal chemistry, and materials synthesis. Cross-coupling of alkyl electrophiles with alkyl nucleophiles traditionally led to poor reaction yields with little-to-no enantioselectivity, however expanding the use of these materials with transition metal catalysts has led to great steps being made. A plethora of alkyl electrophiles exist due to the prevalence of alkyl halides. Alkyl nucleophiles, mostly consisting of Grignard-, zinc-, and boron-alkyl reagents, also have widespread use in the chemical community, but are trickier to mass produce, ship, and handle due to their lack of stability.[57–62] Many of these reagents must be synthesized immediately preceding a reaction or in situ in order to preserve viability. In addition to these complications, a large majority of reagents do not include fluorinated products which have seen heightened use in medicinal and energy applications.[63,64] While some progressions have been made towards the synthesis of di- and mono-fluorinated products, the processes are typically limited to aryl or other π-bond systems.[26–54]

4.2   Results and Discussion

The herein described project began with a reaction that was run between a p-methoxy phenyl cyclopropanol and ethyl 2-bromopropoanate in the presence of copper (I) iodide, potassium carbonate, 1,10-phenanthroline, and acetonitrile. The reaction used one equivalent of the cyclopropanol, four equivalents of ethyl 2-bromopropoanate, 10 mol% copper, 20 mol% ligand, and 0.1 M acetonitrile. The desired product was formed in 27% yield on a 0.3 mmol scale. As it was undesirable for the reaction to be limited to only aromatic cyclopropanols, the reaction scope was then expanded to benzylcyclopropanol as well as phenethylcyclopropanol (Scheme 4.1). Although the product of the

benzylcyclopropanol contains an exceedingly acidic proton in the benzyl/α-carbonyl position, the desired product was recovered in a 30% yield. It was then determined that optimization studies would be performed on the phenethylcyclopropanol due to its ease of synthesis through the Kulinkovich reaction as well as the stability of the product.
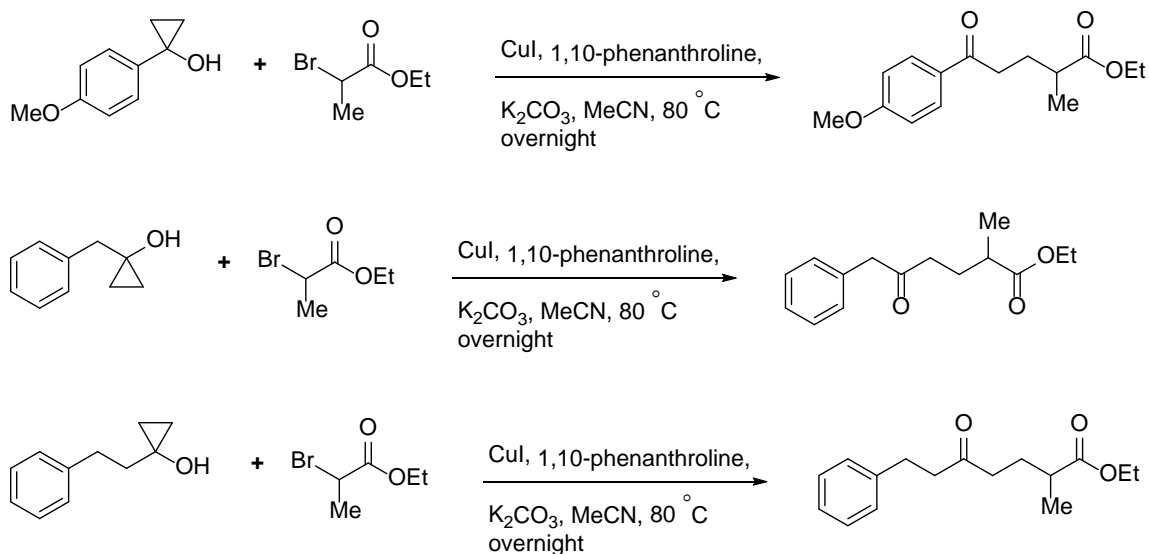
Scheme 4.1 Initial test reactions of cyclopropanol cross-coupling with a brominated ester.

Synthesis of the cyclopropanol can be achieved either through the Simmons-Smith reaction or through a Kulinkovich reaction. It is common knowledge in our group that purification of the Kulinkovich reaction is very tricky due to a commonly made byproduct having the same R_f as the desired product in every tried solvent system. The discovery of a paper written by Kulinkovich that acknowledges these byproducts and uses an equivalent of methyl magnesium bromide to circumvent the formation of these byproducts aided in the complication of purification. This procedure has since been employed and not only eases the complications of purifying the desired product, but also increases reaction yield by preventing the reaction pathway of the undesired intermediates (Scheme 4.2).
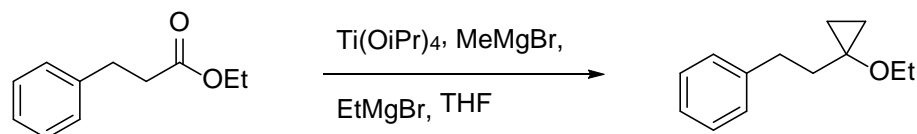
Scheme 4.2 Revised Kulinkovich cyclopropanation reaction.

With phenethylcyclopropanol in hand, the first optimization parameter that was explored was varying the copper (I) catalyst. Reaction conditions still involved using one equivalent of cyclopropanol, four equivalents of α-bromoester, two equivalents of base (potassium carbonate), 10 mol% copper (I), 20 mol% ligand (1,10-phenanthroline), and 0.1 M acetonitrile (Scheme 4.3). Table 4.1 shows the results of this reaction with six different copper catalysts as well as one condition which was run with no copper present. As expected, the reaction does not proceed in the absence of copper. Since little difference was seen between most of the ligands and copper (I) chloride gave the desired product in a 38% yield, it was chosen to be used in further optimization studies. This decision was made based on the price of the catalyst and available quantities.
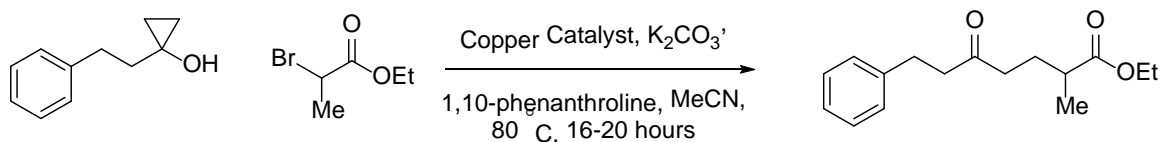
Scheme 4.3 General reaction conditions for optimization of copper catalysts shown in Table 4.1

Table 4.1 Reaction optimization with a variety of copper catalysts and the resulting yields.

Entry	Copper Catalyst	Yield
1	CuI	30%
2	CuBr	37%
3	CuCl	38%
4	CuTc	42%
5	CuCn	38%
6	Cu(MeCN)4BF4	41%
7	None	0%

An observation was made when using CuTc (copper (I) thiophene-2-carboxylate) that a byproduct formed which had a nearly identical R_f as the desired product on TLC. NMR data of the purified byproduct showed that the ligand had reacted with the excess ester to form the byproduct in nearly quantitative yield (Scheme 4.4).
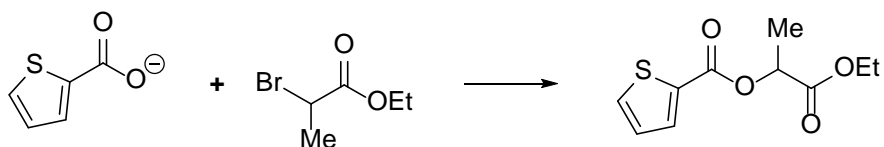
Scheme 4.4 Reactivity of thiophene carboxylate ligand with brominated ester

The second parameter explored was the impact of different bases on the reaction condition. A number of bases, both organic and inorganic, were chosen and the results are shown in Table 4.2 using conditions shown in Scheme 4.5. The organic bases were far more beneficial to the production of the final product than inorganic bases, although, it was noted that, pyridine-type bases resulted in nearly complete recovery of starting material.

Diisopropyl amine provided the highest yield (70%). Again, an experiment was performed to test the reaction in the absence of base which only resulted in recovered starting material. Based on other papers regarding cyclopropanol cross-coupling, it is hypothesized that the base is crucial to the cyclopropanol opening and the reaction cannot proceed in its absence.[55–59]
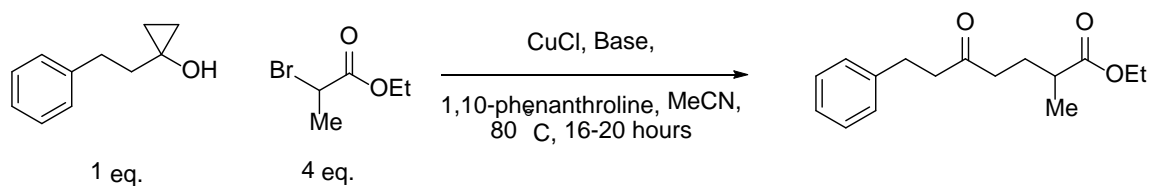
Scheme 4.5 General reaction conditions for optimization of bases shown in Table 4.2

Table 4.2 Reaction optimization with a variety of bases and the resulting yields.

Entry	Base	Yield
8	K_2CO_3	38%
9	Na_2CO_3	35%
10	Cs_2CO_3	34%
11	K_3PO_4	30%
12	KOtBu	No reaction
13	LiOtBu	No reaction
14	Pyridine	No reaction
15	Et_3N	56%
16	DIPEA	61%
17	$^iPr_2NH$	70%
18	Proton sponge	No reaction
19	2,6-lutidine	No reaction
20	Tetramethyl pyridine	67%
21	None	No reaction

Further optimization was achieved by investigating solvent effects (Scheme 4.6). Including the original solvent, acetonitrile, five solvents were investigated however, only dichloromethane resulted in product and it was at significantly a diminished yield (Table 4.3). It was noted that a greater quantity of byproducts were produced from this reaction, such as the β-hydride eliminated product from the cyclopropanol. The effect of concentration on the reaction system was also tested but showed little effect on the overall yield.
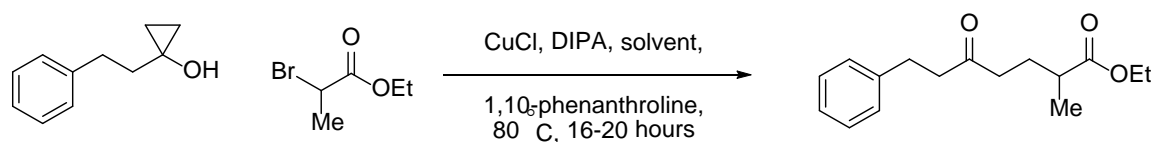
Scheme 4.6 General reaction conditions for optimization of solvent as shown in Table 4.3

Table 4.3 Reaction optimization with a variety of bases and the resulting yields.

Entry	Solvent	Yield
22	MeCN	70%
23	MeOH	No reaction
24	THF	No reaction
25	Toluene	No reaction
26	DCM	41%
27	MeCN (0.2 M)	60%
28	MeCN (0.5 M)	63%

Final testing occurred which probed the sensitivity of the reaction to the original procedure (Table 4.4). Since it is not ideal to use four equivalents of the α-bromoester two reactions were set up using a 1:1 ratio and a 1:2 ratio. Fortunately, the reaction still proceeds but results in a drastically lower yield. Interestingly, the unopened cyclopropanol was still observed even after allowing the reaction to stir at 80 ˚C for over 24 hours. With the previously optimized conditions using copper (I) chloride and di-isopropyl amine there was no starting material left after 16 hours (as observed by crude NMR). Another reaction was performed in which the catalyst loading was doubled to 20 mol% and the ratio of cyclopropanol to α-bromoester was kept at 1:2. Unfortunately, this resulted in a nearly identical yield. This suggests that there is a yet unobserved competing reaction pathway

occurring with the α-bromoester. Further mechanistic probing is required to elucidate the details of this reaction.

A final reaction was run in which the 1,10-phenanthroline was omitted from the reaction to ensure that the organic amine base was not acting as a ligand on the copper (Table 4.4). It was a relief to observe that, without phenanthroline, no reaction of the cyclopropanol took place. Since one of the future goals of this project was to induce an asymmetric addition to the cyclopropanol using chiral ligands, it was important to know if the base, which provided a drastic increase in yield, would act as and compete with the chiral ligand which would in turn prohibit enantioselectivity.
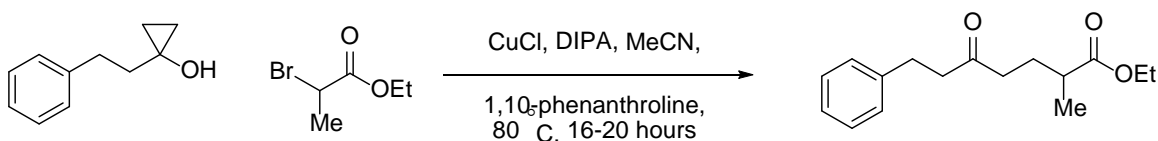
Scheme 4.7 Conditions for final optimization procedures outlined in Table 4.4

Table 4.4 Explorations in reducing the quantity of brominated ester used in synthesis.

Entry	Parameter Explored	Yield
29	Cyclopropanol: ester in a 1:1 ratio	39%
30	Cyclopropanol: ester in a 1:2 ratio	46%
31	Cyclopropanol: ester in a 1:1 ratio with a 20 mol % copper loading	45%
32	Phenanthroline omitted	No reaction

Following the above investigations, it was discovered that conditions using the diisopropyl amine were applicable to synthesis of mono-fluoroesters. Optimization of this reaction proceeded quickly as it only needed minor changes to produce ideal results. It was observed that aryl cyclopropanols performed best in this cross-coupling reaction with yields in the 50% range. Alkyl substituted cyclopropanols underwent cross-coupling but at drastically decreased yields in respect to the alkylation reaction. When conditions were applied to the disubstituted cyclopropanol "**F**" only the β-elimination product was observed.
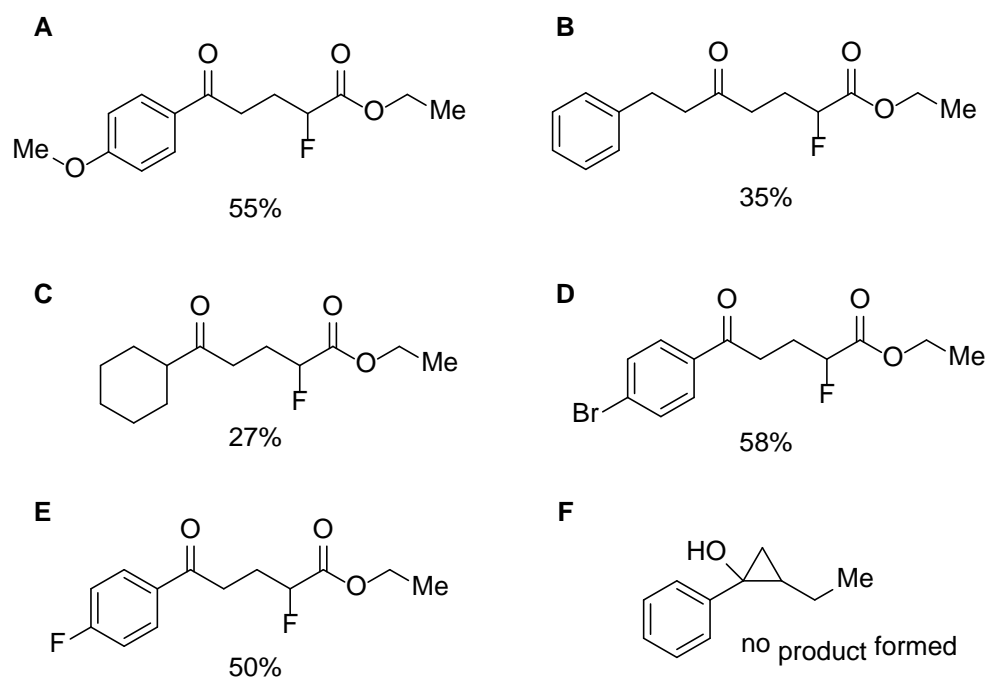
Figure 4.1 Collected data from the cross-coupling of cyclopropanols with fluorinated bromo-esters.

Investigations into the asymmetric application of this reaction were relatively short. After applying a variety of ligands to the reaction conditions, only drastically reduced yields were observed (Scheme 4.8). A method was developed using gas chromatography and a chiral column to separate the enantiomers of this reaction but led to poor results as

there was no enantioselectivity observed. This led to the belief that it is likely a diradical mechanism through which the copper catalyzed cross-coupling reaction is occurring.

   With this knowledge, we investigated identical reaction conditions except using cyclobutanols in place of cyclopropanols. The ring strain of cyclobutanols is only marginally lower than that of cyclopropanols but unfortunately only starting material was recovered from all the reactions which were run.
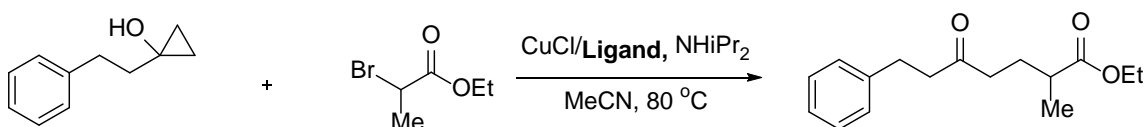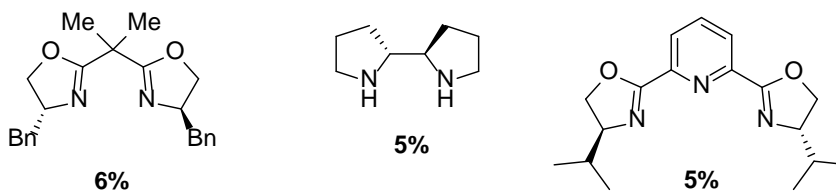
Scheme 4.8 Reaction conditions used for trials with chiral ligands

   With these results in hand, efforts were made to synthesize a library of compounds. The optimized copper catalyzed reaction was effective with a wide variety of substrates including secondary alcohols, terminal alkenes, as well as silyl and phenyl ethers.
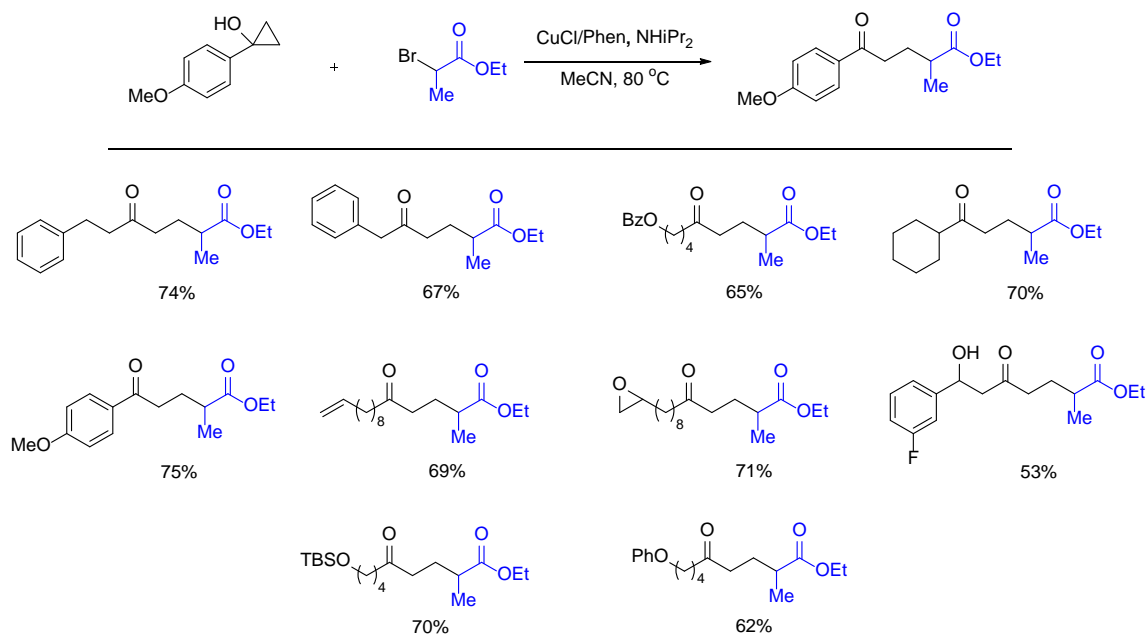
Scheme 4.9 Final products of cyclopropanol alkylation with yields.

Expansion of the previously described reaction to difluoro brominated esters was accomplished and optimized by simply changing the base from diisopropyl amine to potassium carbonate. This reaction produced a similar tolerance to a variety of functional groups as the ones previously described (Scheme 4.10).
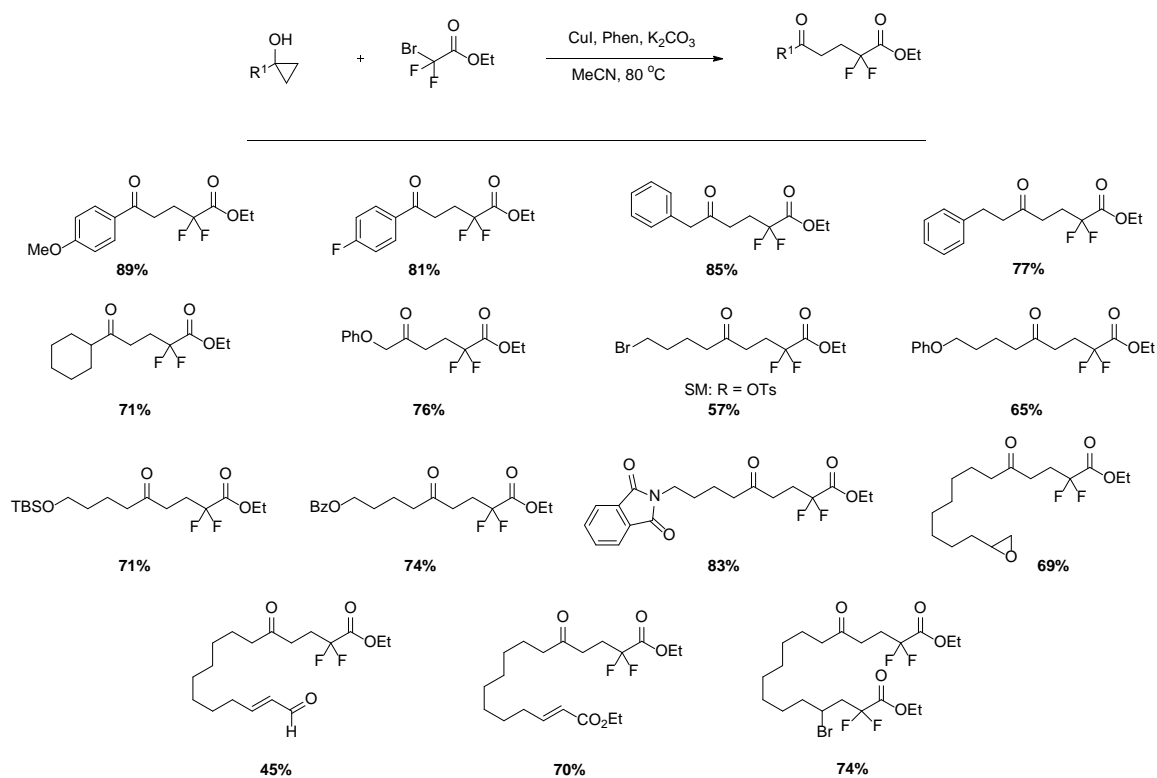
Scheme 4.10 Final products of cyclopropanol difluorination with yields.

Unlike the mono-fluorination reaction, cross coupling with di-substituted cyclopropanols occurred in appreciable yields and produced two cross-coupled products (Scheme 4.11). Production of the two products lends more evidence towards a di-radical mechanism as all of the major products are the result of a secondary radical preferentially formed over a primary radical.
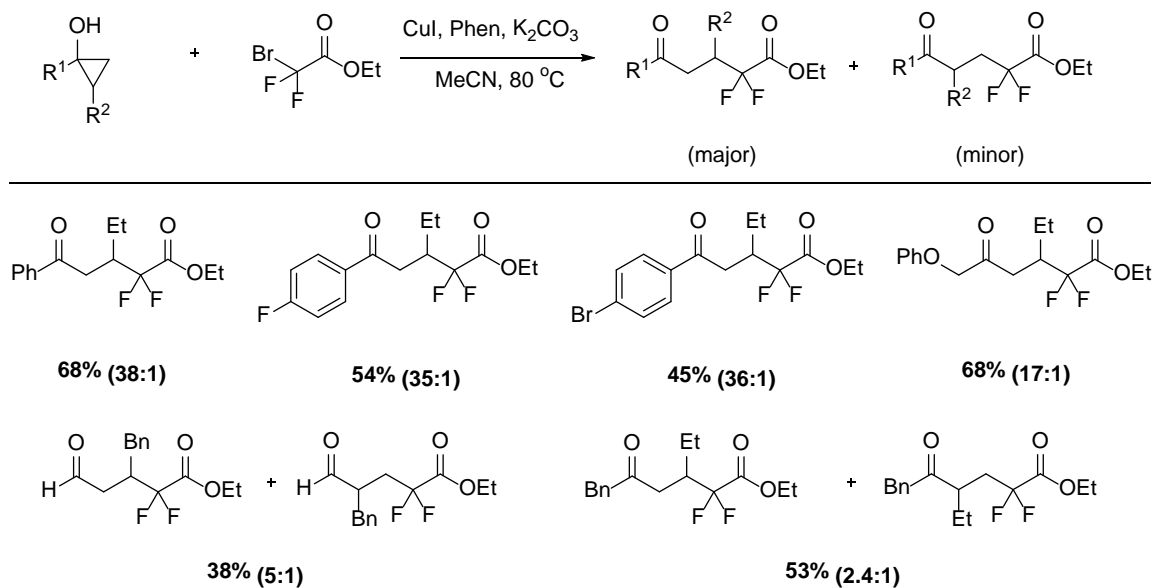
Scheme 4.11 Final products of disubstituted cyclopropanol difluorination with yields.

Extension of the di-fluorinated products was easily accomplished by reaction with a library of difluorinated amides (Scheme 4.12). These amides showed identical tolerance to a wide variety of functional groups as all previous attempts and resulted in a library of compounds made in moderate to good yield.
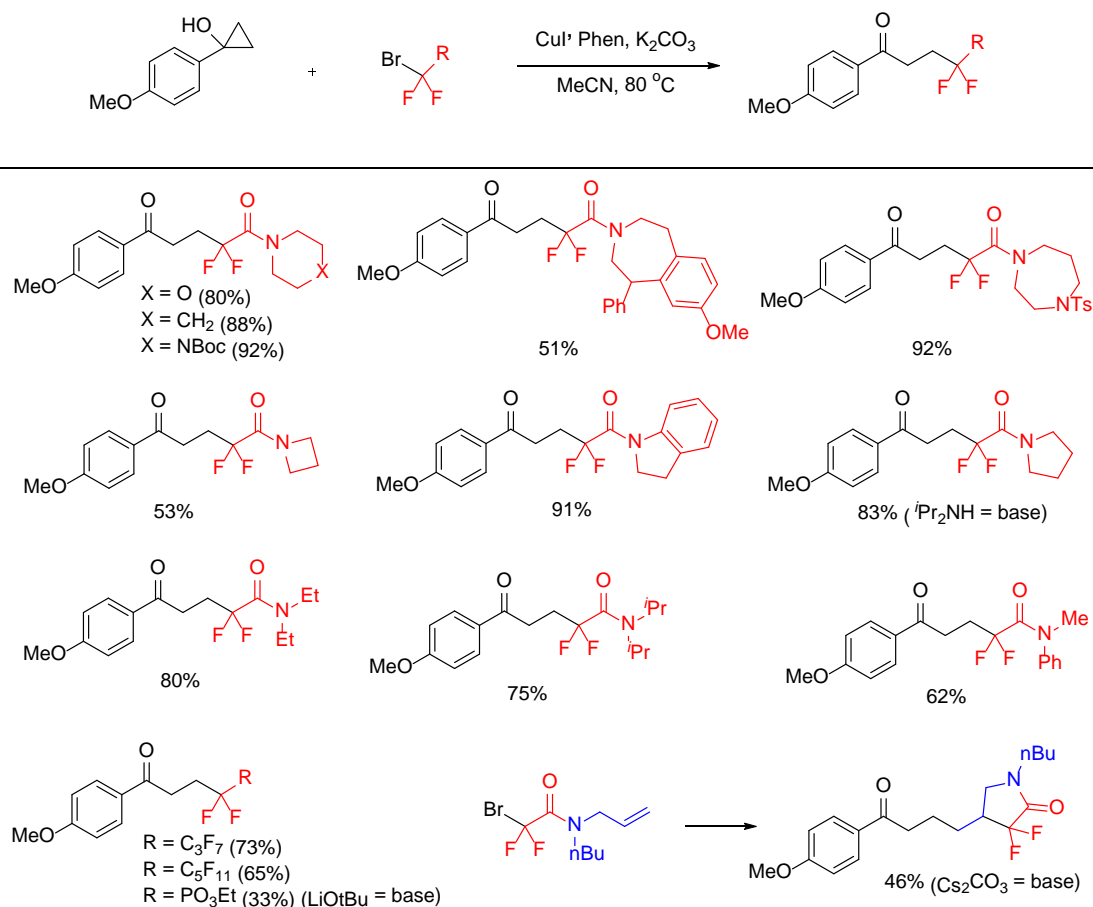
Scheme 4.12 Final products of cyclopropanol difluorination using various difluoro-bromo-amides.

4.3   Experimental

General Methods: NMR spectra were recorded on Bruker spectrometers (^{1}H at 400 MHz, 500 MHz, 800 MHz and ^{13}C at 100 MHz, 125 MHz, 200 MHz). Chemical shifts (δ) were given in ppm with reference to solvent signals [^{1}H NMR: CHCl$_3$ (7.26); ^{13}C NMR: CDCl$_3$ (77.2), C$_6$D$_6$ (128.02), CD$_3$OD (49.0)]. Column chromatography was performed on silica gel. All reactions sensitive to air or moisture were conducted under argon atmosphere in dry and freshly distilled solvents under anhydrous conditions, unless otherwise noted. Anhydrous THF and toluene were distilled over sodium benzophenone ketyl under Argon. Anhydrous CH$_2$Cl$_2$ was distilled over calcium hydride under Argon. All other solvents and reagents were used as obtained from commercial sources without further purification. General procedure for alkylation of cyclopropanols:
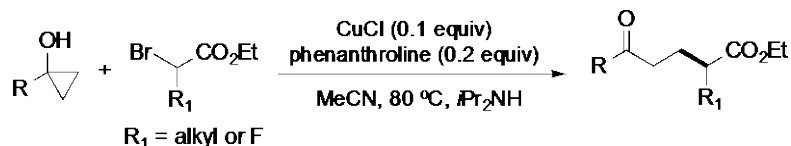
Under argon atmosphere, a mixture of cyclopropanol (0.2 mmol), ethyl 2-bromoester (0.8 mmol), CuCl (0.02 mmol), phenanthroline (0.04 mmol), and ^{i}Pr$_2$NH (0.2 mmol) in 1 mL MeCN was stirred at 80 °C for 16 h. The reaction was quenched with 2 mL ammonium chloride. The organic layer was separated, and the aqueous layer was extracted with EtOAc three times. The combined organic extracts were washed with aq. NaCl three times, dried over Na$_2$SO$_4$, concentrated in vacuo, and purified by silica gel column chromatography to give the desired product.
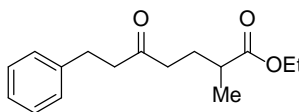
38.9 mg, 74% yield, colorless oil, purified with 5% EtOAc in hexanes; ^{1}H NMR (500 MHz, CDCl$_3$) δ 7.28 – 7.26 (m, 2H), 7.20 – 7.16 (m, 3H), 4.11 (q, J = 7.13 Hz, 2H), 2.89 (t, J = 7.8 Hz, 2H), 2.72 (t, J = 7.9 Hz, 2H), 2.43 – 2.39 (m, 3H), 1.87 – 1.84 (m, 1H), 1.74 – 1.73 (m, 1H), 1.24 (t, J = 7.1 Hz, 3H), 1.14 (d, J = 7.0 Hz, 3H); ^{13}C NMR (125 MHz, CDCl$_3$) δ 209.3, 176.2, 141.1, 128.6, 128.4, 126.2, 60.4, 44.4, 40.4, 38.8, 29.9, 27.4, 17.3, 14.4; IR (cm^{-1}) (neat): v = 1714, 1496, 1453, 1411, 1373, 1260 1177, 1094, 1029, 859 cm^{-1}; GC-MS (EI) [M]$^+$: m/z calcd for C$_{16}$H$_{22}$O$_3$: 262.16, found 262.15.
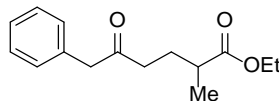
33.3 mg, 67% yield, colorless oil, purified with 5% EtOAc in hexanes; ^{1}H NMR (500 MHz, CDCl$_3$) δ 7.36 – 7.26 (m, 5H), 4.10 (q, J = 7.2 Hz, 2H), 3.70 (s, 2H), 2.52 – 2.39 (m, 3H), 1.91 – 1.72 (m, 2H), 1.25 (t, J = 7.1 Hz, 3H), 1.13 (d, J = 7.0 Hz, 3H); ^{13}C NMR (125 MHz, CDCl$_3$) δ 207.7, 176.2, 134.3, 129.5, 128.8, 127.2, 60.4, 50.3, 39.4, 38.8, 27.5, 17.3, 14.4; IR (cm^{-1}) (neat): v = 2977, 2937, 1729, 1262, 1183, 1096, 1030 cm^{-1}; GC-MS (EI) m/z calcd for C$_{15}$H$_{20}$O$_3$: 248.14, found 248.15.
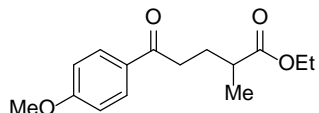
39.8 mg, 75% yield, colorless oil, purified with 5% EtOAc in hexanes; ^{1}H NMR (500 MHz, CDCl$_3$) δ 7.94 (d, J = 8.8 Hz, 2H), 6.93 (d, J = 8.8 Hz, 2H), 4.14 (q, J = 7.1 Hz, 2H), 3.86 (s, 3H), 3.01 – 2.88 (m, 2H), 2.57 – 2.52 (m, 1H), 2.08 – 2.00 (m, 1H), 1.94 – 1.88 (m, 1H), 1.24 (t, J = 7.1 Hz, 1H), 1.20 (d, J = 7.0 Hz, 1H); ^{13}C NMR (125 MHz, CDCl$_3$) δ 198.3, 176.4, 163.6, 130.4, 130.1, 113.8, 60.5, 55.6, 39.1, 35.9, 28.3, 17.5, 14.4; IR (cm^{-1}) (neat): v = 1728, 1678, 1574, 1453, 1416, 1370, 1257, 1170, 1112, 983, 841cm^{-1}; GC-MS (EI) [M]$^+$: m/z calcd for C$_{15}$H$_{20}$O$_4$: 264.14, found 264.15.
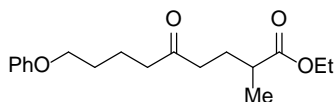
37.9 mg, 62% yield, colorless oil, purified with 5% EtOAc in hexanes; ^{1}H NMR (500 MHz, CDCl$_3$) δ 7.28 – 7.24 (m, 2H), 6.94 – 6.86 (m, 3H), 4.12 (q, J = 7.1 Hz, 2H), 3.95 (t, J = 5.8 Hz, 2H), 2.49 – 2.42 (m, 5H), 1.91 – 1.83 (m, 1H), 1.77 – 1.71 (m, 5H), 1.25 (t, J = 7.1 Hz, 3H), 1.15 (d, J = 7.0, 3H); ^{13}C NMR (125 MHz, CDCl$_3$) δ 210.0, 176.2, 159.0, 129.5, 120.7, 114.5, 67.5, 60.4, 42.4, 40.2, 38.9, 28.8, 27.5, 20.5, 17.3, 14.4; IR (cm^{-1}) (neat): v = 1727, 1713, 1600, 1377, 1243, 1172, 1080, 1036 cm^{-1}; GC-MS (EI) [M]$^+$: m/z calcd for C$_{18}$H$_{26}$O$_4$: 306.18, found 306.20.
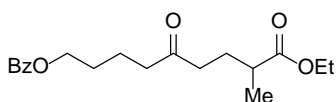
42.0 mg, 65% yield, colorless oil, purified with 5% EtOAc in hexanes; ^{1}H NMR (500 MHz, CDCl$_3$) δ 8.04 – 8.03 (m, 2H), 7.57 – 7.42 (m, 3H), 4.34 – 4.31 (m, 2H), 4.12 (q, J = 7.1 Hz, 2H), 2.50 – 2.42 (m, 5H), 1.94 – 1.72 (m, 6H), 1.25 (t, J = 7.1 Hz, 3H), 1.15 (d, J = 7.0 Hz, 3H); ^{13}C NMR (125 MHz, CDCl$_3$) δ 209.8, 176.2, 166.7, 133.0, 130.4, 129.6, 128.4, 64.6, 60.4, 42.2, 40.3, 38.9, 28.3, 27.5, 20.3, 17.3, 14.3; IR (cm^{-1}) (neat): v = 1714, 1602, 1452, 1314, 1271, 1176, 1111, 1070, 963, 859 cm^{-1}; GC-MS (EI) [M]$^+$: m/z calcd for C$_{19}$H$_{26}$O$_5$: 334.18, found 334.20.
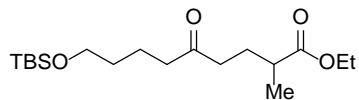
48.2 mg, 62% yield, colorless oil, purified with 5% EtOAc in hexanes; ^{1}H NMR (500 MHz, CDCl$_3$) δ 4.10 (q, J = 7.1 Hz, 2H), 3.57 (t, J = 6.3 Hz, 2H), 2.42-2.38 (m, 5H), 1.88 – 1.80 (m, 1H), 1.75 – 1.69 (m, 1H), 1.62 – 1.56 (m, 2H), 1.49 – 1.44 (m, 2H), 1.22 (t, J = 7.1 Hz, 3H), 1.13 (d, J = 7.0 Hz, 3H), 0.86 (s, 9H), 0.01 (s, 6H); ^{13}C NMR (125 MHz, CDCl$_3$) δ 210.3, 176.2, 62.9, 60.4, 42.7, 40.1, 38.9, 32.3, 27.5, 26.0, 20.4, 18.4, 17.3, 14.3, -5.2; IR (cm^{-1}) (neat): v = 1730, 1462, 1378, 1254, 1179, 1096, 1051, 1006, 835 cm^{-1}; GC-MS (EI) [M]$^+$: m/z calcd for C$_{18}$H$_{36}$O$_4$Si: 344.24, found 344.25.
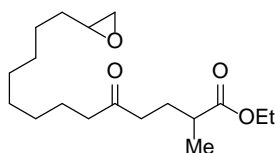
44.4 mg, 71% yield, colorless oil, purified with 5% EtOAc in hexanes; ^{1}H NMR (500 MHz, CDCl$_3$) δ 4.11 (q, J = 7.1 Hz, 2H), 2.90 – 2.87 (m, 1H), 2.74 – 2.72 (m, 1H), 2.45 – 2.35 (m, 6H), 1.88 – 1.82 (m, 1H), 1.77-1.70 (m, 1H), 1.51 – 1.23 (m, 17H), 1.15 (d, J = 7.0 Hz, 3H); ^{13}C NMR (125 MHz, CDCl$_3$) δ 210.6, 176.3, 60.4, 52.5, 47.2, 43.0, 40.2, 38.9, 32.6, 29.4, 29.4, 29.3, 27.5, 26.1, 23.9, 17.3, 14.4; IR (cm^{-1}) (neat): v = 1714, 1463, 1410, 1375, 1259, 1177, 1094, 1051, 1026, 834 cm^{-1}; GC-MS (EI) [M]$^+$: m/z calcd for C$_{18}$H$_{32}$O$_4$: 312.23, found 312.25.
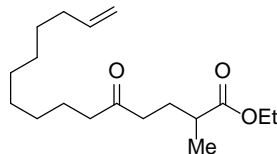
41.1 mg, 62% yield, colorless oil, purified with 5% EtOAc in hexanes; ^{1}H NMR (500 MHz, CDCl$_3$) δ 5.83 – 5.75 (m, 1H), 4.99 – 4.91 (m, 2H), 4.12 (q, J = 7.1 Hz, 2H), 2.44 – 2.35 (m, 5H), 2.04 – 2.00 (m, 2H), 1.89 – 1.82 (m, 1H), 1.77 – 1.70 (m, 1H), 1.55 – 1.53 (m, 2H), 1.37 – 1.34 (m, 2H), 1.26 – 1.23 (m, 11H), 1.15 (d, J = 7.0 Hz, 3H); ^{13}C NMR (125 MHz, CDCl$_3$) δ 210.6, 176.3, 139.3, 114.3, 60.4, 43.0, 40.2, 38.9, 33.9, 29.5, 29.4, 29.3, 29.2, 29.0, 27.6, 24.0, 17.3, 14.4; IR (cm^{-1}) (neat): v = 1730, 1462, 1453, 1376, 1257, 1177, 1027, 994, 909 cm^{-1}; GC-MS (EI) [M]$^+$: m/z calcd for C$_{18}$H$_{32}$O$_3$: 296.24, found 296.25.
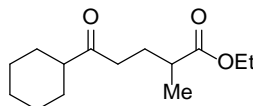
39.6 mg, 70% yield, colorless oil, purified with 5% EtOAc in hexanes; ^{1}H NMR (500 MHz, CDCl$_3$) δ 4.11 (q, J = 7.1 Hz, 2H), 2.45 – 2.41 (m, 3H), 2.32 – 2.27 (m, 1H), 1.86 – 1.68 (m, 6H), 1.33 – 1.20 (m, 9H), 1.30 (d, J = 7.0 Hz, 3H); ^{13}C NMR (125 MHz, CDCl$_3$) δ 213.4, 176.3, 60.4, 51.0, 38.9, 38.0, 28.6, 28.6, 27.5, 25.9, 25.8, 17.3, 14.4; IR (cm^{-1}) (neat): v = 1707, 1450, 1376, 1245, 1160, 1096, 1053, 1026, 991 cm^{-1}; GC-MS (EI) [M]$^+$: m/z calcd for C$_{14}$H$_{24}$O$_3$: 240.17, found 240.20.
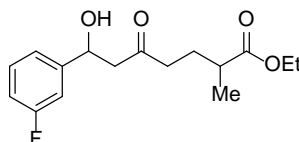
31.2 mg, 53% yield, colorless oil, purified with 5% EtOAc in hexanes. ^{1}H NMR (500 MHz, CDCl$_3$) δ 7.31 – 7.26 (m, 1H), 7.10 – 7.07 (m, 2H), 6.96 – 6.93 (m, 1H), 5.15 – 5.13 (m, 1H), 4.11 (q, J = 7.1 Hz, 2H), 3.45 (br s, 1H), 2.84 – 2.74 (m, 2H), 2.49 – 2.40 (m, 3H), 1.90 – 1.73 (m, 2H), 1.23 (t, J = 7.1 Hz, 3H), 1.15 (d, J = 7.0 Hz, 3H); ^{13}C NMR (125 MHz, CDCl$_3$) δ 210.3, 176.2, 163.2 (d, J = 246.0 Hz), 145.6 (d, J = 6.8 Hz), 130.2(d, J = 8.1 Hz), 121.2, 114.5(d, J = 21.2 Hz), 112.7(d, J = 22.0 Hz), 69.4, 60.6, 51.2, 41.1, 38.8, 27.2, 17.3, 14.3, 14.23; IR (cm^{-1}) (neat): v = 3492, 1711, 1693, 1680, 1613, 1462, 1451, 1433, 1378, 1245.9, 1184, 1133, 1047, 874cm^{-1}; GC-MS (EI) [M][+]: m/z calcd for C$_{16}$H$_{21}$FO$_4$: 296.14, found 296.15.
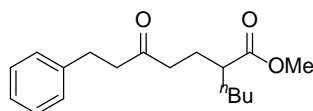

43 mg, 51% yield, colorless oil, purified with 5% EtOAc in hexanes; ^{1}H NMR (500 MHz, CDCl$_3$) δ 7.28 – 7.16 (m, 5H), 3.65 (s, 3H), 2.88 (t, J = 7.6 Hz, 2H), 2.71 (t, J = 7.6 Hz, 2H), 2.41 – 2.30 (m, 3H), 1.82 – 1.76 (m, 2H), 1.62 – 1.58 (m, 1H), 1.44 – 1.41 (m, 1H), 1.31 – 1.21 (m, 4H), 0.87 (t, J = 7.1 Hz, 3H); ^{13}C NMR (125 MHz, CDCl$_3$) δ 209.2, 176.4, 141.1, 128.6, 128.4, 126.2, 51.5, 44. 8, 44.4, 40.5, 32.2, 29.8, 29.5, 25.9, 22.6, 14.0; IR (cm^{-1}) (neat): v = 1714, 1693, 1453, 1192, 1165 cm^{-1}; GC-MS (EI) [M][+]: m/z calcd for C$_{19}$H$_{26}$O$_3$: 296.18, found 296.30.

General Procedure for mono-fluorination:

In a flame dried vial starting cyclopropanol (0.2 mmol) was combined with copper (I) iodide (0.02 mmol, 3.8 mg), 1,10-phenanthroline (0.04 mmol, 7.2 mg), and 2 mL anhydrous acetonitrile (0.1 M). The solution was purged with argon gas before the addition

of ethyl 2-bromo-2-fluoroacetate (0.8 mmol, 100 μL) and diisopropyl amine (0.4 mmol, 60 μL). The resulting solution was stirred at 80 ˚C for 16 hours then quenched with 2 mL ammonium chloride. The mixture was extracted three times with ethyl acetate then washed with brine before being dried over sodium sulfate. Rotary evaporation of the organic phase resulted in a red-brown liquid which was purified with silica based flash chromatography using 20:1 hexane: ethyl acetate as the eluent.
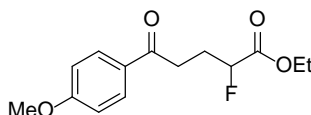
29.5 mg, 66% yield, yellow oil, CuI as catalyst, purified with 25:1 hexanes:EtOAc; ^{1}H NMR (500 MHz, CDCl$_3$) δ 7.94 (d, J = 8.8 Hz, 2H), 6.93 (d, J = 8.8 Hz, 2H), 5.04 (ddd, J = 49.1, 7.8, 4.2 Hz, 1H), 4.26 (q, J = 7.1 Hz, 2H), 3.87 (s, 3H), 3.19 – 3.05 (m, 2H), 2.53 – 2.17 (m, 2H), 1.30 (t, J = 7.1 Hz, 3H); ^{13}C NMR (125 MHz, CDCl$_3$) δ 196.9 (s), 169.7 (d, J = 23.9 Hz), 163.8, 130.4, 129.8, 113.9, 88.2 (d, J = 183.3 Hz), 61.7, 55.6, 32.9, 27.0 (d, J = 20.9 Hz), 14.3; ^{19}F NMR (470 MHz, CDCl$_3$) δ -192.9 (td, J = 49.3, 27.3 Hz); IR (cm^{-1}) (neat): v = 1757, 1677, 1600, 1258, 1214, 1170, 1027; MS (ESI): m/z 291.3 [M+Na]$^+$.
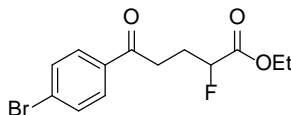
36.0 mg, 58% yield, yellow oil, CuI as catalyst, purified with 25:1 hexanes:EtOAc; ^{1}H NMR (500 MHz, CDCl$_3$) δ 7.84 – 7.81 (m, 2H), 7.63 – 7.59 (m, 2H), 5.04 (ddd, J = 49.0, 7.7, 4.3 Hz, 1H), 4.27 (qd, J = 7.1, 1.4 Hz, 1H), 3.21 – 3.08 (m, 1H), 2.50 – 2.38 (m, 1H), 2.38 – 2.25 (m, 1H), 1.31 (t, J = 7.1 Hz, 1H); ^{13}C NMR (125 MHz, CDCl$_3$) δ 197.4, 169.6 (d, J = 23.7 Hz), 135.4, 132.2, 129.7, 128.7, 88.0 (d, J = 183.7 Hz), 61.9, 32.9, 26.7 (d, J = 20.9 Hz), 14.3; ^{19}F NMR (470 MHz, CDCl$_3$) δ -194.10 (m, 1F); IR (cm^{-1}) (neat): v = 1757, 1688, 1586, 1569, 1484, 1398, 1271, 1178, 1096, 1071, 1027, 1010, 989 cm^{-1}; GC-MS (EI) [M]$^+$: m/z calcd for C$_{13}$H$_{14}$BrFO$_3$: 316.01, found 316.05.
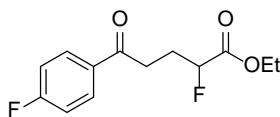
25.1 mg, 50 % yield, yellow oil, CuI as catalyst, purified with 25:1 hexanes:EtOAc; ^{1}H NMR (500 MHz, CDCl$_3$) δ 8.10 – 7.98 (m, 2H), 7.15 – 7.12 (m, 2H), 5.04 (ddd, J = 49.0, 7.7, 4.3 Hz, 1H), 4.27 (qd, J = 7.1, 1.1 Hz, 2H), 3.22 – 3.08 (m, 2H), 2.50 – 2.38 (m, 1H), 2.34 – 2.22 (m, 1H), 1.31 (t, J = 7.1 Hz, 1H); ^{13}C NMR (125 MHz, CDCl$_3$) δ196.8, 169.5 (d, J = 23.8 Hz), 166.0 (d, J = 255.0 Hz), 133.1, 130.8 (d, J = 9.2 Hz), 115.9 (d, J = 21.9 Hz), 88.1 (d, J = 183.6 Hz), 61.8, 32.9, 26.7 (d, J = 20.9 Hz), 14.3; ^{19}F NMR (470 MHz, CDCl$_3$) δ -105.96 (m, 1F), -194.11 (m, 1F); IR (cm^{-1}) (neat): v = 1756, 1685, 15977, 1445, 1372, 1298, 1269, 1157, 1024, 991 cm^{-1}; GC-MS (EI) [M]$^+$: m/z calcd for C$_{13}$H$_{14}$F$_2$O$_3$: 256.09, found 256.10.

General procedure for the synthesis of 2-bromo-2,2-difluoroamides:
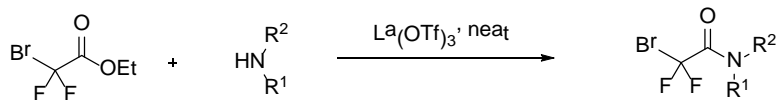
Under argon atmosphere, a 20 mL tube equipped with a magnetic stir bar was charged with lanthanum trifluoromethanesulfonate (0.05 equiv). Ethyl bromodifluoroacetate (1.2 equiv) and amine (1.0 equiv) were added. The mixture was stirred at the room temperature and monitored by TLC. After the amine was consumed, the mixture was concentrated and purified by silica gel column chromatography to give the desired product.

The starting materials **15a**[2], **15b**[2], **15c**[2], **15g**[3], **15i**[4] and **15f**[5] are prepared according to previously reported literature[2].
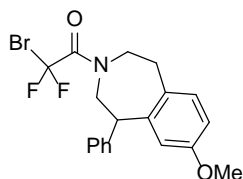
1.902 g, 90% yield, white solid; ^{1}H NMR (500 MHz, CDCl$_3$, a mixture of rotamers) δ 7.42 – 7.18 (m, 3H), 7.16 – 7.06 (m, 3H), 6.76 – 6.66 (m, 1H), 6.59 – 6.54 (m, 0.63 H), 6.39 – 6.36 (m, 0.33 H), 4.64 – 4.61 (m, 1H), 4.46 – 4.21 (m, 2H), 3.97 – 3.82 (m, 1H), 3.80 – 3.62 (m, 4H), 3.32 – 3.10 (m, 1H), 3.04 – 2.82 (m, 1H); ^{13}C NMR (125 MHz, CDCl$_3$, rotamer) δ 159.3 (t, J = 26.4 Hz), 159.0 (t, J = 35.4 Hz), 142.0, 141.8, 141.6, 141.6, 131.5, 131.4, 130.1, 129.2, 129.1, 128.8, 128.2, 127.9, 127.3, 127.0, 116.7, 116.6, 112.3, 111.8, 111.1 (t, J = 309.8 Hz), 110.7 (t, J = 310.8 Hz), 55.2, 52.2, 51.8, 50.0, 49.8, 48.9, 47.8, 33.6, 33.1; ^{19}F NMR (470 MHz, CDCl$_3$, rotamer) δ -55.31 (dd, J = 543.7, 157.9 Hz), -55.02 (dd, J = 985.0, 158.6 Hz); IR (cm^{-1}) (neat): v = 1661, 1502, 1453, 1152, 1128, 1043, 941; MS (ESI): m/z 432.2 [M+Na]$^+$.
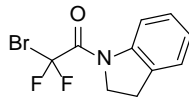
1.000g, 87% yield, white solid; ^{1}H NMR (500 MHz, CDCl$_3$) δ 8.21 (d, J = 8.4 Hz, 1H), 7.28 – 7.25 (m, 2H), 7.17 – 7.14 (m, 1H), 4.32 – 4.29 (m, 2H), 3.25 (t, J = 8.2 Hz, 2H); ^{13}C NMR (125 MHz, CDCl$_3$) δ156.6 (t, J = 27.8 Hz), 142.0, 131.6, 127.8, 125.8, 124.8, 118.7, 111.1 (t, J = 315.4 Hz), 49.0 (t, J = 4.8 Hz), 28.70; ^{19}F NMR (470 MHz, CDCl$_3$) δ -58.0; IR (cm^{-1}) (neat): v = 1678, 1481, 1464, 1412, 1176, 1149, 1072, 925; MS (ESI): m/z 298.2 [M+Na]$^+$.
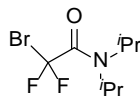
529 mg, 83% yield, white solid; ^{1}H NMR (500 MHz, CDCl$_3$) δ 4.38 (hept, J = 6.6 Hz, 1H), 3.50 (hept, J = 6.8 Hz, 1H), 1.43 (s, 3H), 1.41 (s, 3H), 1.26 (s, 3H), 1.24 (s, 3H); ^{13}C NMR (125 MHz, CDCl$_3$) δ157.50 (t, J = 25.6 Hz), 111.1 (t, J = 314.7 Hz), 49.68, 47.41, 19.96, 19.58; ^{19}F NMR (470 MHz, CDCl$_3$) δ -54.3; IR (cm^{-1}) (neat): v = 1671, 1447, 1376, 1343, 1154, 1141, 1131, 1033; MS (ESI): m/z 280.2 [M+Na]$^+$.
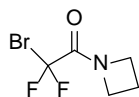
121 mg, 20% yield, colorless oil; ^{1}H NMR (500 MHz, CDCl$_3$) δ 4.37 (t, J = 7.8 Hz, 2H), 4.13 (t, J = 7.9 Hz, 2H), 2.50 – 2.30 (m, 2H); ^{13}C NMR (125 MHz, CDCl$_3$) δ158.5 (t, J = 27.6 Hz), 111.3 (t, J = 316.3 Hz), 52.91, 49.37, 16.34; ^{19}F NMR (470 MHz, CDCl$_3$) δ -57.8; IR (cm^{-1}) (neat): v = 1687, 1441, 1186, 1115, 1007, 947; MS (ESI): m/z 236.3 [M+Na]$^+$.
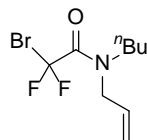
502 mg, 92% yield, colorless oil; ^{1}H NMR (500 MHz, CDCl$_3$, rotamer) δ 6.00 – 5.66 (m, 1H), 5.28 – 5.21 (m, 2H), 4.04 (dd, J = 33.5, 5.6 Hz, 2H), 3.56 – 3.23 (m, 2H), 1.75 – 1.50 (m, 2H), 1.40 – 1.24 (m, 2H), 0.95 – 0.92 (m, 3H); ^{13}C NMR (125 MHz, CDCl$_3$, rotamer) δ, 159.22 (t, J = 26.4 Hz), 159.16 (t, J = 26.2 Hz), 132.28, 131.40, 118.91, 118.22, 111.2 (t, J = 314.9 Hz),111.1 (t, J = 314.9 Hz), 50.9, 49.5, 48.1, 46.8, 30.5, 28.6, 20.1, 20.0, 13.9, 13.8; ^{19}F NMR (470 MHz, CDCl$_3$, , rotamer) δ -55.2, -55.3; IR (cm^{-1}) (neat): v =1681, 1444, 1168, 1139, 1114, 928; MS (ESI): m/z 292.2 [M+Na]$^+$.

Genaral procedure for difluoralkylation of cyclopropanols:
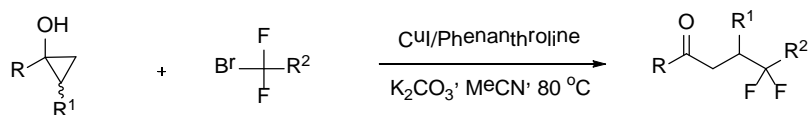
Under argon atmosphere, cyclopropanol (0.1 mmol), difluoroalkyl halide (0.4 mmol), CuI (0.01 mmol), Phenanthroline (0.02 mmol), and K$_2$CO$_3$ (0.2 mmol) in 1 mL MeCN was stirred at 80 °C for 10-12 h. The reaction was then quenched by the water. The organic layer was separated and extracted with EtOAc three times. The combined organic extracts were washed with aq. NaCl three times, dried over Na$_2$SO$_4$, concentrated in vacuo, and purified by silica gel column chromatography to give the desired product.
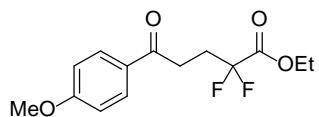
760 mg (3.0 mmol starting material was used) 89% yield, white solid; ^{1}H NMR (500 MHz, CDCl$_3$) δ 8.05 – 7.86 (m, 2H), 7.03 – 6.81 (m, 2H), 4.32 (q, J = 7.1 Hz, 2H), 3.87 (s, 3H), 3.25 – 3.08 (m, 2H), 2.66 – 2.43 (m, 2H), 1.34 (t, J = 7.2 Hz, 3H); ^{13}C NMR (123 MHz, CDCl$_3$) δ 195.7, 164.2 (t, J = 32.6 Hz), 163.9, 130.4, 129.5, 116.1 (t, J = 250.0 Hz), 113.97, 63.1, 55.6, 30.4, 29.2 (t, J = 23.7 Hz), 14.1; ^{19}F NMR (470 MHz, CDCl$_3$) δ -106.3 (t, J = 17.2 Hz); IR (cm^{-1}) (neat): v = 1763, 1679, 1600, 1511, 1259, 1170, 1093, 1029; MS (ESI): m/z 309.2 [M+Na]$^+$.
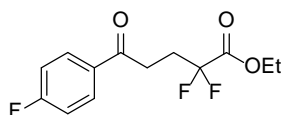
22.2 mg, 81% yield, white solid; ^{1}H NMR (500 MHz, CDCl$_3$) δ 8.08 – 7.90 (m, 2H), 7.17 – 7.08 (m, 2H), 4.32 (q, J = 7.1 Hz, 2H), 3.27 – 3.12 (m, 2H), 2.59 – 2.43 (m, 2H), 1.34 (t, J = 7.2 Hz, 3H); ^{13}C NMR (125 MHz, CDCl$_3$) δ 195.56, 166.1 (d, J = 255.4 Hz), 164.0 (t, J = 32.7 Hz), 132.8, 130.8 (d, J = 9.3 Hz), 116.0 (d, J = 21.9 Hz), 115.9 (t, J = 248.6 Hz), 63.2, 30.7, 29.0 (t, J = 23.8 Hz), 14.0; ^{19}F NMR (470 MHz, CDCl$_3$) δ -104.6, -106.3 (t, J = 17.2 Hz); IR (cm^{-1}) (neat): v = 1761, 1688, 1598, 1286, 1158, 10985, 1045; MS (ESI): m/z 297.2 [M+Na]$^+$.
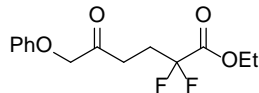
21.7 mg, 76% yield, colorless oil; ^{1}H NMR (500 MHz, CDCl$_3$) δ 7.37 – 7.26 (m, 2H), 7.06 – 6.84 (m, 3H), 4.57 (s, 2H), 4.31 (q, *J* = 7.1 Hz, 2H), 2.99 – 2.79 (m, 2H), 2.48 – 2.32 (m, 2H), 1.34 (t, *J* = 7.2 Hz, 3H); ^{13}C NMR (125 MHz, CDCl$_3$) δ 205.3, 163.9 (t, *J* = 32.6 Hz), 157.7, 129.9, 122.1, 115.6 (d, *J* = 250.4 Hz), 114.6, 72.8, 63.2, 31.5, 28.0 (t, *J* = 24.1 Hz), 14.0; ^{19}F NMR (470 MHz, CDCl$_3$) δ -106.4 (t, *J* = 17.0 Hz); IR (cm^{-1}) (neat): *v* = 1762, 1728, 1241, 1206, 1101, 1054; MS (ESI): *m/z* 309.3 [M+Na]$^+$.
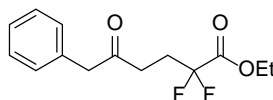
22.9 mg, 85% yield, colorless oil; ^{1}H NMR (500 MHz, CDCl$_3$) δ 7.43 – 7.16 (m, 5H), 4.31 (q, *J* = 7.1 Hz, 2H), 3.74 (s, 2H), 2.79 – 2.65 (m, 2H), 2.45 – 2.30 (m, 2H), 1.34 (t, *J* = 7.2 Hz, 3H); ^{13}C NMR (125 MHz, CDCl$_3$) δ 205.4, 164.0 (t, *J* = 32.7 Hz), 133.8, 129.5, 129.0, 127.4, 115.7 (t, *J* = 250.2 Hz), 63.1, 50.2, 33.9, 28.6 (t, *J* = 23.9 Hz), 14.0; ^{19}F NMR (470 MHz, CDCl$_3$) δ -106.5 (t, *J* = 17.1 Hz); IR (cm^{-1}) (neat): *v* =1764, 1721, 1308, 1191, 1085, 1063; MS (ESI): *m/z* 293.2 [M+Na]$^+$.
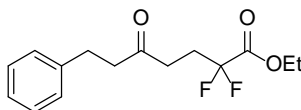
22.0 mg, 77% yield, colorless oil; ^{1}H NMR (500 MHz, CDCl$_3$) δ 7.40 – 7.12 (m, 5H), 4.33 (q, *J* = 7.1 Hz, 2H), 2.93 (t, *J* = 7.6 Hz, 2H), 2.80 (t, *J* = 7.6 Hz, 2H), 2.71 – 2.60 (m, 2H), 2.45 – 2.29 (m, 2H), 1.37 (t, *J* = 7.2 Hz, 3H); ^{13}C NMR (125 MHz, CDCl$_3$) δ 206.9, 164.0 (t, *J* = 32.8 Hz), 140.8, 128.7, 128.4, 126.3, 115.7 (t, *J* = 250.2 Hz), 63.1, 44.4, 34.8, 29.8, 28.5 (t, *J* = 24.0 Hz), 14.0; ^{19}F NMR (470 MHz, CDCl$_3$) δ -106.5 (t, *J* = 17.1 Hz); IR (cm^{-1}) (neat): *v* = 1768, 1718, 1279, 1192, 1095, 1043, 1013; MS (ESI): *m/z* 307.3 [M+Na]$^+$.
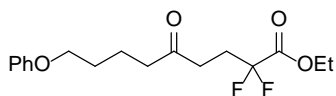
21.3 mg, 65% yield, colorless oil; ^{1}H NMR (500 MHz, CDCl$_3$) δ 7.36 – 7.21 (m, 2H), 7.01 – 6.87 (m, 3H), 4.34 (q, J = 7.1 Hz, 2H), 3.98 (t, J = 5.7 Hz, 2H), 2.72 – 2.29 (m, 6H), 1.88 – 1.72 (m, 4H), 1.38 (t, J = 7.2 Hz, 3H); ^{13}C NMR (125 MHz, CDCl$_3$) δ 207.6, 164.1 (t, J = 32.6 Hz), 1590. 129.6, 120.8, 115.8 (t, J = 249.9 Hz), 114.6, 67.4, 63.1, 42.4, 34.5, 28.8, 28.6 (t, J = 23.8 Hz), 20.6, 14.1; ^{19}F NMR (470 MHz, CDCl$_3$) δ -106.5 (t, J = 17.1 Hz); IR (cm^{-1}) (neat): v = 1764, 1718, 1244, 1194, 1100, 1048; MS (ESI): m/z 351.3 [M+Na]$^+$.
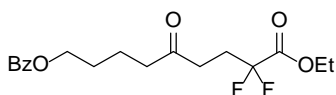
26.5 mg, 74% yield, colorless oil; ^{1}H NMR (500 MHz, CDCl$_3$) δ 8.11 – 7.95 (m, 2H), 7.56 – 7.41 (m, 3H), 4.37 – 4.24 (m, 4H), 2.67 – 2.64 (m, 2H), 2.52 (t, J = 6.8 Hz, 2H), 2.43 – 2.29 (m, 2H), 1.83 – 1.72 (m, 4H), 1.34 (t, J = 7.1 Hz, 3H); ^{13}C NMR (125 MHz, CDCl$_3$) δ 207.3, 166.7, 164.0 (t, J = 32.7 Hz), 133.0, 130.4, 129.6, 128.5, 115.7 (t, J = 250.2 Hz), 64.5, 63.1, 42.2, 34.6, 28.5 (t, J = 23.9 Hz), 28.3, 20.3, 14.0; ^{19}F NMR (470 MHz, CDCl$_3$) δ -106.5 (t, J = 17.1 Hz); IR (cm^{-1}) (neat): v = 1764, 1716, 1274, 1100, 1070; MS (ESI): m/z 379.3 [M+Na]$^+$.
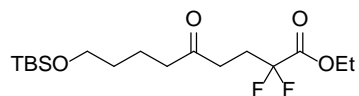
299.7 mg (1.0 mmol starting material was used), 82% yield, colorless oil;^{1}H NMR (500 MHz, CDCl$_3$) δ 4.30 (q, J = 7.1 Hz, 2H), 3.60 (t, J = 6.3 Hz, 2H), 2.64 (t, J = 7.5 Hz, 2H), 2.48 – 2.29 (m, 4H), 1.66 – 1.60 (m, 2H), 1.53 – 1.45 (m, 2H), 1.34 (t, J = 7.1 Hz, 3H), 0.88 (s, 9H), 0.03 (s, 6H); ^{13}C NMR (125 MHz, CDCl$_3$) δ 207.9, 164.1 (t, J = 32.8 Hz), 115.8 (t, J = 250.1 Hz), 63.1, 62.8, 42.7, 34.5, 32.3, 28.6 (t, J = 23.9 Hz), 26.1, 20.4, 18.4, 14.1, -5.2; ^{19}F NMR (470 MHz, CDCl$_3$) δ -106.5 (t, J = 17.2 Hz); IR (cm^{-1}) (neat): v = 1767, 1721, 1256, 1193, 1097, 1058; MS (ESI): m/z 389.4 [M+Na]$^+$.
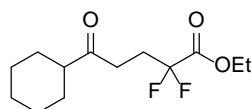
37.0 mg (0.2 mmol starting material was used), 71% yield, colorless oil; ^{1}H NMR (500 MHz, CDCl$_3$) δ 4.30 (q, J = 7.2 Hz, 2H), 2.72 – 2.61 (m, 2H), 2.43 – 2.19 (m, 3H), 1.86 – 1.61 (m, 5H), 1.39 – 1.17 (m, 8H); ^{13}C NMR (125 MHz, CDCl$_3$) δ 211.0, 164.1 (t, J = 32.7 Hz), 115.9 (t, J = 250.0 Hz), 63.0, 50.9, 32.4, 28.6, 28.6 (t, J = 23.8 Hz), 25.9, 25.7, 14.0; ^{19}F NMR (470 MHz, CDCl$_3$) δ -106.5 (t, J = 17.2 Hz); IR (cm^{-1}) (neat): v = 1765, 1711, 1308, 1191, 1095, 1068; MS (ESI): m/z 285.3 [M+Na]$^+$.
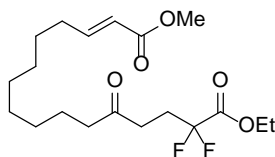
26.2 mg, 70% yield, colorless oil; ^{1}H NMR (500 MHz, CDCl$_3$) δ 6.95 (dt, J = 15.6, 7.0 Hz, 1H), 5.80 (dt, J = 15.6, 1.5 Hz, 1H), 4.31 (q, J = 7.1 Hz, 2H), 3.72 (s, 3H), 2.74 – 2.53 (m, 2H), 2.48 – 2.28 (m, 4H), 2.18 (qd, J = 7.3, 1.6 Hz, 2H), 1.59 – 1.53 (m, 2H), 1.47 – 1.40 (m, 2H), 1.34 (t, J = 7.2 Hz, 3H), 1.27 (br s, 9H); ^{13}C NMR (125 MHz, CDCl$_3$) δ 208.1, 167.3, 164.1 (t, J = 32.8 Hz), 149.8, 120.1, 115.8 (t, J = 250.0 Hz), 63.1, 51.5, 42.9, 34.5, 32.3, 29.4, 29.3, 29.2, 29.2, 28.6 (t, J = 23.9 Hz), 28.1, 23.9, 14.1; ^{19}F NMR (470 MHz, CDCl$_3$) δ -106.5 (t, J = 17.2 Hz); IR (cm^{-1}) (neat): v = 1765, 1718, 1436, 1273, 1195, 1102, 1070; MS (ESI): m/z 399.4 [M+Na]$^+$.
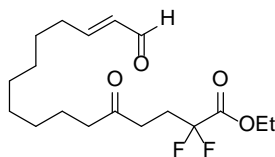
15.5 mg, 45% yield, colorless oil; ^{1}H NMR (500 MHz, CDCl$_3$) δ 9.49 (d, J = 7.9 Hz, 1H), 6.84 (dt, J = 15.6, 6.8 Hz, 1H), 6.10 (ddt, J = 15.6, 7.9, 1.4 Hz, 1H), 4.31 (q, J = 7.1 Hz, 2H), 2.65 –2.62 (m, 2H), 2.45 – 2.29 (m, 6H), 1.60 – 1.46 (m, 4H), 1.37 – 1.25 (m, 11H); ^{13}C NMR (125 MHz, CDCl$_3$) δ 208.0, 194.3, 164.1 (t, J = 32.7 Hz), 159.0, 133.1, 115.8 (t, J = 250.1 Hz), 63.1, 42.9, 34.5, 32.8, 29.3, 29.2, 29.2, 29.2, 28.6 (t, J = 23.9 Hz), 27.9, 23.8, 14.1; ^{19}F NMR (470 MHz, CDCl$_3$) δ -106.5 (t, J = 17.2 Hz); IR (cm^{-1}) (neat): v = 1765, 1718, 1689, 1191, 1100, 1014; MS (ESI): m/z 369.3 [M+Na]$^+$.
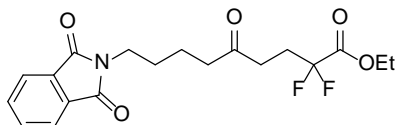
31.6 mg, 83% yield, colorless oil; ^{1}H NMR (500 MHz, CDCl$_3$) δ 7.84 – 7.82 (m, 2H), 7.74 – 7.68 (m, 2H), 4.30 (q, J = 7.1 Hz, 2H), 3.68 (t, J = 6.9 Hz, 2H), 2.67 – 2.61 (m, 2H), 2.50 (t, J = 7.2 Hz, 2H), 2.41 – 2.27 (m, 2H), 1.71 – 1.59 (m, 4H), 1.34 (t, J = 7.2 Hz, 3H); ^{13}C NMR (125 MHz, CDCl$_3$) δ 207.3, 168.5, 164.0 (t, J = 32.8 Hz), 134.1, 132.2, 123.3, 115.7 (t, J = 250.4 Hz), 63.1, 42.0 37.5, 34.6, 28.57 (t, J = 23.8 Hz), 28.0, 20.8, 14.1; ^{19}F NMR (470 MHz, CDCl$_3$) δ -106.5 (t, J = 17.1 Hz); IR (cm^{-1}) (neat): v = 1766, 1709, 1397, 1373, 1188, 1071; MS (ESI); MS (ESI): m/z 404.3 [M+Na]$^+$.
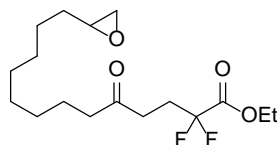
23.1 mg, 69% yield, colorless oil; ^{1}H NMR (500 MHz, CDCl$_3$) δ 4.30 (q, J = 7.2 Hz, 2H), 2.94 – 2.57 (m, 4H), 2.46 – 2.28 (m, 5H), 1.59 – 1.25 (m, 17H); ^{13}C NMR (125 MHz, CDCl$_3$) δ 208.1, 164.0 (t, J = 32.6 Hz), 115.8 (t, J = 250.0 Hz), 63.1, 52.5, 47.2, 42.9, 34.5, 32.6, 29.4, 29.4, 29.3, 29.2, 28.5 (t, J = 23.9 Hz), 26.0, 23.9, 14.0; ^{19}F NMR (470 MHz, CDCl$_3$) δ -106.5 (t, J = 17.2 Hz); IR (cm^{-1}) (neat): v =2928, 1765, 1718, 1305, 1278, 1191, 1103, 1080; MS (ESI): m/z 357.3 [M+Na]$^+$.
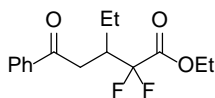
19.4 mg, 68% yield, colorless oil as a 38/1 mixture (determined by ^{1}H and ^{19}F NMR); ^{1}H NMR (500 MHz, CDCl$_3$) δ 8.01 – 7.93 (m, 2H), 7.63 – 7.45 (m, 3H), 4.35 – 4.24 (m, 2H), 3.33 (dd, J = 17.7, 4.4 Hz, 1H), 3.14 – 2.95 (m, 2H), 1.76 – 1.67 (m, 1H), 1.47 – 1.38 (m, 1H), 1.33 (t, J = 7.2 Hz, 3H), 0.95 (t, J = 7.5 Hz, 3H); ^{13}C NMR (125 MHz, CDCl$_3$) δ 197.4, 164.3 (t, J = 33.1 Hz), 136.7, 133.5, 128.8, 128.2, 117.6 (t, J = 253.2 Hz), 63.0, 39.6 (t, J = 21.3 Hz), 36.4, 21.6, 14.5, 11.5; ^{19}F NMR (470 MHz, CDCl$_3$) δ -108.3 (dd, J = 254.7, 14.6 Hz), -111.7 (dd, J = 254.7, 16.3 Hz); IR (cm^{-1}) (neat): v = 1763, 1689,1179, 1099, 1066, 1016; MS (ESI): m/z 307.3 [M+Na]$^+$.
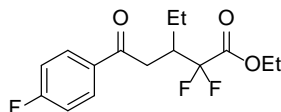
16.4 mg, 54% yield, colorless oil as a 35/1 mixture (determined by ^{1}H and ^{19}F NMR); ^{1}H NMR (500 MHz, CDCl$_3$) δ 8.05 – 7.97 (m, 2H), 7.14 (t, J = 8.5 Hz, 2H), 4.35 – 4.26 (m, 2H), 3.30 (dd, J = 17.7, 4.6 Hz, 1H), 3.12 – 2.90 (m, 2H), 1.76 – 1.65 (m, 1H), 1.45 – 1.39 (m, 1H), 1.33 (t, J = 7.1 Hz, 3H), 0.94 (t, J = 7.5 Hz, 3H); ^{13}C NMR (126 MHz, CDCl$_3$) δ 195.8, 166.0 (d, J = 255.2 Hz), 164.2 (t, J = 32.8 Hz), 133.2, 130.9 (d, J = 9.3 Hz), 11117.5 (d, J = 253.1 Hz), 115.9 (d, J = 21.9 Hz), 63.1, 39.7 (t, J = 21.3 Hz), 36.3, 21.6, 14.1, 11.5; ^{19}F NMR (470 MHz, CDCl$_3$) δ 104.8, -108.2 (dd, J = 255.0, 14.5 Hz), -111.9 (dd, J = 254.9, 16.5 Hz); IR (cm^{-1}) (neat): v = 1765, 1689, 1589, 1231,1155, 1133; MS (ESI): m/z 325.3 [M+Na]$^+$.
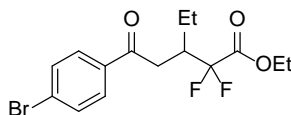
16.4 mg, 45% yield, colorless oil as a 36/1 mixture (determined by ^{1}H and ^{19}F NMR); ^{1}H NMR (500 MHz, CDCl$_3$) δ 7.84 (d, J = 8.4 Hz, 2H), 7.62 (d, J = 8.4 Hz, 2H), 4.35 – 4.26 (m, 2H), 3.29 (dd, J = 17.8, 4.7 Hz, 1H), 3.10 – 2.90 (m, 2H), 1.74 – 1.66 (m, 1H), 1.44 – 1.38 (m, 1H), 1.33 (t, J = 7.1 Hz, 3H), 0.94 (t, J = 7.5 Hz, 3H); ^{13}C NMR (125 MHz, CDCl$_3$) δ 196.4, 164.2 (t, J = 33.0 Hz), 135.4, 132.1, 129.7, 128.7, 117.4 (t, J = 253.3 Hz), 63.1, 39.7 (t, J = 21.3 Hz), 36.3, 21.6, 14.1, 11.5; ^{19}F NMR (470 MHz, CDCl$_3$) δ -108.1 (dd, J = 255.1, 14.4 Hz), -111.9 (dd, J = 255.1, 16.5 Hz); IR (cm^{-1}) (neat): v = 1762, 1690, 1585, 1177, 1069, 1008; MS (ESI) MS (ESI): m/z 385.2 [M+Na]$^+$.
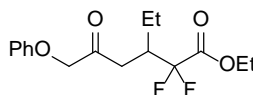
21.4 mg, 68% yield, colorless oil as a 17/1 mixture (determined by ^{1}H and ^{19}F NMR); ^{1}H NMR (500 MHz, CDCl$_3$) δ 7.33 – 7.28 (m, 2H), 7.01 (t, J = 7.4 Hz, 1H), 6.91 – 6.89 (m, 2H), 4.58 (d, J = 1.9 Hz, 2H), 4.30 (q, J = 7.1 Hz, 2H), 3.01 – 2.84 (m, 2H), 2.67 – 2.62 (m, 1H), 1.73 – 1.61 (m, 1H), 1.34 (t, J = 7.1 Hz, 3H), 0.92 (t, J = 7.5 Hz, 3H); ^{13}C NMR (125 MHz, CDCl$_3$) δ 205.1, 164.0 (t, J = 32.6 Hz), 157.6, 129.7, 121.9, 117.1 (t, J = 253.3 Hz), 114.5, 72.7, 63.0, 38.9 (t, J = 21.5 Hz), 36.7, 21.3, 13.9, 11.3; ^{19}F NMR (470 MHz, CDCl$_3$) δ -107.9 (dd, J = 255.7, 13.7 Hz), -112.4 (dd, J = 255.6, 16.3 Hz); IR (cm^{-1}) (neat): v =1760, 1755, 1599, 1496, 1240, 1064; MS (ESI): m/z 337.3 [M+Na]$^+$.
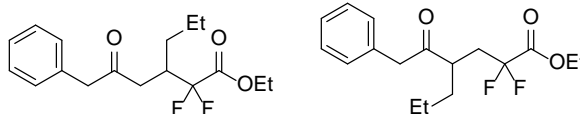
15.8 mg, 53% yield, colorless oil as a 2.4/1 mixture (determined by ^{1}H and ^{19}F NMR); ^{1}H NMR (500 MHz, CDCl$_3$) δ 7.58 – 7.05 (m, 5H), 4.32 – 4.28 (m, 2H), 3.82 (s, 0.58H), 3.75 (s, 1.22H), 3.11 – 2.40 (m, 3H), 2.18 – 1.47 (m, 2H), 1.37 – 1.33 (m, 3H), 1.02 – 0.79 (m, 3H); ^{13}C NMR (125 MHz, CDCl$_3$) δ 209.2, 205.5, 164.2 (t, J = 27.7 Hz), 164.10 (t, J = 32.4 Hz), 133.9, 133.7, 129.8, 129.6, 128.9, 128.7, 127.3, 127.1, 117.3 (t, J = 250.6 Hz), 115.3 (t, J = 250.6 Hz) , 63.2, 63.0, 50.4, 49.8, 45.3, 39.5 (t, J = 23.6 Hz), 35.2 (t, J = 23.1 Hz), 25.6, 21.3, 14.0, 11.3, 11.2; ^{19}F NMR (470 MHz, CDCl$_3$) δ -104.56 (t, J = 17.6 Hz), -108.09 (dd, J = 254.9, 14.0 Hz), -112.19 (dd, J = 254.9, 16.4 Hz); IR (cm^{-1}) (neat): v = 1765, 1711, 1308, 1191, 1095, 1068; MS (ESI): m/z 321.3 [M+Na]$^+$.
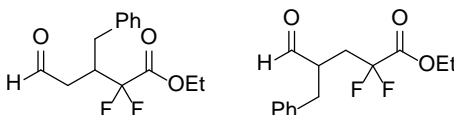
20.2 mg, 38% yield, colorless oil as a 5/1 mixture (determined by ^{1}H and ^{19}F NMR); ^{1}H NMR (500 MHz, CDCl$_3$) δ 9.74 (s, 0.15 H), 9.55 (s, 0.73H), 7.43 – 7.16 (m, 5H), 4.36 – 4.13 (m, 2H), 3.33 – 2.44 (m, 5H), 1.34 (t, J = 7.1 Hz, 3H); ^{13}C NMR (125 MHz, CDCl$_3$) δ 201.5, 198.9, 163.7 (t, J = 32.8 Hz), 137.2, 129.4, 129.2, 129.0, 128.8, 127.2, 116.5(t, J = 253.3 Hz), 63.3, 46.9, 41.4, 39.5 (t, J = 21.9 Hz), 35.7, 34.1, 14.0; ^{19}F NMR (470 MHz, CDCl$_3$) δ -103.8 (dd, J = 19.3, 15.0 Hz), -104.0 (dd, J = 19.7, 15.5 Hz), -107.8 (dd, J = 257.9, 11.8 Hz), -113.69 (dd, J = 257.9, 17.5 Hz); IR (cm^{-1}) (neat): v = 1760, 1754, 1600, 1496, 1240, 1064; MS (ESI): m/z 293.3 [M+Na]$^+$.
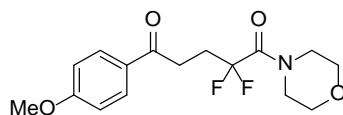
26.1 mg, 80% yield, colorless oil; ^{1}H NMR (500 MHz, CDCl$_3$) δ 7.99 – 7.88 (m, 2H), 6.97 – 6.86 (m, 2H), 3.86 (s, 3H), 3.77 – 3.62 (m, 8H), 3.24 – 3.18 (m, 2H), 2.66 – 2.58 (m, 2H); ^{13}C NMR (125 MHz, CDCl$_3$) δ 196.2, 163.7, 161.9 (t, J = 29.5 Hz), 130.5, 129.7, 119.5 (t, J = 253.9 Hz), 113.9, 66.9, 66.8, 55.6, 46.7, 43.4, 31.1, 29.6 (t, J = 23.7 Hz); ^{19}F NMR (470 MHz, CDCl$_3$) δ -98.9 (t, J = 17.5 Hz); IR (cm^{-1}) (neat): v = 1665, 1600, 1258, 1711, 1116, 1027; MS (ESI): m/z 350.4 [M+Na]$^+$.
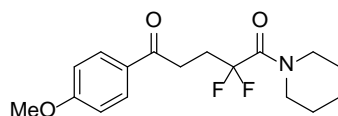
28.8 mg, 88% yield, colorless oil; ^{1}H NMR (500 MHz, CDCl$_3$) δ 7.98 – 7.90 (m, 2H), 6.95 – 6.86 (m, 2H), 3.85 (s, 3H), 3.67 – 3.50 (m, 4H), 3.25 – 3.14 (m, 2H), 2.60 – 2.58 (m, 2H), 1.70 – 1.51 (m, 6H); ^{13}C NMR (125 MHz, CDCl$_3$) δ 196.5, 163.7, 161.6 (t, J = 29.0 Hz), 130.5, 129.7, 119.7 (t, J = 254.1 Hz), 113.8, 55.6, 47.0, 44.5, 31.3, 29.9 (t, J = 23.9 Hz), 26.6, 25.7, 24.6; ^{19}F NMR (470 MHz, CDCl$_3$) δ -98.9 (t, J = 17.4 Hz); IR (cm^{-1}) (neat): v = 1659, 1600, 1257, 1170, 1121, 1028; MS (ESI): m/z 348.4 [M+Na]$^+$.
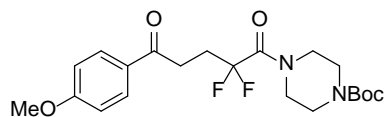
39.4 mg, 92% yield, colorless oil; ^{1}H NMR (500 MHz, CDCl$_3$) δ 7.98 – 7.88 (m, 2H), 6.95 – 6.88 (m, 2H), 3.85 (s, 3H), 3.73 – 3.56 (m, 4H), 3.48 – 3.46 (m, 4H), 3.24 – 3.16 (m, 2H), 2.67 – 2.53 (m, 2H), 1.46 (s, 9H); ^{13}C NMR (125 MHz, CDCl$_3$) δ 196.2, 163.7, 161.9 (t, J = 29.4 Hz), 154.5, 130.4, 129.6, 119.5 (t, J = 254.0 Hz), 113.9, 80.5, 55.6, 45.8, 43.0, 31.1, 29.6 (t, J = 23.6 Hz), 28.4; ^{19}F NMR (470 MHz, CDCl$_3$) δ -98.7 (t, J = 17.0 Hz); IR (cm^{-1}) (neat): v = 1670, 1601, 1418, 1258, 1237, 1169; MS (ESI): m/z 449.4 [M+Na]$^{+}$.
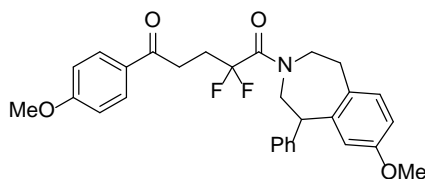
25.0 mg, 51% yield, yellow oil; ^{1}H NMR (500 MHz, CDCl$_3$, rotamer) δ 8.00 – 7.89 (m, 2H), 7.37 – 6.94 (m, 9H), 6.72 – 6.69 (m, 1H), 6.54 (d, J = 2.6 Hz, 0.6H), 6.40 (d, J = 2.6 Hz, 0.34 H), 4.61 – 3.62 (m, 10H), 3.37 – 2.39 (m, 7H); ^{13}C NMR (125 MHz, CDCl$_3$, rotamer) δ 198.8, 196.3, 196.2, 163.7, 163.2 (t, J = 29.9 Hz), 163.0 (t, J = 29.9 Hz), 158.8, 158.6, 142.4, 142.1, 141.6, 131.4, 131.3, 130.5, 130.2, 130.0, 129.7, 129.6, 129.0, 128.7, 128.3, 128.1, 127.1, 126.8, 119.7 (t, J = 253.6 Hz) 119.5 (t, J = 253.6 Hz), 116.8, 116.5, 113.8, 111.9, 111.7, 55.60, 55.2, 55.1, 52.4, 51.3, 50.5, 49.7, 48.1, 47.2, 38.2, 34.4, 33.2, 31.2, 30.0 (t, J = 23.6 Hz), 29.9 (t, J = 23.4 Hz), 24.4; ^{19}F NMR (470 MHz, CDCl$_3$) δ -97.54 (dt, J = 273.7, 14.8 Hz). ^{19}F NMR (470 MHz, CDCl$_3$, rotamer) δ -98.4 (dt, J = 37.2, 16.7 Hz); -98.5 (t, J = 16.9 Hz), -98.64 (t, J = 18.1 Hz), -98.59 (dt, J = 36.2, 17.5 Hz); IR (cm^{-1}) (neat): v = 1663, 1600, 1420, 1258, 1169, 1030; MS (ESI): m/z 516.4 [M+Na]$^{+}$.
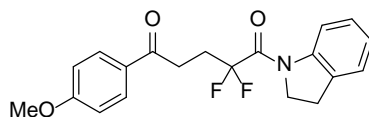
32.8 mg, 91% yield, white solid; ^{1}H NMR (500 MHz, CDCl$_3$) δ 8.24 (d, J = 8.1 Hz, 1H), 8.00 (d, J = 8.8 Hz, 2H), 7.28 – 7.24 (m, 2H), 7.13 (t, J = 7.4 Hz, 1H), 6.96 (d, J = 8.9 Hz, 2H), 4.38 (t, J = 8.2 Hz, 2H), 3.89 (s, 3H), 3.31 – 3.21 (m, 4H), 2.78 – 2.68 (m, 2H); ^{13}C NMR (125 MHz, CDCl$_3$) δ 196.3, 163.7, 161.2 (t, J = 30.2 Hz), 142.7, 131.8, 130.5, 129.7, 127.6, 125.2, 124.8, 119.4 (t, J = 254.3 Hz), 118.0, 113.9, 55.6, 48.0, 31.2, 29.2 (t, J = 23.8 Hz), 28.8; ^{19}F NMR (470 MHz, CDCl$_3$) δ -102.6 (t, J = 17.4 Hz); IR (cm^{-1}) (neat): v = 1671, 1600,1482, 1419, 1259, 1170; MS (ESI): m/z 382.4 [M+Na]$^{+}$.
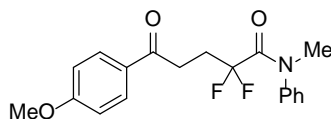
21.5 mg, 62% yield, colorless oil; ^{1}H NMR (500 MHz, CDCl$_3$) δ 7.94 (d, J = 8.5 Hz, 2H), 7.45 – 7.28 (m, 3H), 7.33 – 7.27 (m, 2H), 6.94 (d, J = 8.8 Hz, 2H), 3.88 (s, 3H), 3.34 (s, 3H), 3.16 – 3.07 (m, 2H), 2.58 – 2.49 (m, 2H); ^{13}C NMR (125 MHz, CDCl$_3$) δ 196.3, 163.7, 163.3 (t, J = 28.3 Hz), 142.4, 130.4, 129.7, 129.3, 128.4, 127.6, 118.9 (t, J = 254.8 Hz), 113.9, 55.6, 40.1, 30.1 (t, J = 23.8 Hz), 29.9; ^{19}F NMR (470 MHz, CDCl$_3$) δ -96.7 (t, J = 17.0 Hz); IR (cm^{-1}) (neat): v = 1673, 1599, 1259, 1281, 1171, 1028; MS (ESI): m/z 370.3 [M+Na]$^{+}$.
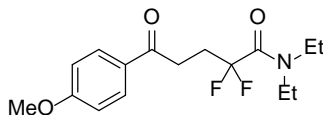
25.1 mg, 80% yield, colorless oil; ^{1}H NMR (500 MHz, CDCl$_3$) δ 7.99 – 7.88 (m, 2H), 6.95 – 6.86 (m, 2H), 3.86 (s, 3H), 3.53 (q, J = 7.0 Hz, 2H), 3.39 (q, J = 7.1 Hz, 2H), 3.25 – 3.16 (m, 2H), 2.67 – 2.53 (m, 2H), 1.21 (t, J = 7.0 Hz, 3H), 1.16 (t, J = 7.1 Hz, 3H); ^{13}C NMR (125 MHz, CDCl$_3$) δ 196.5, 163.7, 162.6 (t, J = 29.1 Hz), 130.5, 129.7, 119.6 (t, J = 254.2 Hz), 113.9, 55.6, 42.0, 41.50 (s), 31.3, 29.9 (t, J = 24.1 Hz), 14.4, 12.5; ^{19}F NMR (470 MHz, CDCl$_3$) δ -99.6 (t, J = 17.5 Hz); IR (cm^{-1}) (neat): v = 1663, 1600,1260, 1171, 1047, 1030; MS (ESI): m/z 336.3 [M+Na]$^+$.
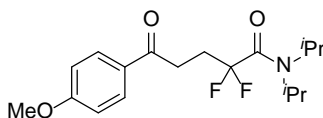
25.5 mg, 75% yield, colorless oil; ^{1}H NMR (500 MHz, CDCl$_3$) δ 7.99 – 7.90 (m, 2H), 6.97 – 6.84 (m, 2H), 4.50 – 4.45 (m, 1H), 3.87 (d, J = 16.5 Hz, 3H), 3.51 – 3.45 (m, 1H), 3.25 – 3.14 (m, 2H), 2.67 – 2.46 (m, 2H), 1.41 (d, J = 6.8 Hz, 6H), 1.21 (d, J = 6.6 Hz, 6H); ^{13}C NMR (125 MHz, CDCl$_3$) δ 196.6, 163.6, 162.0 (t, J = 28.0 Hz), 130.5, 129.8, 119.9 (t, J = 255.2 Hz), 113.8, 55.6, 48.5 (t, J = 7.1 Hz), 47.0, 31.4, 29.9 (t, J = 24.1 Hz), 20.7, 20.0; ^{19}F NMR (470 MHz, CDCl$_3$) δ -99.6 (t, J = 17.6 Hz); IR (cm^{-1}) (neat): v = 1656, 1600, 1311, 1260, 1170, 1022; MS (ESI): m/z 364.4 [M+Na]$^+$.
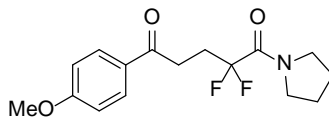
25.7 mg (^{i}Pr$_2$NH was used as base), 83% yield, colorless oil; ^{1}H NMR (500 MHz, CDCl$_3$) δ 7.96 (d, J = 8.8 Hz, 2H), 6.92 (d, J = 8.8 Hz, 2H), 3.86 (s, 3H), 3.70 (t, J = 6.7 Hz, 2H), 3.52 (t, J = 7.0 Hz, 2H), 3.21 (t, J = 7.5 Hz, 2H), 2.64 – 2.54 (m, 2H), 1.99 – 1.83 (m, 4H); ^{13}C NMR (125 MHz, CDCl$_3$) δ 196.5, 163.7, 162.1 (t, J = 30.0 Hz), 130.5, 129.75, 119.0 (t, J = 252.5 Hz), 113.9, 55.6, 47.5, 46.7 (t, J = 5.8 Hz), 31.2, 29.2 (t, J = 23.9 Hz), 26.6, 23.4; ^{19}F NMR (470 MHz, CDCl$_3$) δ -102.9 (t, J = 17.3 Hz); IR (cm^{-1}) (neat): v = 1659, 1600, 1451, 1315, 1259, 1171; MS (ESI): m/z 334.3 [M+Na]$^+$.
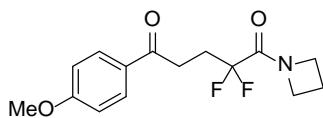
25.8 mg, 53% yield, colorless oil; ^{1}H NMR (500 MHz, CDCl$_3$) δ 7.99 – 7.91 (m, 2H), 6.98 – 6.88 (m, 2H), 4.44 (t, J = 7.8 Hz, 2H), 4.12 (t, J = 7.9 Hz, 2H), 3.86 (s, 3H), 3.21 – 3.12 (m, 2H), 2.57 – 2.47 (m, 2H), 2.39 – 2.33 (m, 2H); ^{13}C NMR (125 MHz, CDCl$_3$) δ 196.2, 163.7, 163.0 (t, J = 30.2 Hz), 130.5, 129.6, 118.90 (t, J = 251.5 Hz), 113.9, 55.6, 52.5, 49.0, 30.8, 29.1 (t, J = 23.8 Hz), 16.5; ^{19}F NMR (470 MHz, CDCl$_3$) δ -103.7 (t, J = 17.4 Hz); IR (cm^{-1}) (neat): v = 1672, 1600, 1313, 1260, 1220, 1172; MS (ESI): m/z 320.3 [M+Na]$^+$.
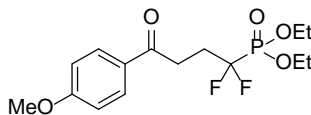
11.3 mg (Li^{t}OBu was used as base), 32% yield, yellow oil; ^{1}H NMR (500 MHz, CDCl$_3$) δ 8.05 – 7.90 (m, 2H), 6.99 – 6.88 (m, 2H), 4.36 – 4.25 (m, 4H), 3.87 (s, 3H), 3.30 – 3.22 (m, 2H), 2.64 – 2.46 (m, 2H), 1.39 (t, J = 7.1 Hz, 6H); ^{13}C NMR (125 MHz, CDCl$_3$) δ 196.1, 163.8, 130.5, 129.7, 113.9, 64.7, 64.6, 55.6, 30.0, 28.8, 28.7, 28.5, 16.6, 16.5; ^{19}F NMR (470 MHz, CDCl$_3$) δ -111.74 (dt, J = 108.2, 19.8 Hz); ^{31}P NMR (203 MHz, CDCl$_3$) δ 6.87 (t, J = 108.2 Hz); IR (cm^{-1}) (neat): v = 1679, 1601, 1260, 1172, 1022, 977; MS (ESI): m/z 373.2 [M+Na]$^+$.
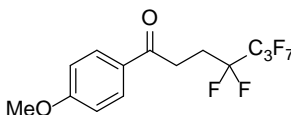
27.8 mg, 73% yield, white solid; ^{1}H NMR (500 MHz, CDCl$_3$) δ 8.05 – 7.85 (m, 2H), 6.99 – 6.88 (m, 2H), 3.88 (s, 3H), 3.36 – 3.16 (m, 2H), 2.64 – 2.54 (m, 2H); ^{13}C NMR (125 MHz, CDCl$_3$) δ 195.0 164.0, 130.5, 129.4, 114.1, 55.6, 29.2, 25.7 (t, J = 21.7 Hz); ^{19}F NMR (470 MHz, CDCl$_3$) δ -81.1 (t, J = 9.6 Hz), -114.4 (br s), -125.4 (br s), -126.0 (dd, J = 12.8, 8.9 Hz); IR (cm^{-1}) (neat): v = 1677, 1601, 1217, 1187, 1134, 980; MS (ESI): m/z 405.1 [M+Na]$^+$.
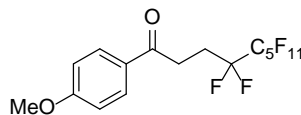
31.3 mg, 65% yield, white solid; ^{1}H NMR (500 MHz, CDCl$_3$) δ 7.96 (d, J = 7.6 Hz, 2H), 6.95 (d, J = 7.6 Hz, 2H), 3.88 (s, 3H), 3.30 – 3.15 (m, 2H), 2.64 – 2.53 (m, 2H); ^{13}C NMR (125 MHz, CDCl$_3$) δ 195.0, 164.0, 130.5, 129.4, 114.1, 55.6, 29.2, 25.8 (t, J = 21.8 Hz); ^{19}F NMR (470 MHz, CDCl$_3$) δ -80.87 (t, J = 9.7 Hz), -114.2(br s), -121.9 (br s), -122.9 (br s), -123.5 (br s), -126.2 (br s); IR (cm^{-1}) (neat): v = 1674, 1606, 1221, 1234, 1189, 1141; MS (ESI): m/z 505.2 [M+Na]$^+$.

Synthetic transformations of ethyl 2,2-difluoro-5-(4-methoxyphenyl)-5-oxopentanoate:
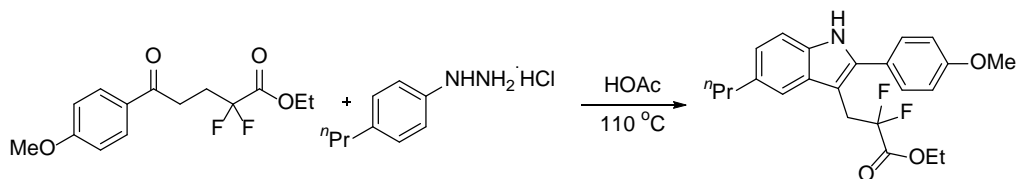
To a stirred solution of the difluoroester (28.6 mg, 0.10 mmol) in acetic acid (1.0 mL), (4-propylphenyl) hydrazine hydrochloride (37.2 mg, 0.20 mmol) was added in one portion. The reaction mixture was then heated at 100 ˚C for 18 h. After it was quenched with a saturated aqueous solution of sodium bicarbonate, the aqueous layer was extracted with ethyl acetate (3 × 10 mL). The combined organic layer was dried over sodium sulfate and concentrated in vacuo. The crude residue was purified by flash column chromatography on silica gel to afford product **19** (37.5mg, 94%) as a yellow solid.

^{1}H NMR (500 MHz, CDCl$_3$) δ 8.10 (s, 1H), 7.58 – 7.41 (m, 3H), 7.28 (d, J = 8.1 Hz, 1H), 7.09 – 7.02 (m, 3H), 4.17 (q, J = 7.1 Hz, 2H), 3.89 (d, J = 7.3 Hz, 3H), 3.64 (t, J = 17.0 Hz, 2H), 2.79 – 2.67 (m, 2H), 1.83 – 1.66 (m, 2H), 1.22 (t, J = 7.2 Hz, 3H), 1.02 (t, J = 7.3 Hz, 3H); ^{13}C NMR (125 MHz, CDCl$_3$) δ164.7 (t, J = 32.7 Hz), 159.7, 137.9, 134.6, 134.1, 129.8, 129.5, 125.1, 123.5, 118.8, 115.9 (t, J = 251.8 Hz), 114.4, 110.5, 101.2, 62.9, 55.5, 38.5, 30.90 (t, J = 24.9 Hz), 25.6, 14.1, 13.9; ^{19}F NMR (470 MHz, CDCl$_3$) δ -103.2 (t, J = 16.9 Hz); IR (cm^{-1}) (neat): v = 3400, 1759, 1508, 1286, 1250, 1180, 1075, 1028; MS (ESI): m/z 424.3 [M+Na]$^+$.
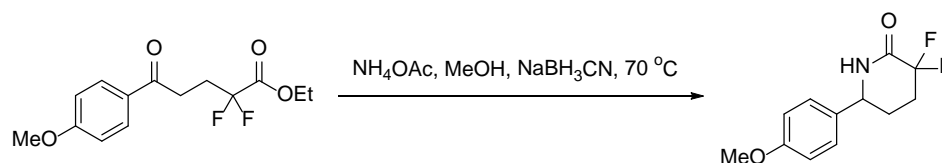
To a stirred solution of the difluoroester (28.6 mg, 0.1 mmol) in methanol (1.0 mL) at room temperature were added solid ammonium acetate (77 mg, 1.0 mmol) and sodium cyanoborohydride (6.2 mg, 0.1 mmol) under argon. Until most of starting material was consumed (monitored by thin layer chromatography), the reaction mixture was quenched with aq NaHCO$_3$. The aqueous layer was extracted with ethyl acetate (3×10 mL). The combined organic layer was dried over sodium sulfate and concentrated in vacuo. The crude residue was purified by flash column chromatography on silica gel to afford product **20** (21.8 mg, 90%) as a white solid.

^{1}H NMR (500 MHz, CDCl$_3$) δ 7.23 – 7.18 (m, 2H), 6.97 – 6.79 (m, 2H), 6.39 (br s, 1H), 4.67 – 4.52 (m, 1H), 3.80 (s, 3H), 2.46 – 2.36 (m, 1H), 2.29 – 2.15 (m, 2H), 2.07 – 1.96 (m, 1H); ^{13}C NMR (125 MHz, CDCl$_3$) δ 163.1 (t, J = 30.2 Hz), 159.8, 132.3, 127.4, 112.4 (t, J = 243.1 Hz), 57.1, 55.5, 30.8 (t, J = 22.8 Hz), 29.1, 29.01; ^{19}F NMR (470 MHz, CDCl$_3$) δ -100.3 (td, J = 283.6, 8.8 Hz), -105.2 (td, J = 283.4, 8.5 Hz); IR (cm^{-1}) (neat): v = 3205, 1724, 1680, 1255, 1201, 1175, 1156, 991; MS (ESI): m/z 264.3 [M+Na]$^+$.
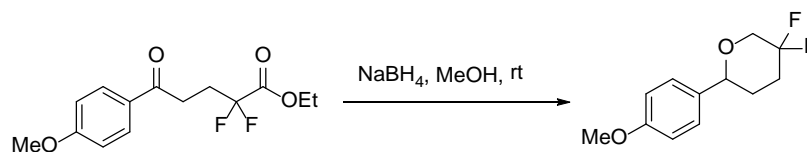
To a stirred solution of the difluoroester (28.6 mg, 0.1 mmol) in methanol (1.0 mL) at room temperature were added NaBH$_4$ (7.5 mg, 0.2 mmol) under argon. Until most of starting material was consumed (monitored by thin layer chromatography), the reaction mixture was quenched with water. The aqueous layer was extracted with ethyl acetate (3 × 10 mL). The combined organic layer was dried over sodium sulfate and concentrated in vacuo. The crude residue was purified by flash column chromatography on silica gel to afford product **20** (19.3 mg, 87%) as colorless oil.

^{1}H NMR (500 MHz, CDCl$_3$) δ 7.33 – 7.28 (m, 2H), 6.92 – 6.87 (m, 2H), 4.38 (dd, J = 9.6, 3.1 Hz, 1H), 4.08 (ddt, J = 12.3, 9.6, 2.7 Hz, 1H), 3.81 (s, 3H), 3.72 – 3.63 (m, 1H), 2.39 – 2.24 (m, 1H), 2.14 – 1.95 (m, 3H); ^{13}C NMR (125 MHz, CDCl$_3$) δ 159.4, 132.9, 127.4, 118.1 (t, J = 244.3 Hz), 114.0, 78.9, 70.3 (dd, J = 34.2, 28.5 Hz), 55.4, 32.64 – 31.66 (m), 30.7, 30.6; ^{19}F NMR (470 MHz, CDCl$_3$) δ -106.6, -107.1, -107.4(m), -107.9(m); IR (cm^{-1}) (neat): v = 1613, 1516, 1253, 1114, 1099, 961; MS (ESI): m/z 229.3 [M+H]$^+$.
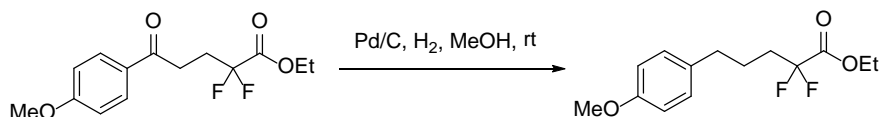
To a stirred solution of the difluoroester (28.6 mg, 0.1 mmol) in methanol (1.0 mL) at room temperature were added 10 % Pd/C (5.7 mg) under H$_2$ (1 atma). Until most of starting material was consumed (monitored by thin layer chromatography), the Pd/C was removed, and the organic layer was concentrated in vacuo. The crude residue was purified by flash column chromatography on silica gel to afford product **20** (21.8 mg, 80%) as colorless oil.

^{1}H NMR (500 MHz, CDCl$_3$) δ 7.09 (d, J = 8.5 Hz, 2H), 6.84 (d, J = 8.5 Hz, 2H), 4.31 (q, J = 7.1 Hz, 2H), 3.79 (s, 3H), 2.62 (t, J = 7.6 Hz, 2H), 2.13 – 1.99 (m, 2H), 1.81 – 1.75 (m, 2H), 1.34 (t, J = 7.1 Hz, 3H); ^{13}C NMR (125 MHz, CDCl$_3$) δ 164.4 (t, J = 33.0 Hz), 158.1, 133.1, 129.4, 116.44 (t, J = 250.1 Hz), 114.0, 62.9, 55.4, 34.3, 34.0 (t, J = 23.2 Hz), 23.4,

14.1; ^{19}F NMR (470 MHz, CDCl$_3$) δ -105.8 (t, J = 16.8 Hz); IR (cm^{-1}) (neat): v = 1765, 1514, 1247, 1180, 1092, 1036; MS (ESI): m/z 295.4 [M+Na]$^+$

CHAPTER 5.   CYCLOPROPANOL CROSS-COUPLING REACTIONS WITH BROMINATED SUBSTITUENTS

5.1   Introduction

As the previous chapter outlined, cyclopropanols are valuable starting materials in that they easily undergo ring opening reactions and provide useful reactive intermediates. These materials can be synthesized in one step from methyl or ethyl esters via the Kulinkovich reaction or from alkenes via the Simmons-Smith reaction. Many groups have used their versatility in the syntheses of complex natural products as well as medicinal targets. Regardless of the reagent or catalyst used in initiating the ring-opening reaction, the reactive intermediate formed has been observed to either be a metallo-homoenolate or a β-alkyl radical intermediate, both of which allow for functionalization of the β-carbon. Unfortunately, competing reaction pathways often result in the en-one byproduct which complicates the use of these reactions. This byproduct was drastically reduced with the switch from palladium to copper catalysts as copper is less prone to the β-hydride reduction pathway.

With the synthesis of mono- and di-fluorinated products as well as the methylated products as described in Chapter 4, we sought to expand the versatility of this reaction. Since the copper catalysts showed poor results with the chiral ligands, the first aim of our studies was to explore the use of nickel catalysts with the reaction conditions as multiple groups have seen great success with nickel catalysts bearing chiral ligands. An alternative route was also proposed which involved a light-promoted copper catalyzed reaction scheme.

In addition to expanding the role of the catalyst in these reactions, other brominated agents were investigated for their versatility in this type of reaction. Favorable results were seen with cyanobromides, fluoro-ethyl-bromo ketones, and, most intriguingly, dimethyl bromo esters. The latter was of great interest because the product of such a reaction would be a ketone with a β-substituted quaternary carbon. Due to the extreme steric bulk of quaternary carbons, they remain a challenging task to synthesize in complex natural products.

5.2   Results and Discussion

Efforts began toward the use of a nickel catalyst in hopes that it would be more amenable to use of chiral ligands and thus, production of a chiral product. The initial reaction was run under argon with NiCl$_2$(DME) which was pre-stirred with bipyridine (Bipy) then added to a solution of phenethylcyclopropanol, the previously used methyl-bromo-ester, and potassium carbonate in acetonitrile (Scheme 5.1). This reaction produced the desired product in a scant 5% yield. With proof of concept in hand, reaction optimization was conducted utilizing the *p*-methoxyphenyl cyclopropanol due to its visibility on TLC.
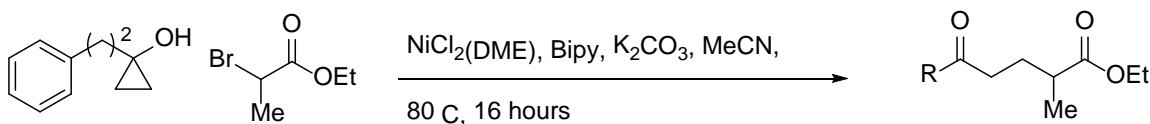
SM: 1 eq, ester: 2 eq, Ni: 5 mol%, Ligand: 5 mol%, base: 2 eq, solvent: 0.1 M

Scheme 5.1 Scheme showing initial reaction conditions with a nickel catalyst.

Since previous reactions had seen drastic improvements with a change of base, this was the first parameter explored. When the catalyst loading was increased to 0.5 equivalents and potassium carbonate was employed as the base, the yield rose to 13% but no other significant increases in yield were observed (Table 5.1).

Table 5.1 Table showing the bases employed in optimization of the nickel catalyzed reaction.

Entry	Ni Catalyst	Ligand	Base	Solvent	Yield
1	NiCl$_2$(DME)	Bipy	K$_2$CO$_3$	MeCN	10%
2	NiCl$_2$(DME)	Bipy	KOtBu	MeCN	No reaction
3	NiCl$_2$(DME)	Bipy	LiOtBu	MeCN	No reaction
4	NiCl$_2$(DME)	Bipy	TMP	MeCN	7%
5	NiCl$_2$(DME)	Bipy	Pyridine	MeCN	No reaction
6	NiCl$_2$(DME)	Bipy	DIPA	MeCN	5%
7	NiCl$_2$(DME)	Bipy	DIPEA	MeCN	6%
8	NiCl$_2$(DME)	Bipy	K$_3$PO$_4$	MeCN	8%
9	NiCl$_2$(DME)	Bipy	Cs$_2$CO$_3$	MeCN	10%

As the changes in base showed no appreciable optimization, the temperature of the reaction was raised to 100 °C. This condition was initially avoided due to high temperatures typically resulting in poor enantioselectivity with chiral catalysts. However, in this case it was seen to be beneficial as the yield rose to 43%. Further optimization was attempted with various nickel catalysts and ligands, however none of the yields produced were over 50%. When the three available chiral ligands were used in combination with the best observed conditions the yields dropped back below 10% and this route was abandoned.

Since the alkylation reaction from chapter four gave excellent results, the idea to expand the scope of the reaction to form a quaternary carbon was proposed. In efforts to lower the temperature of the reaction, the idea of light promoted catalysis was explored. Scheme 5.2 shows the proposed reaction and Table 5.2 shows the initial test results.
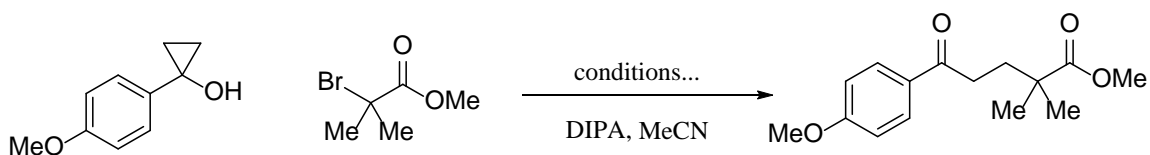
Scheme 5.2 Scheme showing quaternary carbon optimization with light-induced copper catalyzed conditions.

Table 5.2 Table showing preliminary attempts at light-induced copper-catalyzed quaternary carbon formation reaction.

Entry	Catalyst	Ligand	Light Source	Temp (˚C)	Yield
1	CuCl	Phen	CFL bulb	42	51%
2	CuCl	Phen	None	30	Recovered Starting Material
3	CuCl	Phen	None	45	4%
4	CuCl	Phen	CFL bulb	30	21%
5	CuCl	BiPy	CFL bulb	30	42%
6	CuCl	6,6'-Me$_2$BiPy	CFL bulb	30	Recovered Starting Material
7	[Cu(OTf)]$_2$Ph	Phen	CFL bulb	30	<5%
8	CuBr	Phen	CFL bulb	30	54%
9	CuCN	Phen	CFL bulb	30	<5%
10	Cu(MeCN)$_4$*BF$_4$	Phen	CFL bulb	30	53%
11	Cu(MeCN)$_4$*PF$_6$	Phen	CFL bulb	30	55%
12	CuCl	Bipy	None (foil)	45	36%

Unfortunately, although over a hundred attempts were made, conditions which produced the desired product in a yield over 60% were never realized. The reaction did show tolerance to a variety of cyclopropanols and a small library of compounds was synthesized prior to the project being abandoned.

Figure 5.1 Example of reactions stirring in the engineered photo-reactor.

5.3   Experimental

General Methods: NMR spectra were recorded on Bruker spectrometers (^{1}H at 500 MHz and ^{13}C at 125 MHz). Chemical shifts (δ) were given in ppm with reference to solvent signals [^{1}H NMR: CDCl$_3$ (7.26); ^{13}C NMR: CDCl$_3$ (77.2)]. Column chromatography was performed on silica gel obtained from silicycle. All reactions sensitive to air or moisture

were conducted under argon atmosphere in dry and freshly distilled solvents under anhydrous conditions, unless otherwise noted. Anhydrous THF and toluene were distilled over sodium benzophenone ketyl radical under argon. Anhydrous CH_2Cl_2 was distilled over calcium hydride under argon. All other solvents and reagents were used as obtained from commercial sources without further purification.

Under argon atmosphere, a mixture of cyclopropanol (0.2 mmol), α-bromoester (0.8 mmol), CuCl (2.0 mg, 0.02 mmol), Phenanthroline (7.2 mg, 0.04 mmol), and ^{i}Pr$_2$NH (56 μL, 0.4 mmol) in 2 mL of acetonitrile was stirred at 80 ˚C for 16 hours. The reaction was quenched with aqueous NH_4Cl and extracted thrice with DCM (20 mL). The combined organic extract was washed with brine, dried over anhydrous $MgSO_4$, filtered, and concentrated under vacuum. The residue was purified via column chromatography with silica gel to give the desired product.
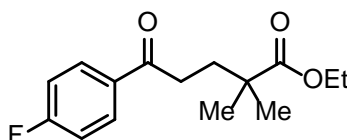
52% yield, colorless oil; ^{1}H NMR (500 MHz, CDCl3) δ 8.08 – 7.88 (m, 2H), 7.13 – 7.09 (m, 2H), 3.67 (s, 3H), 3.00 – 2.81 (m, 2H), 2.10 – 1.90 (m, 2H), 1.23 (s, 6H); ^{13}C NMR (125 MHz, CDCl$_3$) δ 198.2, 178.0, 165.8 (d, J = 254.6 Hz), 133.4, 130.8 (d, J = 9.2 Hz), 115.8 (d, J = 21.8 Hz), 52.0, 41.9, 34.7, 34.5, 25.4
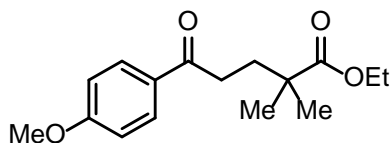
68% yield, colorless oil; 1 H NMR (500 MHz, CDCl3) δ 7.92 (d, J = 8.7 Hz, 2H), 6.91 (d, J = 8.7 Hz, 2H), 3.85 (s, 3H), 3.67 (s, 3H), 2.88 – 2.84 (m, 2H), 2.02 – 1.90 (m, 2H), 1.23 (s, 6H); 13C NMR (125 MHz, CDCl3) δ 198.4, 178.1, 163.5, 130.4, 130.0, 113.8, 55.5, 51.9, 41.9, 35.0, 34.2, 25.4
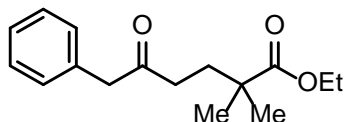
58% yield, colorless oil; 1 H NMR (500 MHz, CDCl3) δ 7.37 – 7.20 (m, 5H), 3.70 (s, 2H), 3.63 (s, 3H), 2.48 – 2.38 (m, 2H), 1.82 – 1.79 (m, 2H), 1.15 (s, 6H); 13C NMR (125 MHz, CDCl3) δ 207.8, 177.9, 134.3, 129.5, 128.8, 127.1, 51.9, 50.2, 41.7, 37.9, 34.0, 25.2
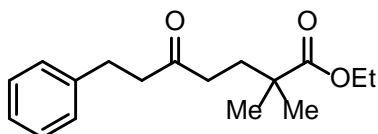
60% yield, colorless oil; 1 H NMR (500 MHz, CDCl3) δ 7.44 – 6.93 (m, 5H), 3.64 (s, 3H), 2.88 (t, J = 7.6 Hz, 2H), 2.73 (t, J = 7.6 Hz, 2H), 2.45 – 2.22 (m, 2H), 1.81 – 1.77 (m, 2H), 1.15 (s, 6H); 13C NMR (125 MHz, CDCl3) δ 209.5, 177.9, 141.1, 128.6, 128.4, 126.2, 51.9, 44.4, 41.7, 38.8, 34.0, 29.9, 25.2
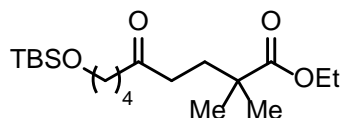
40% yield, colorless oil; 1 H NMR (500 MHz, CDCl3) δ 3.64 (s, 3H), 3.59 (t, J = 6.3 Hz, 2H), 2.43 – 2.40 (m, 2H), 2.38 – 2.31 (m, 2H), 1.85 – 1.76 (m, 2H), 1.63 – 1.46 (m, 4H), 1.17 (s, 6H), 0.88 (s, 9H), 0.03 (s, 6H); 13C NMR (125 MHz, CDCl3) δ 210.5, 178.0, 62.9, 51.9, 42.7, 41.7, 38.5, 34.1, 32.4, 26.1, 25.3, 22.0, 20.5, 18.5, -5.2
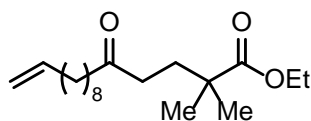
34% yield, colorless oil; 1 H NMR (500 MHz, CDCl3) δ 5.83 – 5.75 (m, 1H), 5.00 – 4.84 (m, 2H), 3.65 (s, 3H), 2.43 – 2.28 (m, 4H), 2.05 – 1.99 (m, 2H), 1.83 – 1.76 (m, 2H), 1.57 – 1.51 (m, 2H), 1.37 – 1.31 (m, 2H), 1.29 – 1.23 (m, 9H), 1.16 (s, 6H); 13C NMR (125 MHz, CDCl3) δ 210.8, S17 178.0, 139.3, 114.3, 51.9, 43.0, 41.7, 38.6, 34.1, 33.9, 29.5, 29.4, 29.3, 29.2, 29.0, 25.3, 24.0
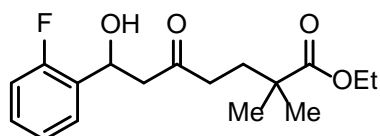
47% yield, colorless oil; 1 H NMR (500 MHz, CDCl3) δ 7.31 – 7.26 (m, 1H), 7.15 – 7.06 (m, 2H), 6.99 – 6.88 (m, 1H), 5.13 (dd, J = 8.6, 3.7 Hz, 1H), 3.64 (s, 3H), 3.46 (s, 1H), 2.87 – 2.72 (m, 2H), 2.46 – 2.36 (m, 2H), 1.87 – 1.76 (m, 2H), 1.16 (s, 6H); 13C NMR (125 MHz, CDCl3) δ 210.4, 177.9, 163.1 (d, J = 246.0 Hz), 145.6 (d, J = 6.9 Hz), 130.2(d, J = 8.1 Hz), 121.3, 114.5 (d, J = 21.2 Hz), 112.8 (d, J = 22.0 Hz), 69.4, 52.0, 51.1, 41.6, 39.6, 33.7, 25.7, 25.2
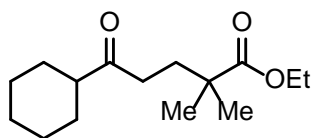
38% yield, colorless oil; 1 H NMR (500 MHz, CDCl3) δ 3.65 (s, 3H), 2.45 – 2.27 (m, 3H), 1.85 – 1.71 (m, 6H), 1.66 – 1.64 (m, 1H), 1.37 – 1.21 (m, 5H), 1.16 (s, 6H); 13C NMR (125 MHz, CDCl3) δ 213.6, 178.1, 51.9, 51.1, 41.8, 36.4, 34.0, 28.7, 25.9, 25.8, 25.324.6 mg, 51% yield, colorless oil; 1 H NMR (500 MHz, CDCl3) δ 3.65 (s, 3H), 2.45 – 2.27 (m, 3H), 1.85 – 1.71 (m, 6H), 1.66 – 1.64 (m, 1H), 1.37 – 1.21 (m, 5H), 1.16 (s, 6H); 13C NMR (125 MHz, CDCl3) δ 213.6, 178.1, 51.9, 51.1, 41.8, 36.4, 34.0, 28.7, 25.9, 25.8, 25.3

REFERENCES

(1)   Anderson, N. H.; Odoh, S. O.; Yao, Y.; Williams, U. J.; Schaefer, B. A.; Kiernicki, J. J.; Lewis, A. J.; Goshert, M. D.; Fanwick, P. E.; Schelter, E. J.; Walensky, J. R.; Gagliardi, L.; Bart, S. C. *Nat. Chem.* **2014**, *6* (10), 919–926.

(2)   Anderson, N. H.; Yin, H.; Kiernicki, J. J.; Fanwick, P. E.; Schelter, E. J.; Bart, S. C. *Angew. Chemie - Int. Ed.* **2015**, *54* (32), 9386–9389.

(3)   Smith, D. P.; Allen, K. D.; Carducci, M. D.; Wigley, D. E. *Inorg. Chem.* **1992**, *31* (8), 1319–1320.

(4)   Morrison, D. L.; Rodgers, P. M.; Chao, Y.-W.; Bruck, M. A.; Grittini, C.; Tajima, T. L.; Alexander, S. J.; Rheingold, A. L.; Wigley, D. E. *Organometallics* **1995**, *14* (5), 2435–2446.

(5)   Bryan, J. C.; Burrell, A. K.; Miller, M. M.; Smith, W. H.; Burns, C. J.; Sattelberger, A. P. *Polyhedron* **1993**, *12* (14), 1769–1777.

(6)   Benson, M. T.; Bryan, J. C.; Burrell, A. K.; Cundari, T. R. *Inorg. Chem.* **1995**, *34* (9), 2348–2355.

(7)   Anhaus, J. T.; Kee, T. P.; Schofield, M. H.; Schrock, R. R. *J. Am. Chem. Soc.* **1990**, *112* (4), 1642–1643.

(8)   Bombieri, G.; Forsellini, E.; Day, J. P. **1978**, 1–4.

(9)   La Pierre, H. S.; Rosenzweig, M.; Kosog, B.; Hauser, C.; Heinemann, F. W.; Liddle, S. T.; Meyer, K. *Chem. Commun.* **2015**, *51* (93), 16671–16674.

(10)   Warner, B. P.; Scott, B. L.; Burns, C. J. *Angew. Chemie - Int. Ed.* **1998**, *37* (7), 959–960.

(11)   Arney, D. S. J.; Burns, C. J. *J. Am. Chem. Soc.* **1993**, *115*, 9840–9841.

(12)   Hayton, T. W.; Boncella, J. M.; Scott, B. L.;Palmer, P. D.; Batista, E. R.; Hay, P. J. *Science (80-.).* **2005**, *310* (5756), 1941–1943.

(13)   Hayton, T. W.; Boncella, J. M.; Scott, B. L.; Batista, E. R.; Hay, P. J. *J. Am. Chem. Soc.* **2006**, *128* (32), 10549–10559.

(14)   Hayton, T. W.; Boncella, J. M.; Scott, B. L.; Batista, E. R. *J. Am. Chem. Soc.* **2006**, *128* (39), 12622–12623.

(15) Anderson, N. H.; Xie, J.; Ray, D.; Zeller, M.; Gagliardi, L.; Bart, S. C. *Nat. Chem.* **2017**, *9* (9), 850–855.

(16) Morrison, D. L.; Wigley, D. E. *J. Chem. Soc. Chem. Commun.* **1995**, No. 1, 79–80.

(17) Anderson, N. H.; Yin, H.; Kiernicki, J. J.; Fanwick, P. E.; Schelter, E. J.; Bart, S. C. *Angew. Chemie - Int. Ed.* **2015**, *54* (32), 9386–9389.

(18) Muetterties, E. L.; Guggenberger, L. J. *J. Am. Chem. Soc.* **1974**, *96* (6), 1748–1756.

(19) Nalewajski, R. F.; Mrozek, J. *Int. J. Quantum Chem.* **2018**, *51* (4), 187–200.

(20) Pangborn, A. B.; Giardello, M. A.; Grubbs, R. H.; Rosen, R. K.; Timmers, F. J. *Organometallics* **1996**, *15*, 1518–1520.

(21) Bruker Advanced X-ray Solutions. Apex2 v2014.7-1, 2014.

(22) Bruker Advanced X-ray Solutions. Saint v8.34A, 2014.

(23) Krause, L.; Herbst-Irmer, R.; Sheldrick, G. M.; Stalke, D. *J. Appl. Crystallogr.* **2015**, *48*, 3–10.

(24) Sheldrick, G. M. TWINABS, 2012.

(25) Bruker Advanced X-ray Solutions. Shelxtl, 2003.

(26) Sheldrick, G. M. *Acta Crystallogr. Sect. A Found. Crystallogr.* **2008**, *64*, 112–122.

(27) Hübschle, C. B.; Sheldrick, G. M.; Dittrich, B. *J. Appl. Crystallogr.* **2011**, *44*, 1281–1284.

(28) Zi, G.; Jia, L.; Werkema, E. L.; Walter, M. D.; Gottfriedsen, J. P.; Andersen, R. A. *Organometallics* **2005**, *24*, 4251–4264.

(29) Zi, G.; Blosch, L. L.; Jia, L.; Andersen, R. A. *Organometallics* **2005**, *24* (19), 4602–4612.

(30) Matson, E. M.; Fanwick, P. E.; Bart, S. C. *Eur. J. Inorg. Chem.* **2012**, *2* (33), 5471–5478.

(31) Ren, W.; Zhou, E.; Fang, B.; Zi, G.; Fang, D.-C.; Walter, M. D. *Chem. Sci.* **2014**, *5*, 3165.

(32) Zhang, C.; Yang, P.; Zhou, E.; Deng, X.; Zi, G.; Walter, M. D. *Organometallics* **2017**, No. I, acs.organomet.7b00212.

(33) Kelly, R. P.; Falcone, M.; Lamsfus, C. A.; Scopelliti, R.; Maron, L.; Meyer, K.; Mazzanti, M. *Chem. Sci.* **2017**, *69*, 2393–2406.

(34) Cleaves, P. A.; Kefalidis, C. E.; Gardner, B. M.; Tuna, F.; McInnes, E. J. L.; Lewis, W.; Maron, L.; Liddle, S. T. *Chem. - A Eur. J.* **2017**, *23*, 2950–2959.

(35) Bart, S. C.; Anthon, C.; Heinemann, F. W.; Bill, E.; Edelstein, N. M.; Meyer, K. *J. Am. Chem. Soc.* **2008**, *130* (37), 12536–12546.

(36) Matson, E. M.; Crestani, M. G.; Fanwick, P. E.; Bart, S. C. *Dalt. Trans.* **2012**, *41*, 7952–7958.

(37) Lu, E.; Cooper, O. J.; McMaster, J.; Tuna, F.; McInnes, E. J. L.; Lewis, W.; Blake, A. J.; Liddle, S. T. *Angew. Chemie - Int. Ed.* **2014**, *53* (26), 6696–6700.

(38) Ren, W.; Zi, G.; Fang, D.-C.; Walter, M. D. *J. Am. Chem. Soc.* **2011**, *133*, 13183–13196.

(39) Spencer, L. P.; Yang, P.; Scott, B. L.; Batista, E. R.; Boncella, J. M. *J. Am. Chem. Soc.* **2008**, *130*, 2930–2931.

(40) Jilek, R. E.; Tomson, N. C.; Scott, B. L.; Boncella, J. M. *Inorganica Chim. Acta* **2014**, *422*, 78–85.

(41) Tatebe, C. J.; Zeller, M.; Bart, S. C. *Inorg. Chem.* **2017**, *56* (4), 1956–1965.

(42) Ren, W.; Zi, G.; Fang, D.-C.; Walter, M. D. *Chem. - A Eur. J.* **2011**, *17*, 12669–12682.

(43) Jilek, R. E.; Tomson, N. C.; Shook, R. L.; Scott, B. L.; Boncella, J. M. *Inorg. Chem.* **2014**, *53* (18), 9818–9826.

(44) Spencer, L. P.; Yang, P.; Scott, B. L.; Batista, E. R.; Boncella, J. M. *Comptes Rendus Chim.* **2010**, *13* (6–7), 758–766.

(45) Graves, C. R.; Vaughn, A. E.; Schelter, E. J.; Scott, B. L.; Thompson, J. D.; Morris, D. E.; Kiplinger, J. L. *Inorg. Chem.* **2008**, *47* (24), 11879–11891.

(46) Schatte, G.; Chivers, T.; Tuononen, H. M.; Suontamo, R.; Laitinen, R.; Valkonen, J. *Inorg. Chem.* **2005**, *44*, 443–451.

(47) Britovsek, G. J. P.; Bruce, M.; Gibson, V. C.; Kimberley, B. S.; Maddox, P. J.; Mastroianni, S.; McTavish, S. J.; Redshaw, C.; Solan, G. A.; Strömberg, S.; White, A. J. P.; Williams, D. J. *J. Am. Chem. Soc.* **1999**, *121* (38), 8728–8740.

(48) Barral, K.; Moorhouse, A. D.; Moses, J. E. *Org. Lett.* **2007**, *9* (9), 1809–1811.

(49) Chakraborty, S.; Chattopadhyay, J.; Guo, W.; Billups, W. E. *Angew. Chemie Int. Ed.* **2007**, *46* (24), 4486–4488.

(50) Kiplinger, J. L.; John, K. D.; Morris, D. E.; Scott, B. L.; Burns, C. J. *Organometallics* **2002**, *21* (21), 4306–4308.

(51) Lam, O. P.; Feng, P. L.; Heinemann, F. W.; O'Connor, J. M.; Meyer, K. *J. Am. Chem. Soc.* **2008**, *130* (9), 2806–2816.

(52) Settineri, N. S.; Shiau, A. A.; Arnold, J. *Chem. Commun.* **2018**, *54* (77), 10913–10916.

(53) Nucciarone, D.; Taylor, N. J.; Carty, A. J. *Organometallics* **1986**, *5* (12), 2565–2567.

(54) Iikubo, T.; Itoh, T.; Hirai, K.; Takahashi, Y.; Kawano, M.; Ohashi, Y.; Tomioka, H. *European J. Org. Chem.* **2004**, *2004* (14), 3004–3010.

(55) Kraft, S. J.; Fanwick, P. E.; Bart, S. C. *Inorg. Chem.* **2010**, *49* (3), 1103–1110.

(56) Miller, J. *J. Org. Chem.* **1959**, *24* (4), 560–561.

(57) Cherney, A. H.; Kadunce, N. T.; Reisman, S. E. *Chem. Rev.* **2015**, *115* (17), 9587–9652.

(58) Swift, E. C.; Jarvo, E. R. *Tetrahedron* **2013**, *69*, 5799.

(59) Rudolph, A.; Lautens, M. *Angew. Chem., Int. Ed.* **2009**, *48*, 2656.

(60) Hu, X. *Chem. Sci.* **2011**, *2*, 1867.

(61) Liang, Y.; Fu, G. C. *J. Am. Chem. Soc.* **2014**, *136*, 5520.

(62) Binder, J. T.; Cordier, C. J.; Fu, G. C. *J. Am. Chem. Soc.* **2012**, *134*, 17003.

(63) Ilardi, E. A.; Vitaku, E.; Njardarson, J. T. *J. Med. Chem.* **2014**, *57*, 2832.

(64) Nelson, D. J.; Brammer, C. N. *Fluorine-Related Nanoscience with Energy Applications*; Nelson, D. J., Brammer, C. N., Eds.; American Chemical Society: Washington D. C., 2011.

(65) Wang, J.; Sánchez-Roselló, M.; Aceña, J. L.; del Pozo, C.; Sorochinsky, A. E.; Fustero, S.; Soloshonok, V. A.; Liu, H. *Chem. Rev.* **2014**, *114*, 2432.

(66) Ni, C.; Hu, M.; Hu, J. *Chem. Rev.* **2015**, *115*, 765.

(67) Guo, Y.; Shreeve, J. M. *Chem. Commun.* **2007**, 3583.

(68) Prakash, G. K. S.; Ganesh, S. K.; Jones, J.-P.; Kulkarni, A.; Masood, K.; Swabeck, J. K.; Olah, G. A. *Angew. Chem., Int. Ed.* **2012**, *51*, 12090.

(69) Qi, Q.; Shen, Q.; Lu, L. *J. Am. Chem. Soc.* **2012**, *134*, 6548.

(70) Fier, P. S.; Hartwig, J. F. *J. Am. Chem. Soc.* **2012**, *134*, 5524.

(71) Ge, S.; Chaladaj, W.; Hartwig, J. F. *J. Am. Chem. Soc.* **2014**, *136*, 4149.

(72)   Min, Q.-Q.; Yin, Z.; Feng, Z.; Guo, W.-H.; Zhang, X. *J. Am. Chem. Soc.* **2014**, *136*, 1230.

(73)   Feng, Z.; Min, Q.-Q.; Xiao, Y.-L.; Zhang, B.; Zhang, X. *Angew. Chem., Int. Ed.* **2014**, *53*, 1669.

(74)   Xiao, Y.-L.; Guo, W.-H.; He, G.-Z.; Pan, Q.; Zhang, X. *Angew. Chem., Int. Ed.* **2014**, *53*, 9909.

(75)   Yu, Y.-B.; He, G.-Z.; Zhang, X. *Angew. Chem., Int. Ed.* **2014**, *53*, 10457.

(76)   Matheis, C.; Jouvin, K.; Goossen, L. J. *Org. Lett.* **2014**, *16*, 5984.

(77)   Yang, X.; Wu, T.; Phipps, R. J.; Toste, F. D. *Chem. Rev.* **2015**, *115*, 826.

(78)   Gu, Y.; Leng, X.; Shen, Q. *Nat. Commun.* **2014**, *5*, 5405.

(79)   Wang, L.; Wei, X.-J.; Jia, W.-L.; Zhong, J.-J.; Wu, L.-Z.; Liu, Q. *Org. Lett.* **2014**, *16*, 5842.

(80)   Shi, S.-L.; Buchwald, S. L. *Angew. Chem., Int. Ed.* **2015**, *54*, 1646.

(81)   Ivanova, M. V; Bayle, A.; Besset, T.; Poisson, T.; Pannecoucke, X. *Angew. Chem., Int. Ed.* **2015**, *54*, 13406.

(82)   Xu, T.; Cheung, C. W.; Hu, X. *Angew. Chem., Int. Ed.* **2014**, *53*, 4910.

(83)   Ma, G.; Wan, W.; Li, J.; Hu, Q.; Jiang, H.; Zhu, S.; Wang, J.; Hao, J. *Chem. Commun.* **2014**, *50*, 9749.

(84)   Yu, C.; Iqbal, N.; Park, S. E.; Cho, J. *Chem. Commun.* **2014**, *50*, 12884.

(85)   Fu, W.; Zhu, M.; Zou, G.; Xu, C.; Wang, Z. *Asian J. Org. Chem.* **2014**, *3*, 1273.

(86)   Riente, P.; Pericàs, M. A. *ChemSusChem* **2015**, *8*, 1841.

(87)   Campbell, M. G.; Ritter, T. *Chem. Rev.* **2015**, *115*, 612.

(88)   Alonso, C.; Martínez de Marigorta, E.; Rubiales, G.; Palacios, F. *Chem. Rev.* **2015**, *115*, 1847.

(89)   Xu, J.; Liu, X.; Fu, Y. *Tetrahedron Lett.* **2014**, *55*, 585.

(90)   Liang, Y.; Fu, G. C. *Angew. Chem., Int. Ed.* **2015**, *54*, 9047.

(91)   Yang, M.-H.; Orsi, D. L.; Altman, R. A. *Angew. Chem., Int. Ed.* **2015**, *54*, 2361.

(92)   Kitazume, T.; Ishikawa, N. *J. Am. Chem. Soc.* **1985**, *107*, 5186.

(93)   Uneyama, K.; Tanaka, H.; Kobayashi, S.; Shioyama, M.; Amii, H. *Org. Lett.* **2004**, *6*, 2733.

(94)   Li, Y.; Ye, Z.; Bellman, T. M.; Chi, T.; Dai, M. *J. Org. Lett.* **2015**, *17*, 2186.

(95) Ye, Z.; Dai, M. **2015**.

(96) Sato, K.; Nakazato, S.; Enko, H.; Tsujita, H.; Fujita, K.; Yamamoto, T.; Omote, M.; Ando, A.; Kumadaki, I. *J. Fluor. Chem.* **2003**, *121*, 105.

(97) Sato, K.; Omote, M.; Ando, A.; Kumadaki, I. *J. Fluor. Chem.* **2004**, *125*, 509.

(98) Kim, B. C.; Park, A.; An, J. E.; Lee, W. K.; Lee, H. B.; Shin, H. *Synthesis (Stuttg).* **2012**, *44*, 3165.

VITA

Kristen Gettys received her B.S. in chemistry at the University of North Carolina at Greensboro in May of 2011. While in her senior year she began doing research in the laboratory of Prof. Mitchel Croatt and worked on the synthesis of targets for GPR55. This research prompted her to stay in Greensboro and pursue a master's degree from the same university. While continuing to study under Prof. Croatt, she completed her thesis on the synthesis of analogs of isocarbacyclin with emphasis on decarboxylation reactions using palladium catalysts.

After graduating again from UNC Greensboro, Kristen joined the research group of Prof. Mingji Dai at Purdue University. Under his guidance she completed multiple studies in copper catalyzed cross-coupling reactions and was also involved in multiple medicinal chemistry projects. Midway through her career at Purdue, Kristen switched to the research group of Prof. Suzanne Bart and began working on high and low valent uranium projects. This switch not only gave Kristen a new lease on life, but also provided her with a greater depth of knowledge and understanding of chemistry.

PUBLICATIONS

Recent Advances in Piperazine Synthesis

Kristen E. Gettys
Zhishi Ye
Mingji Dai*

Department of Chemistry and Center for Cancer Research,
Purdue University, West Lafayette, IN 47907, USA
mjdai@purdue.edu
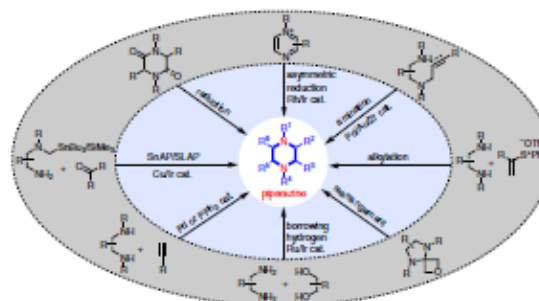
Abstract Piperazine ranks as the third most common N-heterocycle appearing in small-molecule pharmaceuticals. This review highlights recent advances in methods development for the construction of the piperazine ring system with particular emphasis on preparing carbon-substituted piperazines.

1   Introduction

The piperazine scaffold has been classified as a privileged structural motif in drug discovery and continues to have an increasing appearance in lifesaving drug molecules.[1] Recent statistical substructure analysis has shown that piperazine is the third most commonly used N-heterocycle (ranked right behind piperidine and pyridine) in small-molecule pharmaceuticals. Several piperazine-containing drugs are within the top 100 best-selling pharmaceutical products (Figure 1).[2]

Most of the piperazine-containing small-molecule drugs only have substitutions on either both nitrogen atoms or on a single nitrogen atom and piperazine is mainly used as a linker to connect two portions of a drug or as an appendage to tune the drug's physicochemical properties. Piperazine, with its two opposing nitrogen atoms embedded in a six-membered ring, provides a large polar surface area, relative structural rigidity, and additional hydrogen-bond acceptors and donors, which often lead to enhanced target affinity and specificity and improved water solubility, oral bioavailability, and ADME (absorption, distribution, metabolism, and excretion) properties.[3] For the few carbon-substituted piperazine drugs, the substituents are primarily a methyl group, a carboxylate derivative, or an aryl group. Despite the importance of the piperazine structure in therapeutic development, there is a significant lack of carbon substitution diversity on the piperazine ring. The increasing needs of new drugs to combat challenging human diseases require increased structural diversity of piperazines. However, the lack of efficient synthetic methods, particularly those that provide high regio-, stereo- and enantioselectivity for synthesizing carbon-substituted piperazines, represents one of the major hurdles in unleashing the full therapeutic potential of piperazines.[4] The most straightforward way to introduce various substitutions on the carbon atoms is via direct C–H functionalization of the piperazine ring, which has shown to be extremely challenging despite the recent progresses in α-C–H functionalization of amines including piperidines and pyrrolidines. We have already summarized direct C–H functionalization of piperazines,[5] therefore the methods development in this area will not be covered in this review. Herein, we focus on recent advancements in new methods development for de novo construction of the piperazine ring as opposed to functionalization of the existing rings. These new developments have been loosely categorized in the following sections.
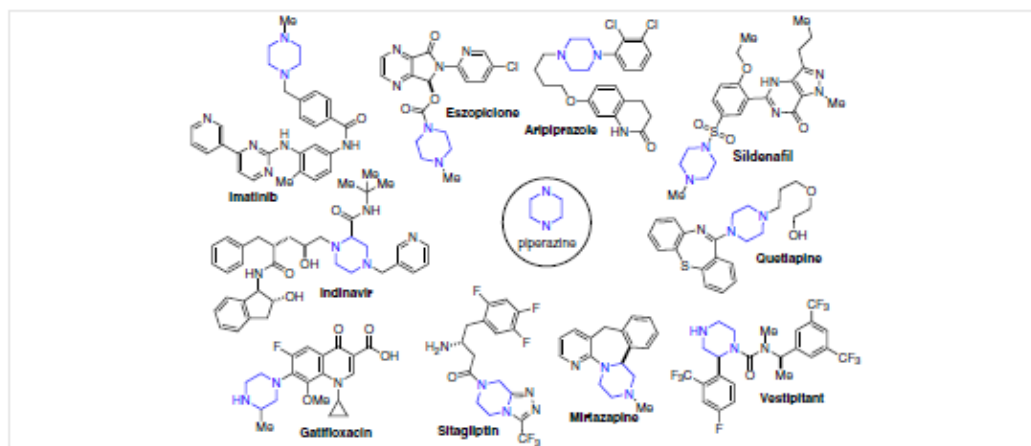
Figure 1 Selected piperazine-containing FDA-approved drugs

Biographical Sketch

Kristen E. Gettys was born in North Carolina (USA) in 1987. She received her B.S. and M.S. degrees from the University of North Carolina at Greensboro in 2011 and 2013 under the supervision of Professor Mitchel Croatt. She then joined the group of Professor Mingji Dai at Purdue University to begin her Ph.D. studies. Her current research focuses on cyclopropanol ring-opening cross-coupling reactions and lead compound optimization in medicinal chemistry.

Zhishi Ye was born in Zhejiang province, China, in 1984. After completing his B.S. degree at Wenzhou University in 2007, he continued to pursue his M.S. degree at the same university in the group of Professor Jiang Cheng and worked on C–H activation as well as transition-metal-catalyzed cascade reactions. He then pursued his graduate studies at Dalian Institute of Chemical Physics, Chinese Academy of Sciences and received his Ph.D. in 2013 under the supervision of Professor Yong-Gui Zhou. His graduate research mainly focused on asymmetric hydrogenation of aromatic compounds. He is currently a postdoctoral research fellow in Professor Mingji Dai's group at Purdue University (USA) and focuses on ring-opening cross-coupling reactions of cyclopropanols and new methods for the synthesis of heterocyclic compounds.

Mingji Dai grew up in Sichuan, China, and received his B.S. from Peking University in 2002. After two years of research with Professors Zhen Yang and Jiahua Chen at the same university, he went to New York (USA) in 2004 to pursue graduate studies under the guidance of Professor Samuel J. Danishefsky and earned his Ph.D. in 2009. He then took a postdoctoral position in the laboratory of Professor Stuart L. Schreiber at Harvard University and the Broad Institute. In August 2012, he began his independent career as an assistant professor in the Chemistry Department of Purdue University (USA). His lab currently focuses on developing new strategies and methodologies for the synthesis of complex natural products and other medicinally and biologically important molecules.

2 Reduction of (DI)ketopiperazine

One of the most commonly used methods to synthesize piperazines is the reduction of the corresponding (di)keto-piperazines, which are generally synthesized from the amino acid chiral pool (for diketopiperazine), 1,2-diamines (ketopiperazine) and other readily available starting materials.[6] These syntheses, while reliable, suffer from lengthy synthetic steps. The carbon substitutions on the piperazine ring are also limited to the availability of the amino acids or 1,2-diamines. Therefore, it is important to develop new (di)ketopiperazine synthesis methods to introduce important substituents which are not readily available from the current amino acid or 1,2-diamine pool. A few such methods are highlighted here.

As shown in Scheme 1, Fustero and co-workers developed a diastereoselective synthesis of trifluoromethyl-substituted piperazines.[7] Instead of using commercially available fluorinated building blocks, the trifluoromethyl group was introduced via a diastereoselective nucleophilic addition of the Ruppert–Prakash reagent (TMSCF$_3$)[8] to Ellman's N-(tert-butanesulfinyl)imines.[9] After a sequence of tert-butanesulfinyl group removal, ketopiperazine formation, reduction and deprotection, both cis- and trans-2-phenyl-3-(trifluoromethyl)piperazines were produced in enantiopure form, which can serve as important building blocks for the development of new therapeutics.
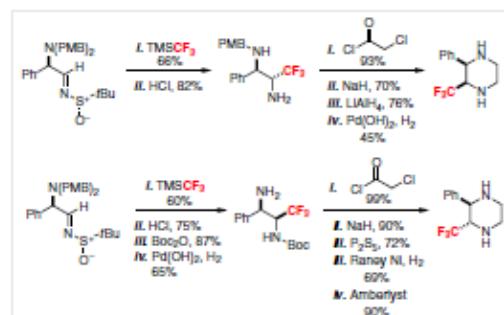
Scheme 1 Diastereoselective synthesis of trifluoromethyl-substituted piperazines

The Stoltz group reported, in 2015, an elegant enantioselective method for the synthesis of ketopiperazines with various carbon substitutions. In continuation of their research in the construction of α-tetrasubstituted carbonyl compounds,[10] they have developed a highly enantioselective palladium-catalyzed decarboxylative allylic alkylation of a variety of N-protected piperazin-2-ones,[11] which can then be converted into the corresponding piperazines via further reductive transformations (Scheme 2). This new synthetic capability utilizes 5 mol% of [Pd$_2$(pmdba)$_3$] cata-

lyst in combination with 12.5 mol% of an electron-deficient PHOX ligand such as (S)-(CF$_3$)$_3$-tBuPHOX. It has a broad substrate scope and products were obtained in high yield and high enantioselectivity. The resulting allyl group can be used as a convenient handle to introduce other substituents and functional groups to further improve the substitution diversity on the carbon atom.

Scheme 2 The Stoltz enantioselective synthesis of piperazin-2-ones
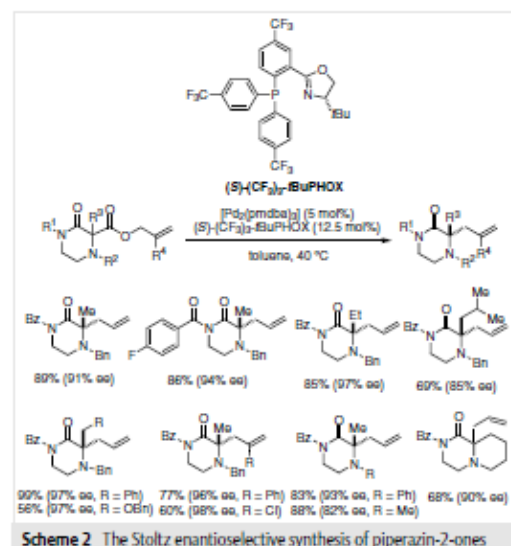
In 2015, Krasavin and co-workers applied the Castagnoli–Cushman reaction[12] with glutaric anhydride analogues to synthesize piperazine and other heterocycles (Scheme 3).[13] A variety of ketopiperazine products could be obtained in high yield and trans-stereoselectivity by utilizing different imine coupling partners.

3 N-Alkylation

Alkylation of amines is another commonly used method to synthesize piperazines.[14] In 2012, Lindsley and O'Reilly combined an organocatalytic enantioselective chlorination of aldehydes[15] with a sequential inter- and intramolecular alkylation (Procedure A) or reductive amination and intramolecular alkylation (Procedure B) to synthesize carbon-functionalized piperazines (Scheme 4).[16] While it is a five-step (Procedure A) or three-step sequence (Procedure B), the overall yield is synthetically useful and the substituted piperazine products are produced in good to high enantioselectivity.
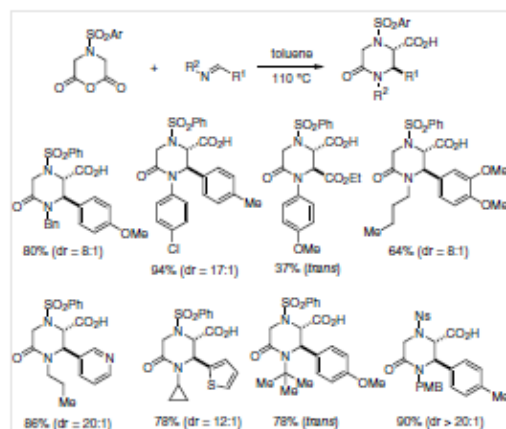
Scheme 3 Synthesis of ketopiperazines via the Castagnoli–Cushman reaction
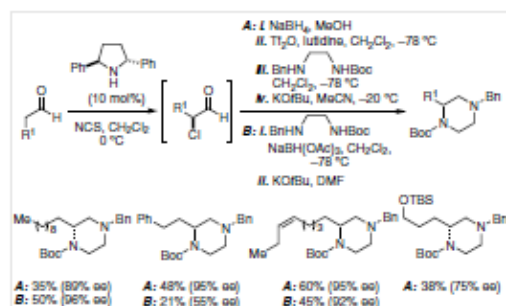
Scheme 4 Synthesis of piperazines via a combination of organocatalytic enantioselective chlorination of aldehydes and alkylation of 1,2-diamines

Another notable development for the synthesis of piperazines via an alkylation of 1,2-diamine derivatives came from the Aggarwal group.[17] They designed a sequence of conjugate addition to vinyl sulfonium salts followed by intramolecular ring closure (Scheme 5). The use of vinyl sulfonium salts as the two-carbon unit avoids some of the problems in using 1,2-dihalogen electrophiles, which are generally poor in terms of reactivity. The latter also suffer from competing elimination processes under basic reaction conditions. The commercially available diphenyl vinyl sulfonium salt can be readily synthesized as well via a base-promoted elimination of the corresponding bromoethylsulfonium salt. It reacts with both free and sulfonamide-protected 1,2-diamines under very mild reaction conditions with triethylamine as base and at 0 °C to room temperature. 1,2-Amino alcohols can be used as nucleophile as well to produce substituted morpholines. Later, the

Aggarwal group discovered that the bromoethylsulfonium salt could be an effective annulation agent for the synthesis of six- and seven-membered 1,4-heterocyclic compounds including piperazines via an in situ generation of the required vinyl sulfonium salts.[18]
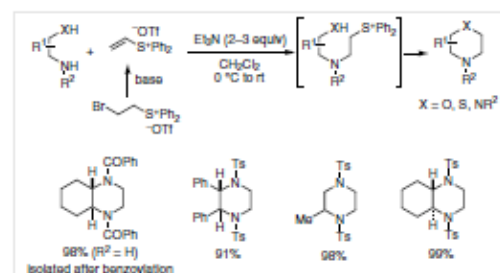
Scheme 5 Annulation with vinyl sulfonium salts

The annulation method with vinyl sulfonium salts was later expanded to synthesize enantiopure *trans*-3-arylpiperazine-2-carboxylic acid derivatives by Chin, Kim, and co-workers (Scheme 6).[19] In this case, they developed an elegant synthesis of the enantiomerically pure 1,2-diamine derivatives via a diaza-Cope rearrangement of a diimine intermediate derived from sequential imine formation between an aryl aldehyde and *trans*-cinnamaldehyde with (*R,R*)/(*S,S*)-1,2-bis(2-hydroxyphenyl)-1,2-diaminoethane (HPEN).
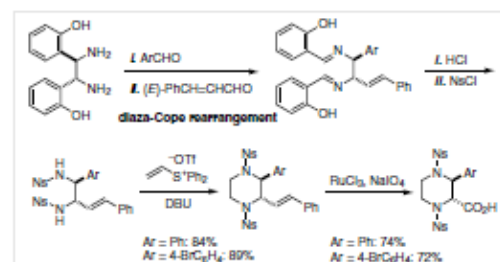
Scheme 6 Annulation with vinyl sulfonium salts for the synthesis of *trans*-3-arylpiperazine-2-carboxylic acids

To further increase the carbon-substitution diversity of the piperazine product, Aggarwal and co-workers discovered that α-phenylvinyl sulfonium salt could be used as an electrophile to react with 1,2- or 1,3-diamines/1,2- or 1,3-amino alcohols to synthesize carbon-substituted piperazines, azepines, morpholines, and oxazepines (Scheme 7).[20] When unsymmetrical 1,2-diamine derivatives were used, the less sterically hindered sulfonamide underwent nucleophilic addition to the α-phenylvinyl sulfonium salt first and the regioselectivity is generally high.
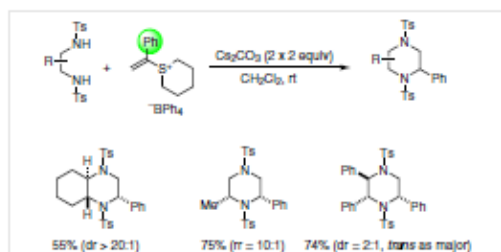
Scheme 7 Annulation with α-phenylvinyl sulfonium salt

In 2011, Bagnoli and co-workers reported a similar annulation process with vinyl selenones as electrophiles (Scheme 8).[21] The desired piperazines were produced in good to excellent yield with either sodium hydride or 1,8-diazabicyclo[5.4.0]undec-7-ene (DBU) as base.
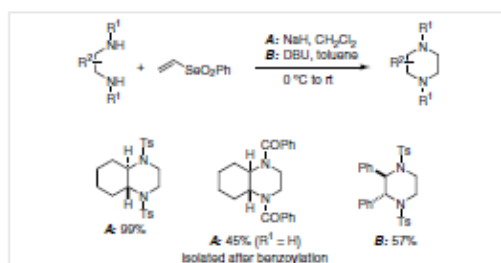
Scheme 8 Annulation with vinyl selenones

Couty and co-workers published a synthesis of fused tri- and tetrazole piperazines by treating the chlorination products of N-cyanomethyl β-amino alcohols with sodium azide under thermal conditions (Scheme 9).[22] In the case of secondary benzylic chlorides, a single isomer was formed. However, in the case of primary alkyl chlorides, two isomers were formed in a nearly 1:1 ratio. The drop in selectivity is presumably due to the formation of an aziridinium intermediate, which can then be opened by sodium azide to provide a mixture of two alkyl azides for the subsequent cycloaddition reactions. It was also discovered that the reaction was not limited to N-cyanomethyl β-amino alcohols. Fused piperazine-triazole products can be formed with propargylic amine substrates. Much better reaction yields were obtained for terminal alkyne substrates than the internal alkyne substrates.
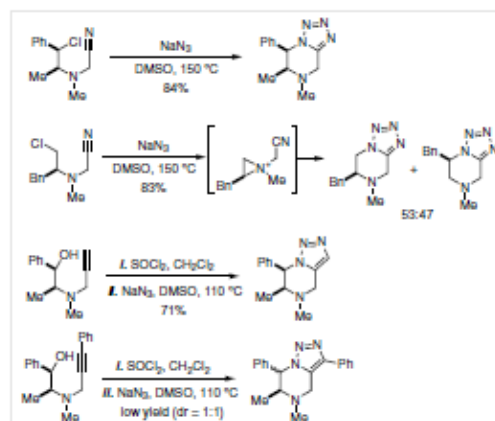
Scheme 9 N-Alkylation followed by [3+2] cycloaddition

4 Transition-Metal-Catalyzed/Mediated Piperazine Synthesis

Recently, several interesting transition-metal-catalyzed/mediated piperazine syntheses have been developed. The commonly used transition metals include copper, palladium, gold, ruthenium, iridium, and zirconium. In comparison to the traditional (di)ketopiperazine and alkylation approaches, the transition-metal-catalyzed piperazine syntheses provide new reaction modes, new retrosynthetic analyses in planning, and new avenues to access various substitution patterns in the products.

4.1 The SnAP and SLAP Methods

The Bode group has developed a series of stannyl amine protocol (SnAP) reagents for the synthesis of a variety of N-heterocycles.[23] A significant amount of the SnAP reagents are now commercially available or can be synthesized via an alkylation with tributyl(iodomethyl)stannane. In the presence of 1.0 equivalent of Cu(OTf)$_2$, the SnAP reagents react with a variety of aldehydes via a sequence of condensation, radical formation, and cyclization to provide a wide range of N-heterocycles including piperazines (Scheme 10).[24] Later, a set of catalytic conditions with 10 mol% of Cu(OTf)$_2$ was developed as well.[25] In addition to aldehydes, the reaction was further expanded to ketone substrates, including cyclic ketones to synthesize poly-carbon-substituted piperazines and spirocyclic piperazines.[26] These discoveries represent a breakthrough in N-heterocycle synthesis, particularly carbon-substituted piperazine synthesis, due to the existence of a large amount of readily available alde-

hydes and ketones. Because of the radical cyclization nature, developing an enantioselective version is difficult and has not been reported so far, but is worthy of attempt.
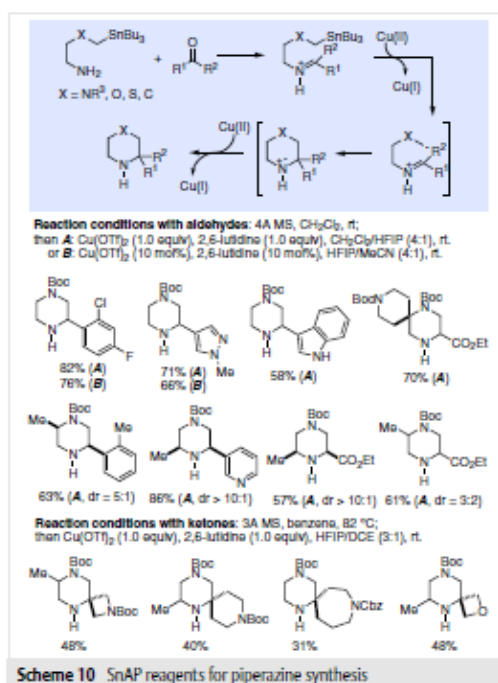
Scheme 10 SnAP reagents for piperazine synthesis

Direct condensations of acyclic ketones with the SnAP reagents are sometimes problematic. Bode and co-workers overcame this challenge by using azido SnAP reagents (Scheme 11) to access the required ketimine via a Staudinger–aza-Wittig reaction with a polymer-bound phosphine reducing reagent.[26] When 2,2,2-trifluoromethyl ketones were used, several trifluoromethyl-substituted piperazines were synthesized in modest yield.
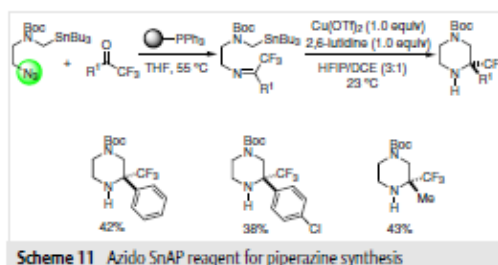
Scheme 11 Azido SnAP reagent for piperazine synthesis

One major drawback for the SnAP process is the use and production of toxic tin reagents. To solve this problem, a series of silicon amine protocol (SLAP) reagents were developed by the Bode group to provide a tin-free alternative (Scheme 12).[27] Under photocatalytic conditions (blue light with Ir[(ppy)$_2$dtbbpy]PF$_6$ as catalyst), a wide range of aldehydes including aromatic, heteroaromatic, and aliphatic aldehydes could couple with the SLAP reagents. When ketones were used, the reaction yields dropped significantly.
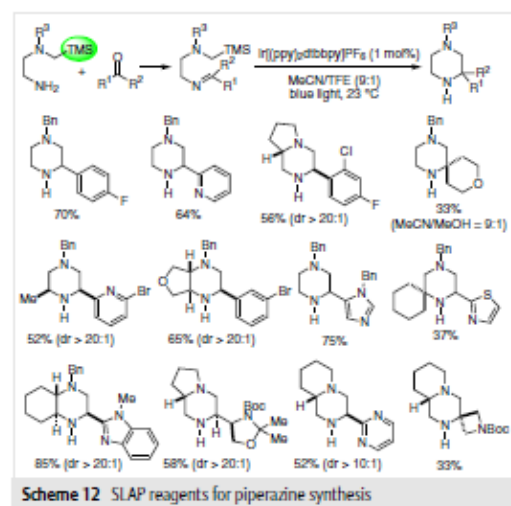
Scheme 12 SLAP reagents for piperazine synthesis

4.2 Palladium-Catalyzed Cyclization

In 2007, the Wolfe group described a piperazine synthesis via a palladium-catalyzed carboamination reaction which closes the heterocyclic ring and functionalizes the terminal alkene carbon in one step (Scheme 13).[28] The stereochemical outcome is presumably determined by the favored six-membered-ring transition state in which the terminal olefin is pseudo-equatorial and the bulky aryl N-substituent is rotated to avoid $A_{1,3}$ interaction and allow for pseudo-equatorial positioning of the R^1 group. Generally the products were formed in good to high yields with high diastereoselectivity and a variety of aryl halides can be used to introduce structural diversity.

Following this work, Michael and Cochran published a palladium-catalyzed intramolecular hydroamination that yielded trans-2,6-disubstituted piperazines (Scheme 14).[29] Although this methodology provided high yields and excellent diastereoselectivity, this route is limited to terminal olefins and produces only a methyl group at the C6 position. Interestingly, analysis of the crystal structure of this type of piperazine showed that they prefer the twist-boat conformation to the traditional chair, presumably to avoid $A_{1,3}$ strain. The trans stereochemical outcome is explained by

Scheme 13 Palladium-catalyzed carboamination for *cis*-2,6-disubstituted piperazines
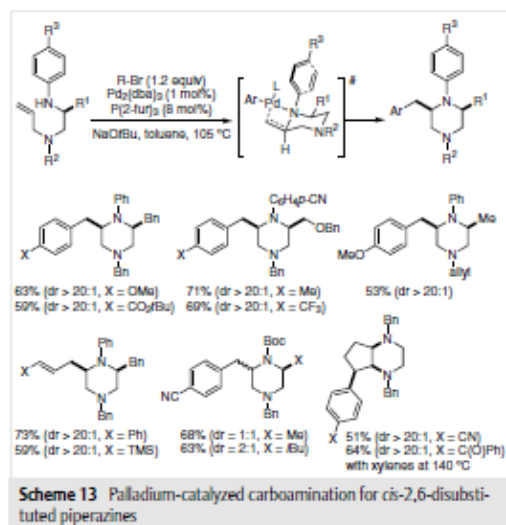
the transition state shown in Scheme 14. During the *anti*-aminopalladation process, the terminal olefin orients pseudo-equatorially while the R¹ group takes the pseudo-axial position to avoid $A_{1,3}$ interaction with the carbamate group. Eventually, *trans*-2,6-disubstituted piperazines are produced, which complements the *cis*-stereochemical outcome of Wolfe's work.

Scheme 14 Palladium-catalyzed hydroamination for *trans*-2,6-disubstituted piperazines
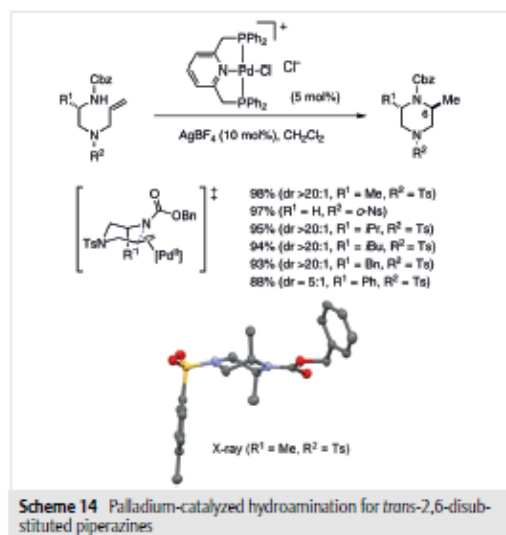
In 2012, Stahl and Lu reported a base-free palladium-catalyzed oxidative amination with oxygen as the oxidant to synthesize six-membered *N*-heterocycles including morpholines, piperazinones, piperidines, and piperazines (Scheme 15).[30] While poor yields were observed under 1 atmosphere of oxygen, under 4.1 atmospheres the reaction proceeded with good to excellent yield. Since the use of high oxygen pressure with organic solvents is a potential safety hazard, the authors provided a solution for this by diluting oxygen with an inert gas. In principle, either an allylic C–H amination[31] or an aminopalladation process could provide the same *N*-heterocycle product. Investigation of the mechanism with the homoallyl ether yielded the seven-membered ring as the major product, thus suggesting the aminopalladation pathway is preferred over the allylic C–H activation process.

Scheme 15 Aerobic and base-free oxidative amination for piperazine synthesis
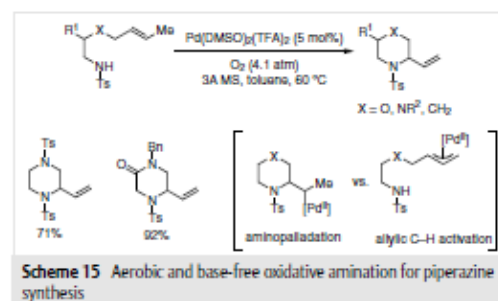
Recently, the Rawal group produced a novel palladium-catalyzed method of constructing highly substituted piperazines and related *N*-heterocycles from 1,2-diamine derivatives and Boc-protected propargyl alcohols under mild conditions (Scheme 16).[32] This process could be viewed as a formal [4+2]-diamination process to couple two of the carbons of the propargyl unit with the 1,2-diamine derivative. In general, good to excellent yields and regioselectivities were obtained. Mechanistically, the reaction is proposed to go through a Pd(II)–π-allyl species (shown in brackets) which is derived from nucleophilic attack of the sulfonamide nitrogen to the middle carbon of a cationic palladium allene species generated from the Boc-protected propargyl alcohol.

Expansion of this work to include aryl amide and sulfonamide groups progressed nicely and a library of complex piperazinones were constructed with good to nearly quantitative yields as shown in Scheme 17.[32] Reaction times ranged from 30 minutes to 28 hours and it was noted that electron-deficient aryl amides reacted faster than the corresponding electron-rich equivalents. Finally, the easily removable nosyl sulfonamides were synthesized with yields similar to those of the tosyl analogues, but the reactions required more time to reach completion.
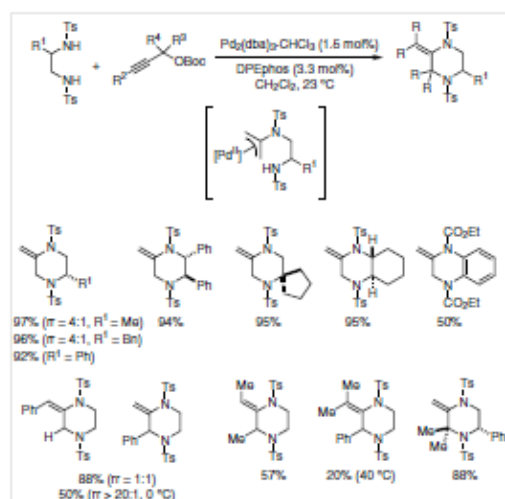
Scheme 16 Palladium-catalyzed formal [4+2] cycloaddition of Boc-protected propargyl alcohols
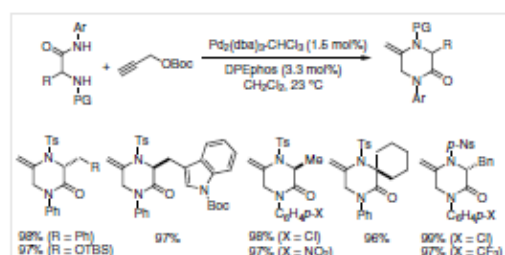
Scheme 17 Rawal's synthesis of substituted ketopiperazines

4.3 Gold-Catalyzed Cyclization

While palladium continues to be the transition metal of choice for many reactions, its drawbacks (including the β-hydride elimination pathway) cannot be ignored. Alternatively, several groups have explored gold-catalyzed cyclization strategies to synthesize piperazines. In 2013, Nelson and co-workers described a gold-catalyzed cyclization of propargylic sulfonamides derived from ring opening of cyclic sulfamidates to provide tetrahydropyrazines (Scheme 18, A).[33] Further reduction of the tetrahydropyrazine products with the treatment of trifluoroacetic acid and triethylsilane yielded piperazines in good yields. After removal of the Boc- or Cbz-protecting group, a Ugi-type multicomponent reaction of the resultant tetrahydropyrazines with tri-

fluoroacetic acid and substituted isonitriles afforded differentially protected piperazines and introduced another carboxamide group at the α-position.

In the case that the kinetic ketone product is formed preferentially over the thermodynamic cyclization under the gold-catalyzed reaction conditions (Scheme 18, B), the resulting ketone product could undergo a reductive amination cyclization with the treatment of trifluoroacetic acid and triethylsilane to provide the desired piperazine in high yield and diastereoselectivity.
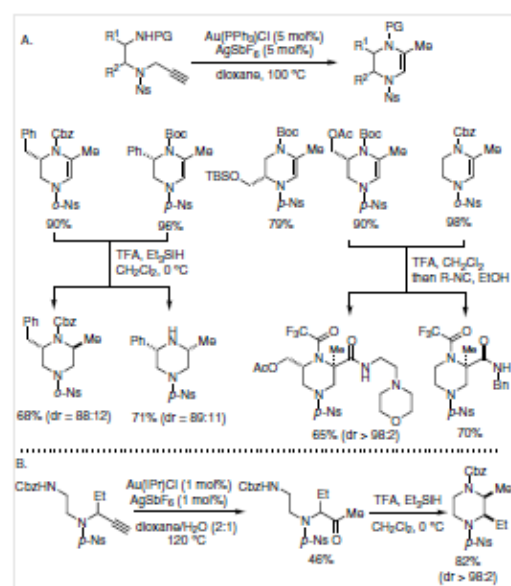
Scheme 18 Gold-catalyzed piperazine synthesis developed by Nelson

Following Nelson's work, Huang and co-workers reported their synthesis of tetrahydropyrazines utilizing similar gold-catalyzed cyclization of propargylic sulfonamides (Scheme 19).[34] Most of the reactions were completed at 40 °C and required a lower catalyst loading than in Nelson's protocols. Deuterium labeling experiments suggested a reaction pathway in which the product is formed through a 6-exo-dig cyclization where the nucleophilic nitrogen attacks the internal carbon of the triple bond activated by the gold catalyst.

4.4 Other Metal-Catalyzed/Mediated Cyclization

Several transition metals other than palladium and gold have been utilized to synthesize piperazines as well. The Schafer group has used a special titanium–amidate catalyst developed in their group to catalyze a regioselective intramolecular hydroamination to produce a tetrahydropyrazine
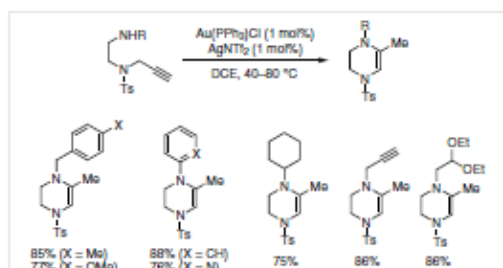
Scheme 19 Gold-catalyzed intramolecular cyclization as described by Huang

which was then reduced to piperazine utilizing the Noyori asymmetric hydrogenation[35] in 80% yield and 70% ee (Scheme 20, A).[36] The requisite aminoalkyne starting materials can be tedious to synthesize and often require multiple steps. The Schafer group has also shown that a zirconium–urea catalyst developed in their laboratory is able to promote intramolecular hydroamination of alkenes.[37] They then developed a novel protocol toward 2,5-substituted piperazines by taking advantage of the unique hydroamination reactivity of their titanium–amidate catalyst and zirconium–urea catalyst. The last step of this protocol is to convert substituted diaminoalkene substrates into 2,5-substituted piperazines using their zirconium–urea catalyst (Scheme 20, B). The substituted diaminoalkene substrates were synthesized via the titanium–amidate-catalyzed regioselective intermolecular hydroamination and a sequence of a modified Strecker reaction, alkylation and reduction. This new approach is very effective for the synthesis of N-benzyl-substituted piperazines and the overall yields are good with high stereoselectivity. When the method was used to access N-benzhydryl-substituted piperazines, a motif commonly used in medicinal chemistry, it proved to be much less effective and the desired products were produced in only 20–30% yields. This new approach uses commercially available starting materials. Due to the ready availability of a large number of allyl bromides and alkynes, it has the potential to provide new avenues to access substituted piperazines that are otherwise difficult to prepare.

An attractive but challenging strategy toward piperazines would be the direct [4+2] cyclization of an olefin and a 1,2-diamine or its derivative. Paul and co-workers reported a mercury-mediated oxidative diamination of olefins (Scheme 21).[38] Both terminal and internal olefins are effective substrates and a variety of piperazines could be produced in good to excellent yield. The proposed mechanism involves an intermolecular aminomercuration to form a β-aminomercury(II) tetrafluoroborate complex which then undergoes an intramolecular cyclization after attack by the second amino group to yield the desired piperazine. Obviously, the major drawback of this method is the use of more
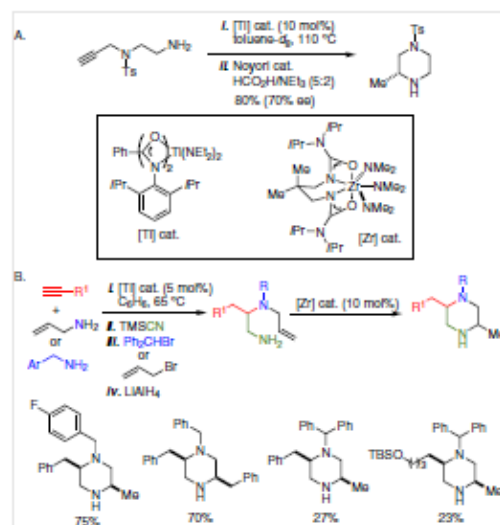
Scheme 20 Schafer's synthesis of piperazines via zirconium- and titanium-catalyzed hydroaminations

than a stoichiometric amount of highly toxic mercuric oxide. Only symmetrical bis-methylated or benzylated ethylene diamines have been explored so far.
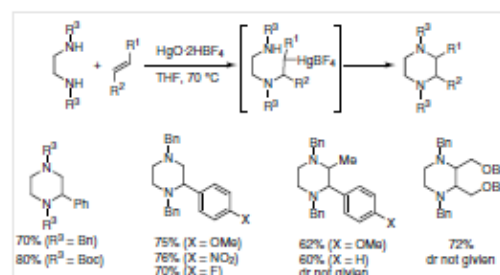
Scheme 21 Mercuric oxide mediated cyclization of 1,2-diamines with olefins

4.5 Borrowing Hydrogen Strategy

Amines and alcohols are common and readily available starting materials. Direct substitution of an alcohol by an amine[39] is an alternative and attractive alkylation approach to substituted amines. In principle, this redox-neutral approach could avoid the use of oxidants and reducing reagents and the only byproduct from the reaction would be water, therefore rendering this approach to be highly environmentally friendly. This type of reaction has been termed 'borrowing hydrogen'. The approach has been widely stud-

142

ied from an academic perspective[40] and it has been applied in the pharmaceutical industry.[41] The first application of 'borrowing hydrogen' for piperazine synthesis appeared in 1985. Watanabe and co-workers published a pioneering ruthenium-catalyzed reaction to convert 1,5-diols and primary amines into *N*-alkylated or *N*-arylated piperazines (Scheme 22).[42] As opposed to the reductive amination approach which requires unstable aldehydes and stoichiometric reducing reagent, this process uses inexpensive and readily available alcohols and only a catalytic amount of ruthenium catalyst.
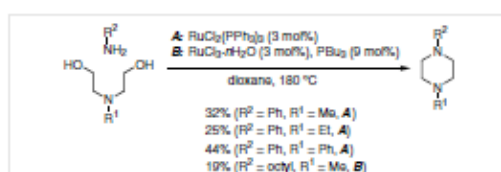
Scheme 22 Ruthenium-catalyzed 'borrowing hydrogen' synthesis of piperazines

In 2007, Madsen and co-workers utilized the 'borrowing hydrogen' concept and developed an iridium-catalyzed synthesis of piperazines (Scheme 23).[43] Under their catalytic conditions at elevated reaction temperatures, various 1,2-diamines and 1,2-diols underwent cyclocondensation to yield substituted piperazines in good to excellent yield and high stereoselectivity. Both toluene and water can be used as solvent. Use of benzylamine with two equivalents of ethylene glycol works as well (eq. 1). Impressively, two different 1,2-diols could be incorporated into one piperazine to provide unsymmetrical product (eq. 2).

4.6 Imine Reductive Cyclization

Intramolecular reductive coupling of 1,2-diimines is an efficient method to synthesize 2,3-substituted piperazines. The cyclization precursor can be prepared readily from condensation of a 1,2-diamine and two aldehydes. Sigman and Mercer described a manganese and Brønsted acid promoted reductive cyclization of diimines which yielded *trans*-2,3-(hetero)aryl-substituted piperazines in moderate to high yields (Scheme 24).[44] Unfortunately, the reaction was not productive when applied to non-aromatic diimines. The reasoning for the *trans*-substitution of the products lies in the proposed six-membered transition state when the diradical intermediate cyclizes to piperazine. In the transition state, the aryl substituents are oriented *trans* to each other in equatorial sites.
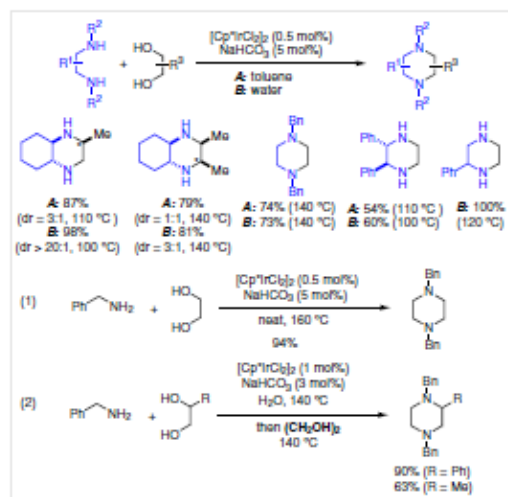
Scheme 23 Iridium-catalyzed 'borrowing hydrogen' synthesis of piperazines
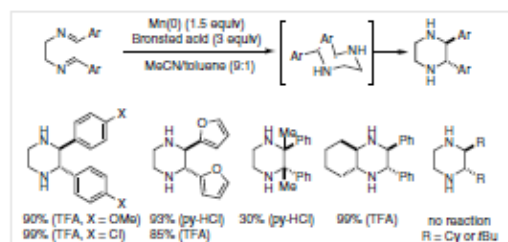
Scheme 24 Manganese-mediate reductive cyclization of 1,2-diimines

Similarly to Sigman's work, the Periasamy group reported a zinc and titanium promoted reductive cyclization that was also limited to aryl substitutions as seen in Scheme 25.[45] Periasamy also described a procedure to yield the desired piperazine product in 99% ee after chiral resolutions using tartaric and oxalic acids.

5 Reduction of Pyrazines

Pyrazines are common nitrogen heteroaromatics and can be accessed or modified readily. Direct reduction of pyrazines via hydrogenation or hydride reaction is undoubtedly an efficient and convenient way to synthesize piperazines. Significant progress has been made in this area, but the enantioselective reduction of pyrazines is still challenging[46] and only a few examples have been reported.
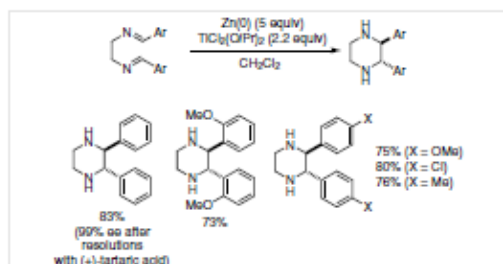
Scheme 25 Zinc/titanium-mediated reductive coupling of 1,2-diimines

During their synthesis of the HIV protease inhibitor indinavir, which contains a piperazine 2-carboxamide, a group of Merck scientists led by Rossen reported a sequential reduction of a 2-tert-butyl amide substituted pyrazine to provide the piperazine core in high enantioselectivity.[47] Controlled partial hydrogenation of the 2-tert-butyl pyrazine amide followed by nitrogen protections gave the N-Boc- and N-Cbz-protected tetrahydropyrazine for an asymmetric hydrogenation. With a (R)-BINAP–Rh complex as catalyst and under high pressure (70 bar), the desired piperazine was furnished in 96% yield with 99% ee, and was then subjected to hydrogenolytic removal of the Cbz group and crystallization to yield the mono-protected piperazine in 96% yield and with 99% ee (Scheme 26).
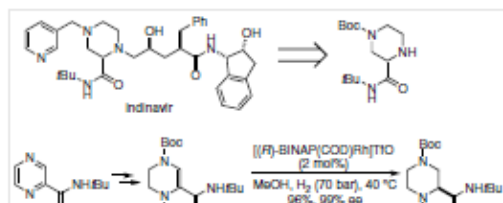
Scheme 26 Asymmetric hydrogenation for the synthesis of indinavir

Advances on this protocol were later made by Rossen and co-workers using a unique cationic PhanePhos–Rh complex (Scheme 27).[48] The previously described BINAP–Rh catalyst system, while effective for the tetrahydropyrazine bearing bulky tert-butyl amide, gave only 56% ee and 88% yield when applied to tetrahydropyrazines bearing ester substitutions. The products of the latter are desirable for the synthesis of other HIV protease inhibitors such as indinavir. The new PhanePhos–Rh complex gave the desired 2-ester-substituted piperazine product with 100% conversion in 86% ee at significantly lower pressure (1.5 bar) and temperature (–40 °C).
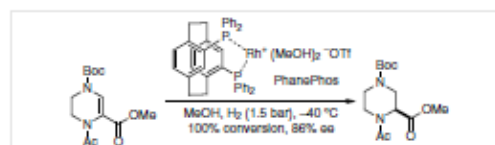
Scheme 27 Asymmetric hydrogenation with PhanePhos–Rh complex

In 1999, Ito and Kuwano described an asymmetric reduction of 2-amide-substituted tetrahydropyrazines with the (R,R)-(S,S)-TRAP–Rh complex (Scheme 28).[49] The conversion and enantioselectivity of the reaction are quite sensitive to the substituents on the two nitrogen atoms in the six-membered ring, with conversions ranging from 16 to 85% and enantiomeric excess values ranging from 51 to 96%.
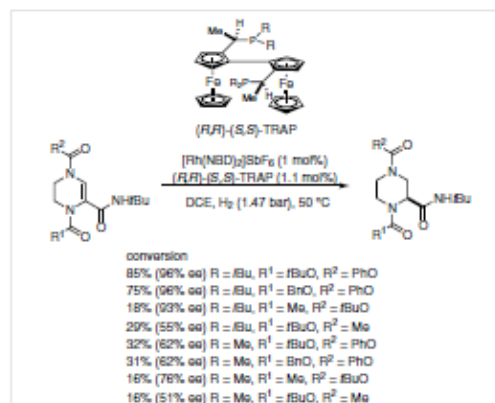
Scheme 28 Asymmetric hydrogenation with the (R,R)-(S,S)-TRAP–Rh complex

In 1997, Fuchs reported a direct asymmetric hydrogenation of pyrazinecarboxylic acid derivatives to piperazines without isolating the tetrahydropyrazine intermediates and masking the two nitrogen atoms (Scheme 29).[50] Using a JosiPhos–Rh complex, good yield and enantioselectivity could be obtained with a bulky carboxylate derivative at the 2-position. This method offers nitrogen-unprotected piperazine products directly, thereby avoiding protecting group manipulations, but the enantioselectivity needs to be improved.

The challenge for direct enantioselective hydrogenation of pyrazine lies in its high aromaticity and the presence of two strong coordinative nitrogen atoms which may interfere with the transition-metal catalyst of choice. The resulting nitrogen-unprotected piperazine product may also deactivate the catalyst used due to its two secondary amines. Recently, Zhou and co-workers developed an elegant solu-
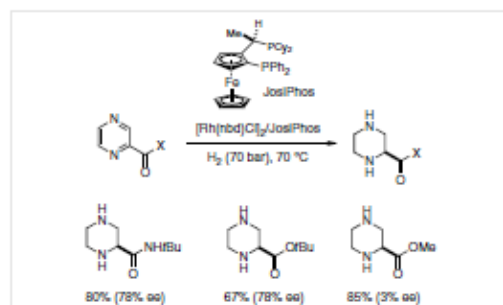
Scheme 29   Direct asymmetric hydrogenation of pyrazines

tion for these issues by using alkyl halides to activate the pyrazine via the formation of pyrazinium salt and weaken the coordinating ability of the nitrogens in the starting material and product (Scheme 30).[31] They have reported a set of reaction conditions using chiral iridium–bidentate phosphine complexes to reduce a variety of benzyl pyrazinium salts to piperazines with different carbon substitution patterns. In general, the yields and enantioselectivities are excellent and many functional groups are tolerated. This strategy provides mono-*N*-protected products, allowing for further modification to be made without selective deprotection or differentiation of two free nitrogens. The benzyl group can be removed easily by a simple catalytic hydrogenation. This method was used to synthesize vestipitant (Figure 1), a selective NK1 receptor antagonist with potential application as an antiemetic and anxiolytic drug, in an overall yield of 47%. It was also applied to a formal synthesis of (*S*)-mirtazapine (Figure 1) with the potential to treat insomnia and climacteric symptoms. Mechanistically, this catalytic process is proposed to go through sequential iridium-catalyzed hydride reductions initiated with a 1,4-hydride addition. The resultant 1,4-dihydropyrazine intermediate then tautomerizes to an iminium salt, which upon Ir–H reduction delivers a tetrahydropyrazine with the introduction of the chiral center. The chiral tetrahydropyrazine is then further reduced to the desired piperazine.

Fagnou and Leclerc reported a combination of palladium-catalyzed C–H arylation of pyrazine *N*-oxides and Pt₂O-catalyzed hydrogenation to synthesize piperazines (Scheme 31).[52] The palladium-catalyzed C–H functionalization of pyrazine *N*-oxides enables rapid introduction of various aryl groups at the C2-position, but the Pt₂O-catalyzed hydrogenation gave racemic piperazine products.

Pyrazine derivatives can also be reduced by stoichiometric hydride sources. In 1965, Lyle and Thomas described the reduction of *N*-benzylpyrazinium salts with sodium borohydride to afford the *trans*- and *cis*-substituted piperazines in a 9:1 ratio (Scheme 32, eq. 1).[53] This work was later expanded by Horne and co-workers in their syntheses of dragmacidins A, B, and C (Scheme 32, eq. 2).[54]
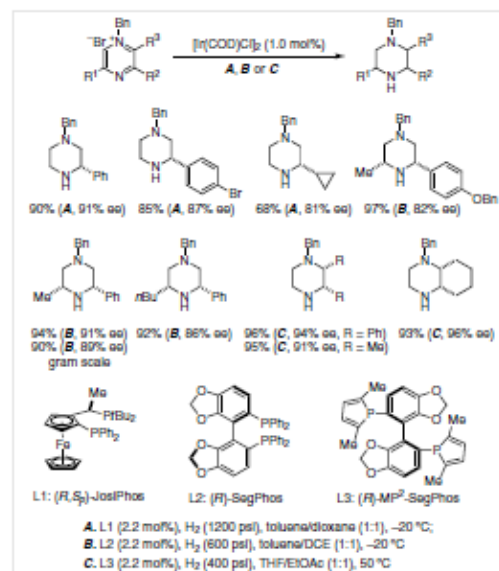
Scheme 30   Zhou's asymmetric hydrogenation of pyrazinium salts
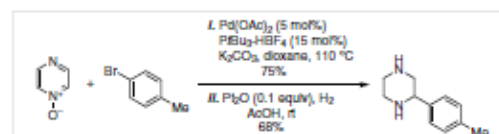
Scheme 31   Synthesis of piperazines via C–H arylation of pyrazine *N*-oxides and Pt₂O-catalyzed hydrogenation

Pyrazine *N*-oxides are activated pyrazine derivatives and can react with nucleophiles like Grignard reagents. Olsson, Almqvist and co-workers published a regioselective Grignard addition followed by sodium borohydride reduction and Boc protection to synthesize *N*-hydroxypiperazines in moderate to excellent yields (Scheme 33).[55] The presence of either electron-donating or electron-withdrawing substituents on the aryl rings had little effect on the overall yields. Application of heterocycles as well as allyl substituents dropped the yields, and use of alkyl Grignard reagents drastically decreased the yield. It was noted that the final Boc protection step was unnecessary, but allowed for easy handling of the final products.
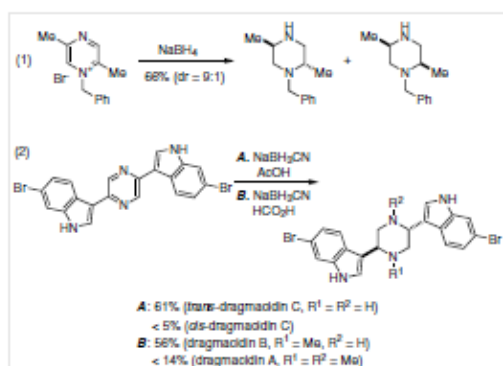
Scheme 32 Hydride reduction of pyrazines
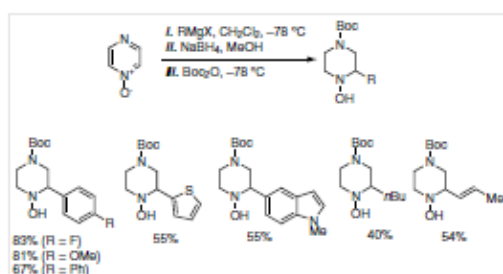
Scheme 33 Grignard addition and hydride reduction to pyrazine N-oxides

With the desire for an enantioselective synthesis, Olsson and Almqvist explored the addition of (–)-sparteine to the Grignard addition and discovered that the desired product was formed with good to high enantioselectivity, but at drastically decreased yields (Scheme 34).[55] By increasing the reaction time and decreasing the equivalents of Grignard reagent coupled with (–)-sparteine, they were able to increase the enantioselectivity, but at the cost of total yield. This promising asymmetric addition deserves further investigation.
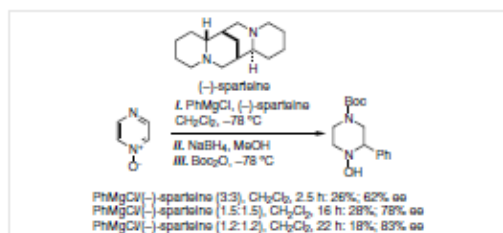
Scheme 34 Asymmetric Grignard addition to pyrazine N-oxide

In related studies, the hydropyrazine intermediates formed during the reduction of pyrazines could be prepared by other methods. Taylor and co-workers published a tandem oxidative cyclization and reduction for the production of piperazines (Scheme 35).[56] The starting reagents were simple α-hydroxy ketones and unprotected 1,2-diamines, and the dihydropyrazine intermediates formed from the oxidative condensation of the two substrates were then reduced to piperazine products with sodium borohydride in good to excellent yields. Notably, without the addition of $NaBH_4$, pyrazine products could be produced.
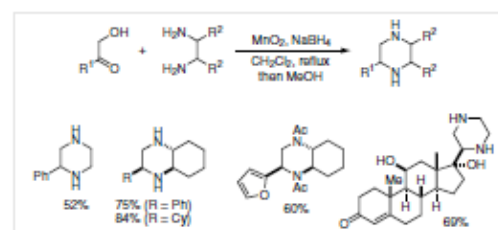
Scheme 35 Oxidation of α-hydroxy ketones with 1,2-diamines followed by reduction

González and co-workers published a piperazine synthesis using a sequence of nitroepoxide and 1,2-diamine cyclocondensation followed by hydride reduction of the resultant tetrahydropyrazine intermediates (Scheme 36).[57] The nitroepoxides can be synthesized readily from nitroalkenes via nucleophilic epoxidation with basic hydrogen peroxide. This one-pot protocol gave substituted piperazines in moderate yield with slight preference for the cis product.
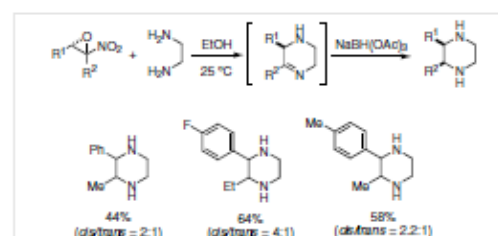
Scheme 36 [4+2]-Cycloaddition of nitroepoxides with diamines

6   Miscellaneous

In 2012, Luisi and co-workers reported an interesting Lewis acid catalyzed dimerization of aziridines to produce 2,5-disubstituted piperazines (Scheme 37).[58] In the presence of 5 mol% magnesium bromide, non-activated N-alkyl arylaziridines underwent ring-opening with another aziridine followed by ring-closure to afford the desired piperazines in good to excellent yield. Unfortunately, this formal

[3+3] process lacked stereochemical control and 2,5-disubstituted piperazines were produced as a 1:1 diastereomeric mixture. When enantio-enriched aziridines were used, the enantio-enriched *cis*-isomer and meso *trans*-isomer were produced.

Scheme 37 Dimerization of aziridines catalyzed by magnesium bromide
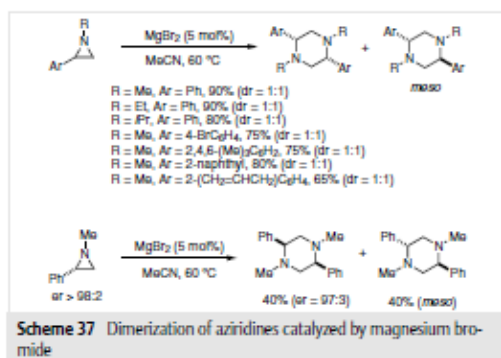
Another example of dimerization to produce piperazines came from the Mendoza group in 2015 (Scheme 38).[59] Using trimethylaluminum coupled with white LED lamps, and tetrahydrofuran as solvent, they were able to convert azomethine ylides with aromatic substituents into piperazines in high yields, high stereoselectivity, and on gram scale. Remarkably, in addition to symmetrical imines, unsymmetrical imines bearing imidazole and pyridine or pyrazine substituents underwent dimerization smoothly and gave the piperazine products as single regioisomers. The regioselectivity is very sensitive to the imine substituents and is not yet understood. This process represents a nice example of visible-light photochemistry of main-group organometallics.

Scheme 38 Photochemical dimerization of azomethine ylides
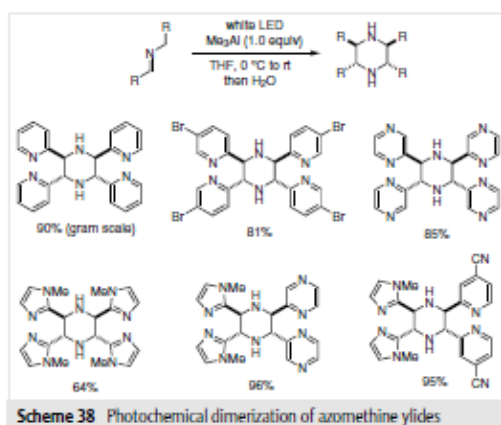
In continuation of their work in phosphine catalysis, Lu and Lu reported a phosphine-catalyzed tandem umpolung addition and intramolecular conjugate addition to synthesize piperazines in high yield (Scheme 39).[60] This strategy can be viewed as a formal [4+2] cycloaddition between protected 1,2-diamines and electron-deficient allenes or alkynes. It only requires a catalytic amount of triphenylphosphine as catalyst and offers a simple and highly atom-economic method for constructing synthetically useful nitrogen heterocycles. This method is currently limited to symmetrical 1,2-diamine derivatives.

Scheme 39 [4+2]-Cycloaddition of 1,2-diamines with allenes and alkynes
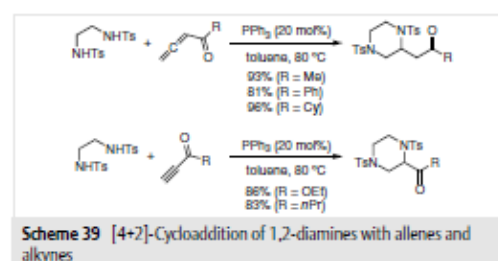
The multicomponent Ugi reaction is very efficient for building structural complexity and has been utilized to synthesize piperazines and related compounds.[61] Rossen and co-workers developed an efficient synthesis of piperazine-2-carboxamides by reacting a mixture of a carboxylic acid, chloroacetaldehyde, an *N*-alkylethylenediamine, and an isonitrile (Scheme 40).[62]

Scheme 40 The Ugi multicomponent reaction for piperazines
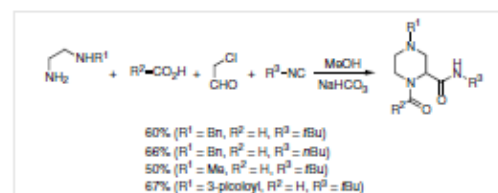
Unsymmetrical *N*-substituted piperazines are useful in medicinal chemistry yet can be complicated to synthesize. Through the use of a copper-catalyzed C–N bond formation, Yavari and co-workers developed a facile synthesis from readily available 1,4-diazabicyclo[2.2.2]octane (DABCO).[63] As shown in Scheme 41 (A), the ring-opening cross-coupling gave differentially *N*-substituted piperazines in high yields. Another DABCO functionalization method was described in 2015 by Xie and co-workers (Scheme 41, B).[64] A library of over fifty piperazines was created from the reaction of DABCO with an electron-deficient acetylene and an

aryl acid. Both of these methods are limited to the production of N-substituted piperazines due to the use of DABCO as starting material.

Scheme 41 Synthesis of differentially functionalized piperazines from DABCO
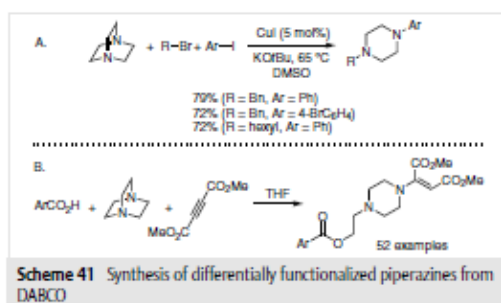
A conceptually new and facile synthesis of piperazines and other nitrogen heterocycles was reported by the Carreira group (Scheme 42).[65] Their method utilizes an indium-catalyzed ring expansion of 3-oxetanone-derived spirocycles, which can be assembled by cyclization of 1,2-diamine derivatives with 3-oxetanone. Under the Strecker reaction conditions with trimethylsilyl cyanide and indium(III) triflate, the ring expansion process is speculated to proceed with an opening of the imidazoline ring followed by cyanide addition to give an oxetane intermediate. The latter then undergoes an intramolecular 6-exo-tet cyclization via a transition state with the R^3 group occupying the equatorial position thus forcing the nitrile into the axial conformation. Cleavage of the weakened C–O bond yields the final product in good to excellent yield and high stereoselectivity.

Scheme 42 Rearrangement of oxetanes to piperazines
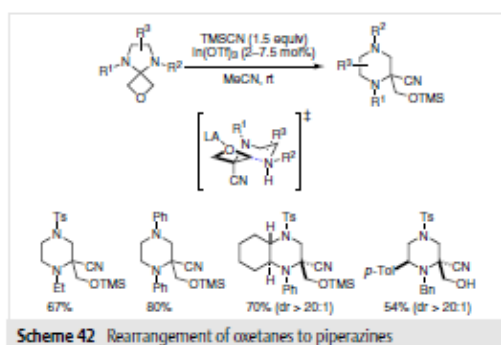
7   Conclusion

In summary, a plethora of methods by which substituted piperazines are synthesized have been highlighted in this review. The piperazine scaffold has become increasingly utilized in drug molecules and other bioactive molecules.

Despite these progresses, efficient and facile methods to quickly increase structural diversity as well as enantioselective methods are still highly desirable.

References

(1) (a) Taylor, R. D.; MacCoss, M.; Lawson, A. D. G. *J. Med. Chem.* **2014**, *57*, 5845. (b) Zhang, T. Y. *Adv. Heterocycl. Chem.* **2017**, *121*, 1.
(2) Vitaku, E.; Smith, D. T.; Njardarson, J. T. *J. Med. Chem.* **2014**, *57*, 10257.
(3) Walker, M. A. *Expert Opin. Drug Discov.* **2014**, *9*, 1421.
(4) For a review, see: Vo, C.-V. T.; Bode, J. W. *J. Org. Chem.* **2014**, *79*, 2809.
(5) Ye, Z.; Gettys, K. E.; Dai, M. *Beilstein J. Org. Chem.* **2016**, *12*, 702.
(6) (a) For an excellent review, see: Dinsmore, C. J.; Beshore, D. C. *Org. Prep. Proced. Int.* **2002**, *34*, 367 For examples. (b) Schanen, V.; Riche, C.; Chiaroni, A.; Quirion, J.-C.; Husson, H.-P. *Tetrahedron Lett.* **1994**, *35*, 2533. (c) König, B.; Maity, P. *Org. Lett.* **2008**, *10*, 1473. (d) Mickelson, J. W.; Belonga, K. L.; Jacobsen, E. J. *J. Org. Chem.* **1995**, *60*, 4177. (e) Jung, M. E.; Rohloff, J. C. *J. Org. Chem.* **1985**, *50*, 4909. (f) Viso, A.; de la Pradilla, R. F.; López-Rodríguez, M. L.; García, A.; Tortosa, M. *Synlett* **2002**, 755. (g) Yokoshima, S.; Watanabe, K.; Uehara, F.; Usui, Y.; Tanaka, H. *Bioorg. Med. Chem. Lett.* **2014**, *24*, 5749. (h) Opatz, T. *Eur. J. Org. Chem.* **2004**, 4113. (i) Ashton, K. S.; Denti, M.; Norman, M. H.; St. Jean, D. J. Jr. *Tetrahedron Lett.* **2014**, *55*, 4501. (j) Jida, M.; Laconde, G.; Soueidan, O.-M.; Lebegue, N.; Revelant, G.; Pelinski, L.; Agbossou-Niedercorn, F.; Deprez, B.; Deprez-Poulain, R. *Tetrahedron Lett.* **2012**, *53*, 5215.
(7) (a) Sanchez-Rosello, M.; Delgado, O.; Mateu, N.; Trabanco, A. A.; Van Gool, M.; Fustero, S. *J. Org. Chem.* **2014**, *79*, 5887. (b) Napolitano, C.; Borriello, M.; Cardullo, F.; Donati, D.; Paio, A.; Manfredini, F. *Synth. Commun.* **2011**, *41*, 2031. (c) Bourbeau, M. P.; Siegmund, A.; Allen, J. G.; Shu, H.; Fotsch, C.; Bartberger, M. D.; Kim, K.-W.; Komorowski, R.; Graham, M.; Busby, J.; Wang, M.; Meyer, J.; Xu, Y.; Salyers, K.; Fielden, M.; Véniant, M. M.; Gu, W. *J. Med. Chem.* **2013**, *56*, 10132. (d) Katz, J.; Knowles, S. L.; Jewell, J. P.; Sloman, D. L.; Stanton, M. G.; Noucti, N. Patent WO2010017046 A1, **2010**.
(8) (a) Ruppert, I.; Schlich, K.; Volbach, W. *Tetrahedron Lett.* **1984**, *25*, 2195. (b) Prakash, G. K. S.; Krishnamurti, R.; Olah, G. A. *J. Am. Chem. Soc.* **1989**, *111*, 393.
(9) Robak, M. T.; Herbage, M. A.; Ellman, J. A. *Chem. Rev.* **2010**, *110*, 3600.
(10) Liu, Y.; Han, S.-J.; Liu, W.-B.; Stoltz, B. M. *Acc. Chem. Res.* **2015**, *48*, 740.
(11) Korch, K. M.; Eidamshaus, C.; Behenna, D. C.; Nam, S.; Horne, D.; Stoltz, B. M. *Angew. Chem. Int. Ed.* **2015**, *54*, 179.
(12) (a) Castagnoli, N. Jr. *J. Org. Chem.* **1969**, *34*, 3187. (b) Cushman, M.; Castagnoli, N. Jr. *J. Org. Chem.* **1972**, *37*, 1268.
(13) Dar'in, D.; Bakulina, O.; Chizhoba, M.; Krasavin, M. *Org. Lett.* **2015**, *17*, 3930.
(14) For examples: (a) Liu, K. G.; Robichaud, A. J. *Tetrahedron Lett.* **2005**, *46*, 7921. (b) Mishani, E.; Dence, C. S.; McCarthy, T. J.; Welch, M. J. *Tetrahedron Lett.* **1996**, *37*, 319. (c) Van Brabandt,

W.; Vanwalleghem, M.; D'hooghe, M.; De Kimpe, N. *J. Org. Chem.* **2006**, *71*, 7083. (d) Balsells, J.; DiMichele, L.; Liu, J.; Kubryk, M.; Hansen, K.; Armstrong, J. D. III *Org. Lett.* **2005**, *7*, 1039. (e) Gao, R.; Canney, D. J. *J. Org. Chem.* **2010**, *75*, 7451. (f) Crestey, F.; Witt, M.; Jaroszewski, J. W.; Franzyk, H. *J. Org. Chem.* **2009**, *74*, 5652. (g) Huang, J.; Xu, W.; Xie, H.; Li, S. *J. Org. Chem.* **2012**, *77*, 7506.

(15) (a) Halland, N.; Braunton, A.; Bachmann, S.; Marigo, M.; Jørgensen, K. A. *J. Am. Chem. Soc.* **2004**, *126*, 4790. (b) Marigo, M.; Bachmann, S.; Halland, N.; Braunton, A.; Jørgensen, K. A. *Angew. Chem. Int. Ed.* **2004**, *43*, 5507.

(16) (a) O'Reilly, M. C.; Lindsley, C. W. *Org. Lett.* **2012**, *14*, 2910. (b) O'Reilly, M. C.; Lindsley, C. W. *Tetrahedron Lett.* **2012**, *53*, 1539.

(17) Yar, M.; McGarrigle, E. M.; Aggarwal, V. K. *Angew. Chem. Int. Ed.* **2008**, *47*, 3784.

(18) Yar, M.; McGarrigle, E. M.; Aggarwal, V. K. *Org. Lett.* **2009**, *11*, 257.

(19) Kwon, S. H.; Lee, S. M.; Byun, S. M.; Chin, J.; Kim, B. M. *Org. Lett.* **2012**, *14*, 3664.

(20) Matlock, J. V.; Svejstrup, T. D.; Songara, P.; Overington, S.; McGarrigle, E. M.; Aggarwal, V. K. *Org. Lett.* **2014**, *16*, 5044.

(21) Bagnoli, L.; Scarponi, C.; Rossi, M. G.; Testaferri, L.; Tiecco, M. *Chem. Eur. J.* **2011**, *17*, 993.

(22) Couty, F.; Durrat, F.; Prim, D. *Tetrahedron Lett.* **2004**, *45*, 3725.

(23) (a) Leuscher, M. U.; Geoghegan, K.; Nichols, P.; Bode, J. W. *Aldrichimica Acta* **2015**, *48*, 43. (b) Vo, C.-V. T.; Leuscher, M. U.; Bode, J. W. *Nat. Chem.* **2014**, *6*, 310. (c) Vo, C.-V. T.; Mikutis, G.; Bode, J. W. *Angew. Chem. Int. Ed.* **2013**, *52*, 1705.

(24) (a) Luescher, M. U.; Vo, C.-V. T.; Bode, J. W. *Org. Lett.* **2014**, *16*, 1236. (b) Geoghegan, K.; Bode, J. W. *Org. Lett.* **2015**, *17*, 1934.

(25) Leuscher, M. U.; Bode, J. W. *Angew. Chem. Int. Ed.* **2015**, *54*, 10884.

(26) Siau, W-Y.; Bode, J. W. *J. Am. Chem. Soc.* **2014**, *136*, 17726.

(27) Hsieh, S-Y.; Bode, J. W. *Org. Lett.* **2016**, *18*, 2098.

(28) (a) Nakhla, J. S.; Wolfe, J. P. *Org. Lett.* **2007**, *9*, 3279. (b) Nakhla, J. S.; Schultz, D. M.; Wolfe, J. P. *Tetrahedron* **2009**, *65*, 6549.

(29) Cochran, B. M.; Michael, F. E. *Org. Lett.* **2008**, *10*, 329.

(30) Lu, Z.; Stahl, S. S. *Org. Lett.* **2012**, *14*, 1234.

(31) (a) Chen, M. S.; White, M. C. *J. Am. Chem. Soc.* **2004**, *126*, 1346. (b) Chen, M. S.; Prabagaran, N.; Labenz, N. A.; White, M. C. *J. Am. Chem. Soc.* **2005**, *127*, 6970. (c) Fraunhoffer, K. J.; White, M. C. *J. Am. Chem. Soc.* **2007**, *129*, 7274.

(32) Montgomery, T. D.; Rawal, V. H. *Org. Lett.* **2016**, *18*, 740.

(33) James, T.; Simpson, I.; Grant, J. A.; Sridharan, V.; Nelson, A. *Org. Lett.* **2013**, *15*, 6094.

(34) Yao, L.-F.; Wang, Y.; Huang, K.-W. *Org. Chem. Front.* **2015**, *2*, 721.

(35) Haack, K.-J.; Hashiguchi, S.; Fujii, A.; Ikariya, T.; Noyori, R. *Angew. Chem. Int. Ed.* **1997**, *36*, 285.

(36) Zhai, H.; Borzenko, A.; Lau, Y. Y.; Ahn, S. H.; Schafer, L. L. *Angew. Chem. Int. Ed.* **2012**, *51*, 12219.

(37) Leitch, D. C.; Schafer, L. L. *Organometallics* **2010**, *29*, 5162.

(38) Kour, H.; Paul, S.; Singh, P. P.; Gupta, M.; Gupta, R. *Tetrahedron Lett.* **2013**, *54*, 761.

(39) (a) Watanabe, Y.; Tsuji, Y.; Ohsugi, Y. *Tetrahedron Lett.* **1981**, *22*, 2667. (b) Grigg, R.; Mitchell, T. R. B.; Sutthivaiyakit, S.; Tongpenyai, N. *J. Chem. Soc., Chem. Commun.* **1981**, 611. (c) Khai, B.-T.; Concilio, C.; Porzi, G. *J. Org. Chem.* **1981**, *46*, 1759.

(40) For reviews: (a) Dobereiner, G. E.; Crabtree, R. H. *Chem. Rev.* **2010**, *110*, 681. (b) Guillena, G.; Ramón, D. J.; Yus, M. *Chem. Rev.* **2010**, *110*, 1611. (c) Gunanathan, C.; Milstein, D. *Science* **2013**, *341*, 249.

(41) Leonard, J.; Blacker, A. J.; Marsden, S. P.; Jones, M. F.; Mulholland, K. R.; Newton, R. *Org. Process Res. Dev.* **2015**, *19*, 1400.

(42) Tsuji, Y.; Huh, K-T.; Ohsugi, Y.; Watanabe, Y. *J. Org. Chem.* **1985**, *50*, 1365.

(43) (a) Nordstrøm, L. U.; Madsen, R. *Chem. Commun.* **2007**, 5034. (b) Lorentz-Petersen, L. L. R.; Nordstrøm, L. U.; Madsen, R. *Eur. J. Org. Chem.* **2012**, 6752.

(44) Mercer, G. J.; Sigman, M. S. *Org. Lett.* **2003**, *5*, 1591.

(45) Vairaprakash, P.; Periasamy, M. *J. Org. Chem.* **2006**, *71*, 3636.

(46) Chen, Z.-P.; Zhou, Y.-G. *Synthesis* **2016**, *48*, 1769.

(47) Rossen, K.; Weissman, S. A.; Sager, J.; Reamer, R. A.; Askin, D.; Volante, R. P.; Reider, P. J. *Tetrahedron Lett.* **1995**, *36*, 6419.

(48) Pye, P. J.; Rossen, K.; Reamer, R. A.; Tsou, N. N.; Volante, R. P.; Reider, P. J. *J. Am. Chem. Soc.* **1997**, *119*, 6207.

(49) Kuwano, R.; Ito, Y. *J. Org. Chem.* **1999**, *64*, 1232.

(50) (a) Fuchs, R. EP 0803502, **1997**. (b) Fuchs, R. US 5945534, **1999**.

(51) (a) Huang, W.-X.; Liu, L.-J.; Feng, G.-S.; Wang, B.; Zhou, Y.-G. *Org. Lett.* **2016**, *18*, 3082. (b) Huang, W.-X.; Yu, C.-B.; Shi, L.; Zhou, Y.-G. *Org. Lett.* **2014**, *16*, 3324.

(52) Leclerc, J.-P.; Fagnou, K. *Angew. Chem. Int. Ed.* **2006**, *45*, 7781.

(53) Lyle, R. E.; Thomas, J. J. *J. Org. Chem.* **1965**, *30*, 1907.

(54) Miyake, F. Y.; Yakushijin, K.; Horne, D. A. *Org. Lett.* **2000**, *2*, 3185.

(55) Andersson, H.; Banchelin, T. S.-L.; Das, S.; Gustafsson, M.; Olsson, R.; Almqvist, F. *Org. Lett.* **2010**, *12*, 284.

(56) Raw, S. A.; Wilfred, C. D.; Taylor, R. J. K. *Chem. Commun.* **2003**, 2286.

(57) Vidal-Albalat, A.; Rodríguez, S.; González, F. V. *Org. Lett.* **2014**, *16*, 1752.

(58) Trinchera, P.; Musio, B.; Degennaro, L.; Moliterni, A.; Falcicchio, A.; Luisi, R. *Org. Biomol. Chem.* **2012**, *10*, 1962.

(59) (a) Suárez-Pantiga, S.; Colas, K.; Johansson, M. J.; Mendoza, A. *Angew. Chem. Int. Ed.* **2015**, *54*, 14094. (b) Chen, Z.; Wu, J.; Chen, Y.; Li, L.; Xia, Y.; Li, Y.; Liu, W.; Lei, T.; Yang, L.; Gao, D.; Li, W. *Organometallics* **2012**, *31*, 6005. (c) Cariou, R.; Gibson, V. C.; Tomov, A. K.; White, A. J. P. *J. Organomet. Chem.* **2009**, *694*, 703. (d) Trepanier, S. J.; Wang, X. *Can. J. Chem.* **1996**, *74*, 2032.

(60) Lu, C.; Lu, X. *Org. Lett.* **2002**, *4*, 4677.

(61) (a) For a review: Dömling, A.; Huang, Y. *Synthesis* **2010**, 2859. (b) Zhu, D.; Xia, L.; Pan, L.; Chen, R.; Mou, Y.; Chen, X. *J. Org. Chem.* **2012**, *77*, 1386.

(62) Rossen, K.; Sager, J.; DiMichele, L. M. *Tetrahedron Lett.* **1997**, *38*, 3183.

(63) Yavari, I.; Bayat, M. J.; Ghazanfarpour-Darjani, M. *Tetrahedron Lett.* **2014**, *55*, 5595.

(64) Dong, H.-R.; Chen, Z.-B.; Li, R.-S.; Dong, H.-S.; Xie, Z.-X. *RSC Adv.* **2015**, *5*, 10768.

(65) Ruider, S. A.; Müller, S.; Carreira, E. M. *Angew. Chem. Int. Ed.* **2013**, *52*, 11908.

Copper-Catalyzed Cyclopropanol Ring Opening C$_{sp^3}$–C$_{sp^3}$ Cross-Couplings with (Fluoro)Alkyl Halides

Zhishi Ye, Kristen E. Gettys, Xingyu Shen, and Mingji Dai*

Department of Chemistry and Center for Cancer Research, Purdue University, 560 Oval Drive, West Lafayette, Indiana 47907, United States

⑤ *Supporting Information*

ABSTRACT: Novel and general copper-catalyzed cyclopropanol ring opening cross-coupling reactions with difluoroalkyl bromides, perfluoroalkyl iodides, monofluoroalkyl bromides, and 2-bromo-2-alkylesters to synthesize various β-(fluoro)alkylated ketones are reported. The reactions feature mild conditions and excellent functional group compatibility and can be scaled up to gram scale. Preliminary mechanistic studies suggest the involvement of radical intermediates. The difluoroalkyl–alkyl cross-coupling products can also be readily converted to more valuable and diverse gem-difluoro-containing compounds by taking advantage of the carbonyl group resulting from cyclopropanol ring opening.
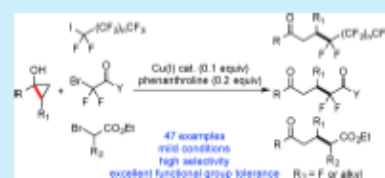
Recently, significant progress has been made in the development of transition metal-catalyzed cross-coupling reactions of alkyl electrophiles and alkyl nucleophiles, including enantioselective variants. Most of the commonly used alkyl nucleophiles in these alkyl–alkyl cross-coupling processes are alkyl Grignard reagents, alkyl zinc reagents, and alkyl boron reagents.[1] Some of these reagents suffer from poor functional group compatibility, have to be generated in situ or right before use, and are not stable for long-term storage. Due to the importance of alkyl–alkyl cross-couplings in medicinal chemistry, natural product synthesis, and other related areas, there is a great need to expand the scope of alkyl nucleophiles. Furthermore, due to the importance of fluorinated molecules in medicinal chemistry and many other fields,[2] the demand for efficient and reliable methods for their synthesis has increased dramatically. Despite recent advances,[3] direct difluoroalkylation or monofluoroalkylation of alkyl nucleophiles has been limited[4] in comparison to the introduction of such groups on aromatic systems[5] and unsaturated systems such as olefins and alkynes.[6] Efficient methods for direct fluoroalkyl–alkyl cross-coupling reactions are highly desirable. Recently, Liang and Fu reported an elegant nickel-catalyzed alkyl–alkyl cross-coupling of fluorinated secondary electrophiles (see **1 → 2**, Figure 1A).[4a]

Cyclopropanols are important and useful functional groups and can be readily accessed via the Kulinkovich reaction or the Simmons–Smith protocols.[7] They are bench stable and can be stored for a relatively long time. Due to the intrinsic ring strain, cyclopropanols are prone to ring opening reactions and are often viewed as homoenolate equivalents. Therefore, cyclopropanols could be important alkyl nucleophiles in alkyl–alkyl cross-coupling reactions. Moreover, the resulting coupling products would be equipped with a ketone functional group, which can be transformed to a variety of products due to the rich carbonyl chemistry. Currently, most of the transition-metal-catalyzed cyclopropanol ring opening cross-couplings

A. Ni-catalyzed alkyl-alkyl cross-couplings of fluorinated secondary electrophiles (Fu, et al.)

B. S$_N$2' alkylation of cyclopropanols via homoenolates (Cha, et al.)
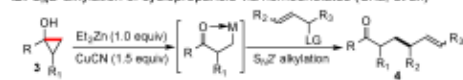
C. This work: Cu-catalyzed ring opening (fluoro)alkyl-alkyl cross-couplings
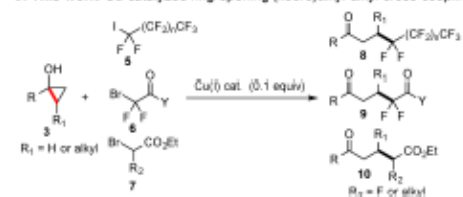
Figure 1. Selected examples and this work.

focus on palladium-catalyzed C–C bond formation,[8] which is significantly limited by the proclivity of β-H elimination. Copper, in comparison to palladium, is more abundant, cheaper, and less prone to β-H elimination chemistry.[9] However, copper-promoted or copper-catalyzed cyclopropanol ring opening cross-coupling reactions have been very rare.[10] Recently, Cha and co-workers have developed elegant S$_N$2' alkylations of the Zn(II)/Cu(I)-homoenolate derived from treating cyclopropanols with more than stoichiometric amount of CuCN and 1 equiv of ZnEt$_2$ (see **3 → 4**, Figure 1B)[10c] and

applied this chemistry in total synthesis of natural products.[10d,e] We have developed copper-catalyzed cyclopropanol ring opening electrophilic cross-coupling reactions to synthesize various β-CF$_3$, β-SCF$_3$, and β-amino-substituted carbonyl products.[11a,b] Herein, we report novel and unprecedented copper-catalyzed cyclopropanol ring opening alkyl–alkyl cross-coupling reactions with difluoroalkyl bromides, perfluoroalkyl iodides, monofluoroalkyl bromides, and 2-bromo-2-alkylesters as electrophiles (Figure 1C). In addition to the catalytic nature, the selectivity of breaking the strained Walsh bond of unsymmetrical cyclopropanols is opposite from the previous cases,[10c,11b] presumably due to a radical ring opening process.

Due to the importance and prevalence of difluoroalkyl groups in bioactive molecules,[12] we started our exploration with 2-bromo-2,2-difluoroacetate (11, Figure 2) as the electrophilic coupling partner with cyclopropanols. After extensive reaction condition optimizations (see the Supporting Information), we discovered that (i) CuI is superior to CuCN, CuTc, and Cu(MeCN)$_4$PF$_6$, (ii) 2,2'-bipyridine or 1,10-phenanthroline ligand is critical, (iii) the reaction is very sensitive to solvent and MeCN is much better than other solvents such as THF, PhMe, DMF, DCE, 1,4-dioxane, and DMSO, and (iv) a base is necessary to neutralize the acid generated in the reaction system. Under the conditions of a catalytic amount of CuI/1,10-phenanthroline in MeCN at 80 °C with K$_2$CO$_3$ as base, optimal yields of 2,2-difluoro-1,5-dicarbonyl products[13] (12) could be obtained from various cyclopropanols and 11.

We then investigated the substrate scope in terms of both cyclopropanols and the electrophilic bromodifluoroalkyl coupling partners (Figures 2–4). To our satisfaction, the reaction has broad substrate scope and tolerates a variety of functional groups. Both aryl and alkyl substituted cyclopropanols underwent the desired ring opening reactions with 11 to provide various β-difluoroalkylated ketone products in good to excellent yield (Figure 2). Alkyl/aryl ether (12a, 12c, 12f), benzoate (12g), TBS-ether (12h), α,β-unsaturated ester (12j) and aldehyde (12k), amide (12l), and epoxide (12m) are
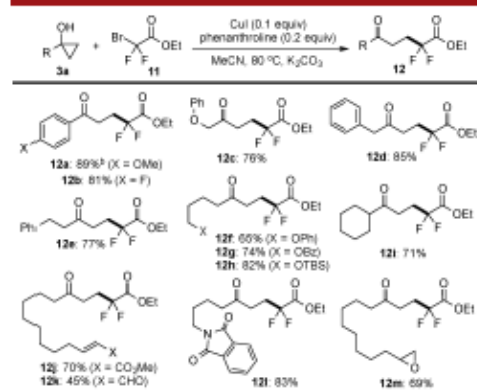
Figure 2. Cyclopropanol substrate scope. General reaction conditions: solution of 3a (0.1 mmol), 11 (0.4 mmol), CuI (0.01 mmol), phenanthroline (0.02 mmol), and K$_2$CO$_3$ (0.2 mmol) were stirred in MeCN (1 mL) at 80 °C for 10–12 h. The reaction process was monitored by thin-layer chromatography. Isolated yield from flash chromatography was given. The b indicates gram scale.

well tolerated. The reaction could also be conducted at gram scale (12a, Figure 2).

We next explored unsymmetrical cyclopropanol substrates (3, Figure 3). In this scenario, one question was apparent to us: which Walsh bond "a" the less substituted bond "a" or the more substituted bond "b", would be selectively broken for the cross-coupling? It has been shown that radical promoted cyclopropanol ring opening tends to break bond "b" to provide the more stable and more substituted β-alkyl radical[14] and formation of metallo-homoenolate favors breaking bond "a" to generate less substituted metallo-homoenolate.[10c,11b] In our case, the more substituted Walsh bond "b" was selectively cleaved, and the difluoroalkylation occurred at the more substituted carbon, which indicates a radical cyclopropanol ring opening process. The selectivity is excellent for the cases of aryl substituted cyclopropanols and products 13a–c were produced as the dominant products. While 13d was produced in high selectivity (17/1), the selectivity dropped significantly in the case of 13e (2.4/1). Additionally, aldehyde product 13f could be obtained in good selectivity as well.
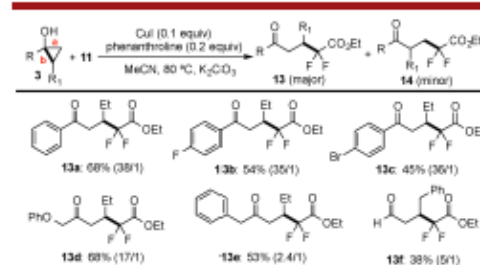
Figure 3. Unsymmetrical cyclopropanol substrate scope. Isolated yield with 13/14 ratio in parentheses.

Other halodifluoroalkyl electrophiles such as 2-bromo-2,2-difluoroamides, (bromodifluoromethyl)phosphonates, and perfluoroalkyl iodides work smoothly under the reaction conditions (Figure 4). Morpholine- (16a), Boc-protected piperazine- (16c), benzoazepane- (16d), indoline- (16e), and azitidine-derived (16j) difluoroamides can be produced in good to excellent yield. With (bromodifluoromethyl)phosphonate as electrophile, a strong base, LiOtBu, has to be used and the reaction yield was relatively low (16k, 32%). In the case of perfluoroalkylation (16l and 16m), the corresponding alkyl iodides were used and good yields were obtained.

We then moved beyond difluoroalkyl electrophiles and explored the use of other alkyl electrophiles (Figure 5). To our delight, simply switching the base from K$_2$CO$_3$ to iPr$_2$NH and using CuI or CuCl as catalyst, electrophiles such as 2-bromo-2-alkyl acetates and 2-bromo-2-fluoroacetates became effective coupling partners. We also observed some changes in comparison to the difluoroalkylation cases. Free alcohol (18j) and terminal olefin (18h), which are not compatible in the previous cases, are well tolerated in the slightly modified conditions. In general, good reaction yields could be obtained, and a variety of functional groups including benzoate (18e), primary TBS-ether (18f), epoxide (18g), and aryl bromide (18n) are compatible under the reaction conditions.

One advantage of using cyclopropanols as nucelophilic alkyl cross-coupling partners is that the coupling products are

Organic Letters
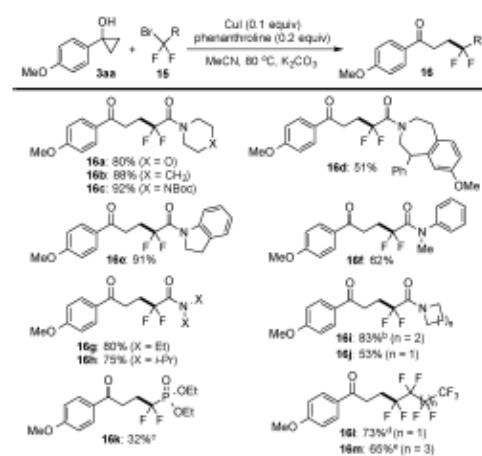
Figure 4. Difluoroalkyl halides substrate scope. Yield of isolated product is provided: [b]iPr$_2$NH as base; [c]LiOtBu as base; [d]with perfluorobutyl iodide; [e]with perfluorohexyl iodide.
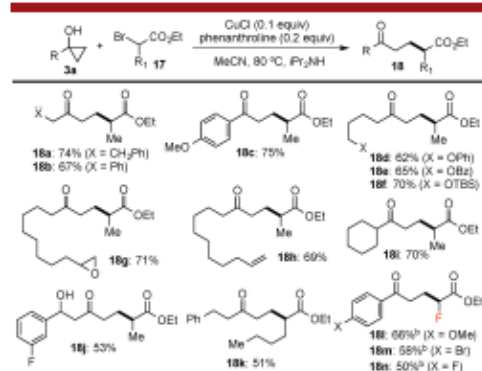
Figure 5. Other alkyl halides substrate scope. Isolated yield is given; b indicates that CuI was used.

equipped with a ketone functional group. Due to rich chemistry of the carbonyl group, the coupling products can be converted to a diverse collection of products using standard carbonyl transformations. For example (Figure 6), Fisher indole synthesis was used to convert 12a to indole-containing biaryl product 19 in 94% yield.[15] Reductive amination followed by lactam formation provided α,α-difluorolactam 20 in excellent
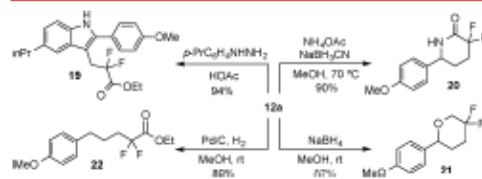
Figure 6. Synthetic transformations of 12a.

yield.[16] When NaBH$_4$ was used, 3,3-difluoro-6-aryltetrahydro-pyran product 21 was obtained in 87% yield.[17] These scaffolds are of great medicinal importance but are otherwise challenging to access.[15–17] The ketone carbonyl group could be reduced to a methylene group as well (12a → 22), which further expands the potential use of cyclopropanols as alkyl cross-coupling partners.

Mechanistically, both the conversion of 15n with a double bond to 23 and the formation of 24 when TEMPO was added to the reaction of 3aa and 11 (Figure 7) suggest the formation
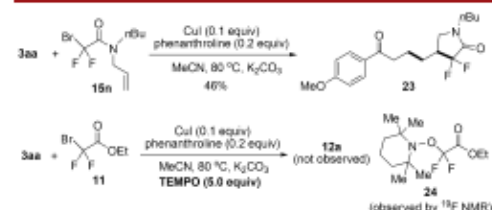
Figure 7. Preliminary mechanistic studies.

of a radical at the α-carbon bearing the two fluorine atoms presumable via a single electron transfer (SET) process between CuI and the bromides (15n or 11). The resulting Cu(II) salt would then oxidize cyclopropanols via another SET process to promote a radical cyclopropane ring cleavage as evidenced by the use of unsymmetrical cyclopropanols to generate a more stable β-alkyl radical for following cross-couplings.[14,18]

In summary, we have developed a novel umpolung strategy for the synthesis of β-(fluoro)alkylated ketones via copper-catalyzed cyclopropanol ring opening C$_{sp}$³–C$_{sp}$³ cross-couplings with various alkyl halides including difluoroalkyl bromides, perfluoroalkyl iodides, monofluoroalkyl bromides, and 2-bromo-2-alkylesters. Many functional groups are tolerated under the mild reaction conditions. The reaction can also be scaled up. In addition to its catalytic nature, a different cyclopropane ring opening mode has been observed in comparison to the previous cases. Preliminary mechanistic studies indicate the involvement of radical intermediates. The coupling products could be converted to a diverse collection of important compounds. This chemistry demonstrates the significant potential of cyclopropanol and related systems as useful nucleophiles in alkyl–alkyl cross-coupling reactions. We are currently investigating the detailed reaction mechanisms as well as developing enantioselective versions of this type of transformation.

■ ASSOCIATED CONTENT

S Supporting Information

The Supporting Information is available free of charge on the ACS Publications website at DOI: 10.1021/acs.or-glett.5b03096.

> Experimental procedures and characterization for new compounds (PDF)

■ AUTHOR INFORMATION

Corresponding Author

*E-mail: mjdai@purdue.edu.

Notes

The authors declare no competing financial interest.

■ REFERENCES

(1) For reviews, see: (a) Cherney, A. H.; Kadunce, N. T.; Reisman, S. E. Chem. Rev. 2015, 115, 9587. (b) Swift, E. C.; Jarvo, E. R. Tetrahedron 2013, 69, 5799. (c) Rudolph, A.; Lautens, M. Angew. Chem., Int. Ed. 2009, 48, 2656. (d) Hu, X. Chem. Sci. 2011, 2, 1867. (e) Liang, Y.; Fu, G. C. J. Am. Chem. Soc. 2014, 136, 5520. (f) Binder, J. T.; Cordier, C. J.; Fu, G. C. J. Am. Chem. Soc. 2012, 134, 17003.

(2) (a) Ilardi, E. A.; Vitaku, E.; Njardarson, J. T. J. Med. Chem. 2014, 57, 2832. (b) Fluorine-Related Nanoscience with Energy Applications; Nelson, D. J., Brammer, C. N., Eds.; American Chemical Society: Washington, DC, 2011.

(3) For reviews, see: (a) Wang, J.; Sánchez-Roselló, M.; Aceña, J. L.; del Pozo, C.; Sorochinsky, A. E.; Fustero, S.; Soloshonok, V. A.; Liu, H. Chem. Rev. 2014, 114, 2432. (b) Ni, C.; Hu, M.; Hu, J. Chem. Rev. 2015, 115, 765. (c) Yang, X.; Wu, T.; Phipps, R. J.; Toste, F. D. Chem. Rev. 2015, 115, 826. (d) Campbell, M. G.; Ritter, T. Chem. Rev. 2015, 115, 612. (e) Alonso, C.; Martinez de Marigorta, E.; Rubiales, G.; Palacios, F. Chem. Rev. 2015, 115, 1847. (f) Xu, J.; Liu, X.; Fu, Y. Tetrahedron Lett. 2014, 55, 585.

(4) For leading references, see: (a) Liang, Y.; Fu, G. C. Angew. Chem., Int. Ed. 2015, 54, 9047. (b) Yang, M.-H.; Orsi, D. L.; Altman, R. A. Angew. Chem., Int. Ed. 2015, 54, 2361. (c) Kitazume, T.; Ishikawa, N. J. Am. Chem. Soc. 1985, 107, 5186.

(5) (a) Uneyama, K.; Tanaka, H.; Kobayashi, S.; Shioyama, M.; Amii, H. Org. Lett. 2004, 6, 2733. (b) Guo, Y.; Shreeve, J. M. Chem. Commun. 2007, 3583. (c) Prakash, G. K. S.; Ganesh, S. K.; Jones, J.-P.; Kulkarni, A.; Masood, K.; Swabeck, J. K.; Olah, G. A. Angew. Chem., Int. Ed. 2012, 51, 12090. (d) Qi, Q.; Shen, Q.; Lu, L. J. Am. Chem. Soc. 2012, 134, 6548. (e) Pier, P. S.; Hartwig, J. F. J. Am. Chem. Soc. 2012, 134, 5524. (f) Ge, S.; Chaładaj, W.; Hartwig, J. F. J. Am. Chem. Soc. 2014, 136, 4149. (g) Ge, S.; Arlow, S. I.; Mormino, M. G.; Hartwig, J. F. J. Am. Chem. Soc. 2014, 136, 14401. (h) Min, Q.-Q.; Yin, Z.; Feng, Z.; Guo, W.-H.; Zhang, X. J. Am. Chem. Soc. 2014, 136, 1230. (i) Peng, Z.; Min, Q.-Q.; Xiao, Y.-L.; Zhang, B.; Zhang, X. Angew. Chem., Int. Ed. 2014, 53, 1669. (j) Xiao, Y.-L.; Guo, W.-H.; He, G.-Z.; Pan, Q.; Zhang, X. Angew. Chem., Int. Ed. 2014, 53, 9909. (k) Yu, Y.-B.; He, G.-Z.; Zhang, X. Angew. Chem., Int. Ed. 2014, 53, 10457. (l) Matheis, C.; Jouvin, K.; Goossen, L. J. Org. Lett. 2014, 16, 5984. (m) Gu, Y.; Leng, X.; Shen, Q. Nat. Commun. 2014, 5, 5405. (n) Wang, L.; Wei, X.-J.; Jia, W.-L.; Zhong, J.-J.; Wu, L.-Z.; Liu, Q. Org. Lett. 2014, 16, 5842. (o) Shi, S.-L.; Buchwald, S. L. Angew. Chem., Int. Ed. 2015, 54, 1646. (p) Ivanova, M. V.; Bayle, A.; Besset, T.; Poisson, T.; Pannecoucke, X. Angew. Chem., Int. Ed. 2015, 54, 13406.

(6) For leading references, see: (a) Xu, T.; Cheung, C. W.; Hu, X. Angew. Chem., Int. Ed. 2014, 53, 4910. (b) Ma, G.; Wan, W.; Li, J.; Hu, Q.; Jiang, H.; Zhu, S.; Wang, J.; Hao, J. Chem. Commun. 2014, 50, 9749. (c) Yu, C.; Iqbal, N.; Park, S. E.; Cho, J. Chem. Commun. 2014, 50, 12884. (d) Fu, W.; Zhu, M.; Zou, G.; Xu, C.; Wang, Z. Asian J. Org. Chem. 2014, 3, 1273. (e) Riente, P.; Pericàs, M. A. ChemSusChem 2015, 8, 1841.

(7) For reviews, see: (a) Gibson, D. H.; DePuy, C. H. Chem. Rev. 1974, 74, 605. (b) Kulinkovich, O. G. Chem. Rev. 2003, 103, 2597.

(8) (a) For a review, see: Rosa, D.; Nikolaev, A.; Nithiy, N.; Orellana, A. Synlett 2015, 26, 441. For examples, see: (b) Aoki, S.; Fujimura, T.; Nakamura, E.; Kuwajima, I. J. Am. Chem. Soc. 1988, 110, 3296. (c) Fujimura, T.; Aoki, S.; Nakamura, E. J. Org. Chem. 1991, 56, 2809. (d) Rosa, D.; Orellana, A. Org. Lett. 2011, 13, 110. (e) Rosa, D.; Orellana, A. Chem. Commun. 2012, 48, 1922. (f) Parida, B. B.; Das, P. P.; Niocel, M.; Cha, J. K. Org. Lett. 2013, 15, 1780. (g) Cheng, K.;

Walsh, P. J. Org. Lett. 2013, 15, 2298. (h) Rosa, D.; Orellana, A. Chem. Commun. 2013, 49, 5420. (i) Nithiy, N.; Orellana, A. Org. Lett. 2014, 16, 5854. (j) Nikolaev, A.; Nithiy, N.; Orellana, A. Synlett 2014, 25, 2301.

(9) For leading references, see: (a) Ren, P.; Stern, L.-A.; Hu, X. Angew. Chem., Int. Ed. 2012, 51, 9110. (b) Yang, C.-T.; Zhang, Z.-Q.; Liang, J.; Liu, J.-H.; Lu, X.-Y.; Chen, H.-H.; Liu, L. J. Am. Chem. Soc. 2012, 134, 11124. (c) You, W.; Brown, M. K. J. Am. Chem. Soc. 2014, 136, 14730. (d) Yang, Y.; Shi, S.-L.; Niu, D.; Liu, P.; Buchwald, S. L. Science 2015, 349, 62.

(10) (a) Ryu, I.; Ando, M.; Ogawa, A.; Murai, S.; Sonoda, N. J. Am. Chem. Soc. 1983, 105, 7192. (b) Ryu, I.; Matsumoto, K.; Kameyama, Y.; Ando, M.; Kusumoto, N.; Ogawa, A.; Kambe, N.; Murai, S.; Sonoda, N. J. Am. Chem. Soc. 1993, 115, 12330. (c) Das, P. P.; Belmore, K.; Cha, J. K. Angew. Chem., Int. Ed. 2012, 51, 9517. (d) Rao, N. N.; Parida, B. B.; Cha, J. K. Org. Lett. 2014, 16, 6208. (e) Rao, N. N.; Cha, J. K. J. Am. Chem. Soc. 2015, 137, 2243. (f) Murali, R. V. N. S.; Rao, N. N.; Cha, J. K. Org. Lett. 2015, 17, 3854.

(11) (a) Ye, Z.; Dai, M. J. Org. Lett. 2015, 17, 2190. (b) Li, Y.; Ye, Z.; Bellman, T. M.; Chi, T.; Dai, M. J. Org. Lett. 2015, 17, 2186. (c) Kananovich, D. G.; Konik, Y. A.; Zubrytski, D. M.; Järving, I.; Lopp, M. Chem. Commun. 2015, 51, 8439. (d) He, X.-P.; Shu, Y.-J.; Dai, J.-J.; Zhang, W.-M.; Feng, Y.-S.; Xu, H.-J. Org. Biomol. Chem. 2015, 13, 7159.

(12) (a) Han, C.; Salyer, A. E.; Kim, E. H.; Jiang, X.; Jarrard, R. E.; Powers, M. S.; Kirchhoff, A. M.; Salvador, T. K.; Chester, J. A.; Hockerman, G. H.; Colby, D. A. J. Med. Chem. 2013, 56, 2456. (b) Han, C.; Kim, E. H.; Colby, D. A. J. Am. Chem. Soc. 2011, 133, 5802. (c) Bégué, J.-P.; Bonnet-Delpon, D. Bioorganic and Medicinal Chemistry of Fluorine; Wiley: Hoboken, NJ, 2008; Chapter 7, pp 246–256.

(13) (a) Sato, K.; Nakazato, S.; Enko, H.; Tsujita, H.; Fujita, K.; Yamamoto, T.; Omote, M.; Ando, A.; Kumadaki, I. J. Fluorine Chem. 2003, 121, 105. (b) Sato, K.; Omote, M.; Ando, A.; Kumadaki, I. J. Fluorine Chem. 2004, 125, 509. (c) Kim, B. C.; Park, A.; An, J. E.; Lee, W. K.; Lee, H. B.; Shin, H. Synthesis 2012, 44, 3165.

(14) (a) Zhao, H.; Fan, X.; Yu, J.; Zhu, C. J. Am. Chem. Soc. 2015, 137, 3490. (b) Booker-Milburn, K. I.; Barker, A.; Brailsford, W.; Cox, B.; Mansley, T. E. Tetrahedron 1998, 54, 15321.

(15) Nicolaou, K. C.; Estrada, A. A.; Freestone, G. C.; Lee, S. H.; Alvarez-Mico, X. Tetrahedron 2007, 63, 6088.

(16) (a) Surmont, R.; Verniest, G.; Thuring, J. W.; Macdonald, G.; Deroose, F.; De Kimpe, N. J. Org. Chem. 2010, 75, 929. (b) Fustero, S.; Báez, C.; Sánchez-Roselló, M.; Asensio, A.; Miro, J.; del Pozo, C. Synthesis 2012, 44, 1863.

(17) (a) Chen, Z.-H.; Wang, R.-W.; Qing, F.-L. Tetrahedron Lett. 2012, 53, 2171. (b) Tang, W.; Liu, S.; Degen, D.; Ebright, R. H.; Prusov, E. V. Chem. - Eur. J. 2014, 20, 12310. (c) Zhang, R.; McCarter, J. D.; Braun, C.; Yeung, W.; Brayer, G. D.; Withers, S. G. J. Org. Chem. 2008, 73, 3070.

(18) (a) De Schutter, C.; Pfund, E.; Lequeux, T. Tetrahedron 2013, 69, 5920. (b) Hasegawa, E.; Tateyama, M.; Nagumo, R.; Tayama, E.; Iwamoto, H. Beilstein J. Org. Chem. 2013, 9, 1397. (c) Snider, B. B.; Kwon, T. J. Org. Chem. 1992, 57, 2399. (d) Jiao, J.; Nguyen, L. X.; Patterson, D. R.; Flowers, R. A., II Org. Lett. 2007, 9, 1323. (e) Wang, Y.-F.; Toh, K. K.; Ng, E. P. J.; Chiba, S. J. Am. Chem. Soc. 2011, 133, 6411.